THE UNIVERSITY OF
WAIKATO
Te Whare Wānanga o Waikato

Investigations on the surge withstand capability of SCALED system

by

Pranav Nandkishor Udas

A thesis submitted in fulfilment for the degree of Master of Engineering

in the

Faculty of Science and Engineering

Department of Engineering

September 2020

Abstract

Simple resistor-capacitor (RC) circuit theory is extended in developing Supercapacitor Assisted (SCA) technique by placing supercapacitor (SC) in series with the useful load. Part of wasted energy in a RC loop is utilised by this useful load resulting in increased overall efficiency of the circuit.

In Supercapacitor Assisted Light Emitting Diode (SCALED) converter, developed for a DC microgrid system, two SC banks with LEDs form the modified RC loops. A complete SCALED system prototype is in field trial at Ports of Auckland Limited (POAL).

Target of this project was to test transient surge withstand capability of SCALED system so that its vulnerability to lightning surges could be minimised. Noiseken LSS-6110 Lightning Surge Simulator (LSS) was used to generate high voltage transient surges as per IEEE C62.41 standards. Surge propagation through different parts of SCALED was studied stage by stage with PV panel providing two different paths for surge energy to travel. Tests revealed that SCALED itself is able to withstand limited transient surges due to the buffer SC bank connected across its input ports. However, some operational time delay was observed which is due to processing circuits sensitive to transients. Thesis provides an initial approach towards developing surge protected SCALED system.

Acknowledgements

I would like to thank my parents, Mr. Nandkishore Udas and Mrs. Megha Udas for their tremendous love, unwavering support and help who made me what I am today. No words can express my gratitude for all they have provided me with. I am very much thankful to all my family members for their emotional and moral support.

I am very much indebted to my academic supervisor, Associate Professor Nihal Kularatna for providing me with this opportunity. His brilliance, guidance, enthusiasm, advice and direction supported me in completion of my thesis. I would also like to mention my colleague Mrs. Dilini Jayananda who developed Supercapacitor Assisted LED system (SCALED) as her PhD project and would like to thank her for all the necessary help she has provided me with.

I would like to acknowledge Mr. Benson Chang, laboratory technician for providing me with the components I asked for. I am thankful to the Division registrar Mrs. Hannah Te Puia for helping me through my VISA and enrolment conditions.

My loving gratitude to two special girls in my life, Kasturi and Soha for helping me to stay calm and focused throughout this whole journey. I would like to express my appreciation to my dearest friend, brother and flatmate Mr. Thushanth Chandrakumar.

Table of Contents

Chapter 3: Overview of Surge

Chapter 4: Use of Supercapacitor in Surge protection and in SCALED system

Chapter 5: Effect of surges on SCALED

Chapter 6: Conclusion and Future Development

Appendices

References

List of Tables

List of Figures

Acronyms and Abbreviations

SC	supercapacitor
ESR	Equivalent Series Resistance
SCA	Supercapacitor Assisted
DC	Direct Current
AC	Alternating Current
LED	Light Emitting Diode
SCALDO	Supercapacitor Assisted Low Dropout Regulator
SCASA	Supercapacitor Assisted Surge Absorber
SCATMA	Supercapacitor Assisted Temperature Modification Apparatus
SCAHDI	Supercapacitor Assisted High Density Inverter
SCALED	Supercapacitor Assisted Light Emitting Diode
PV	Photovoltaic
MPP	Maximum Power Point
ETTE	End To End Efficiency
DM	Differential Mode
CM	Common Mode
LSS	Lightning Surge Simulator
EUT	Equipment Under Test
TVSS	Transient Voltage Surge Suppressors
SPD	Surge Protection Devices
MOV	Metal Oxide Varistor
GDT	Gas Discharge Tube
BBD	Bipolar Breakdown Devices

Chapter 1

Introduction

1.1 Extended RC circuit theory

Supercapacitors (SCs) also referred as ultracapacitors have typical capacitance values million times larger than the conventional electrolytic capacitors. SCs have higher power densities than rechargeable batteries and higher energy densities than electrolytic capacitors. Compared to traditional capacitors, SCs have lower DC voltage ratings, low equivalent series resistance (ESR) and large time constant.

Completely uncharged capacitor starting from zero-charge condition stores the energy $\frac{1}{2}CV^2$ after about five time constants where input source voltage is *V*. Resistive components in the loop dissipates equal amount of energy during this period making the charging process only 50% efficient. This electrical circuit is extended by (i) replacing the capacitor bank with supercapacitor providing large time constant (ii) inserting useful load in the series to utilize part of the wasted energy and (iii) pre-charging the supercapacitor connected; giving rise to Supercapacitor Assisted (SCA) techniques developed by power electronics research group at University of Waikato.

1.2 Efficiency improvement

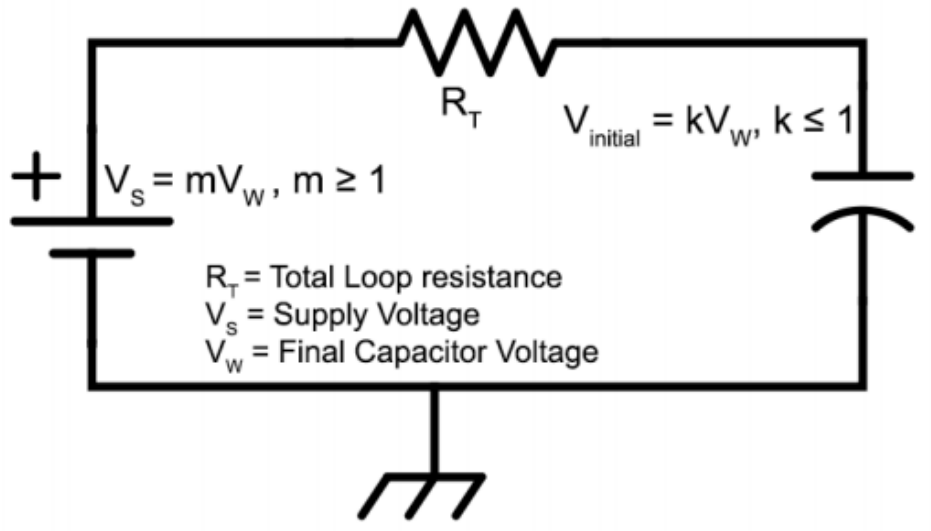

(a)

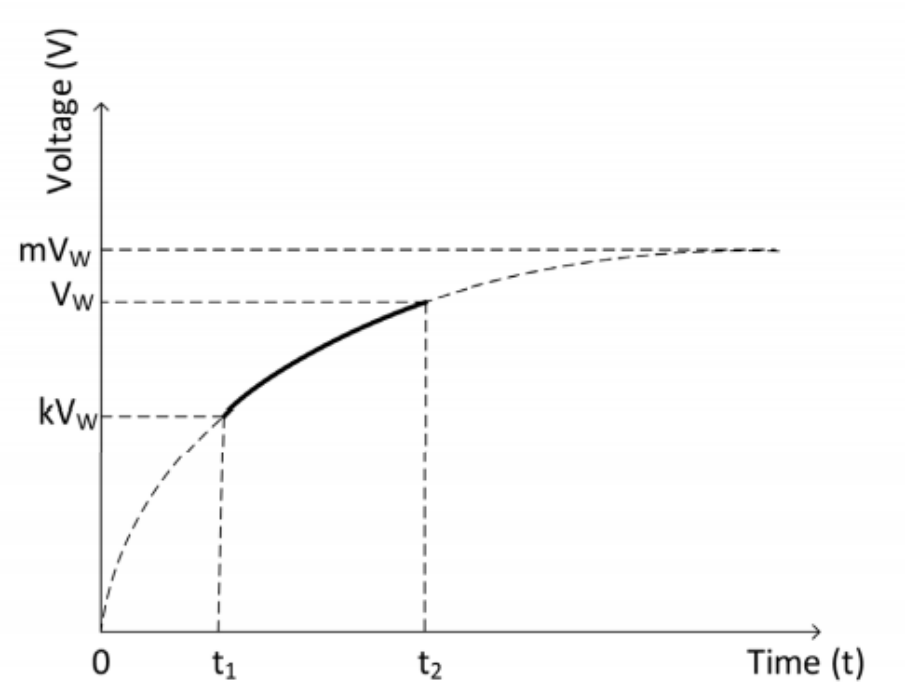

(b)

Fig 1.1 (a) capacitor charging loop (b) Capacitor charging curve [1]

As analysed in [1],

When a fully discharged capacitor is charged from 0 to V_w from a DC supply of mV_w (m ≥ 1), capacitor voltage at time *'t'* is given as

$$V(t) = mV_w(1 - e^{-t/RC}) \tag{1.1}$$

V(t) reaches to kV_w in time t_1 and V_w in time t_2 as shown in Figure 1.1(b), where *'k'* is the initial voltage fraction and *'m'* is the power supply overvoltage factor.

Time taken to reach target voltages kV_w and V_w are given as

$$e^{-t_1/RC} = \frac{m-k}{m} \qquad e^{-t_2/RC} = \frac{m-1}{m} \tag{1.2}$$

Energy stored in the capacitor during this time interval is,

$$E_c(t_2, t_1) = \frac{1}{2}CV_w^2 - \frac{1}{2}C(kV_w^2) = \frac{1}{2}CV_w^2(1 - k^2) \tag{1.3}$$

Energy dissipated in across the resistor during this time is,

$$E_R(t_2, t_1) = \int_{t_1}^{t_2} \frac{(mV_w - V(t))^2}{R}\, dt$$

$$E_R(t_2, t_1) = \frac{m^2V_w^2}{R}\left(\frac{-RC}{2}\right)[e^{-2t_2/RC} - e^{-2t_1/RC}] \tag{1.4}$$

Substituting eq^{n} (1.2) in eq^{n} (1.4)

$$E_R(t_2, t_1) = \frac{1}{2} C V_w^2 (k^2 - 2mk + 2m - 1)$$

Energy efficiency ratio is given by,

$$\eta = \frac{E_C}{E_c + E_R} = \frac{1+k}{2m} \quad (1.5)$$

When $k \rightarrow 0$ (no capacitor precharge) and $m \rightarrow 1$ (no power supply over-voltage factor) efficiency = $\frac{1}{2}$, recovering the standard result. Equation (1.5) depicts that efficiency can be enhanced if the capacitor carries percentage charge before charging commences [1].

Supercapacitor have lower ESR compared to standard electrolytic capacitor making SCs less dissipative. Due to small ESR, dissipative voltage across the series connected SC can be negligible while the potential difference across the capacitor can be large. This property makes the series connected SC as lossless voltage dropper in circuit. Connecting useful load like LED lamps in series with the supercapacitor, minimises the energy loss in circuit resulting in increased overall efficiency [1].

1.3 SCA topologies

A research team in the school of Science and Engineering at University of Waikato has been developing SC assisted electronic circuit topologies for almost a decade. Gradually, the team started to build some novel circuit topologies from basic theoretical concepts to practical implementation. The circuit topologies developed so far are listed below:

1. SCALDO (Supercapacitor assisted low dropout regulator)
2. SCASA (Supercapacitor assisted surge absorber)
3. SCATMA (Supercapacitor assisted temperature modification apparatus)
4. SCAHDI (Supercapacitor assisted high density inverter)
5. SCALED (Supercapacitor assisted light emitting diode)

SCALDO was one of the very first applications developed by combining a low dropout linear voltage regulator with SC or an array of SCs, achieving a significant improvement in the ETEE. This successful technique provided a gateway to the development of many other SC-assisted applications [2].

One important application relies on the fact that SCs are capable of absorbing very high surges. This is due to their large time constants, allowing them to be

used in surge protection circuits. This circuit topology, named SCASA, has better surge handling capability than traditional surge protectors [3].

SCATMA is an instant water heating technique based on the use of stored energy in supercapacitor to overcome the delayed delivery of the hot water in domestic water systems. This application makes use of supercapacitor's feature of high power density which enables it to deliver high level of power for short periods [4].

SCAHDI was developed by placing resistive inverter load in the capacitor charging loop to generate high density inverter. While internal resistance of the supply, loop resistance and ESR of the supercapacitor waste energy, resistive load inverter usefully utilises the wasted energy causing improved charging efficiency [5].

Connecting LED as a useful load in series with the supercapacitor bank forms a modified RC loop giving rise to SCALED technique. These series connected SC banks act as energy storage elements within an overall SCALED system powering up the LEDs. This SCALED topology is another novel application in the field of DC microgrid [6].

1.4 Objective of the project

SCALED technique utilises solar energy to power up the LEDs in a DC microgrid environment. Solar panels are installed on the rooftops of the buildings or in open large spaces and hence are exposed to natural calamities like lightning surges. Surge appearance at the solar panel also results in injecting a high energy transient pulse current through SCALED. Therefore, surge withstand capability of the SCALED circuit needs to be tested as it is vulnerable to these high voltage transients.

The design of SCALED is primarily based on supercapacitors and hence chosen for the special Masters task where surge withstand capability of the system has been tested. Surges were generated by Noiseken LSS-6110 lightning surge simulator, which is capable of producing maximum surge voltage of 6.6 kV and maximum surge current of 3.3 kA. To understand the response of SCALED towards surges, PV panel was also subjected to surge condition. Practical study shows that PV panel absorbs surges and hence indirectly plays an important role in surge protection of SCALED circuit.

1.5 Thesis outline

Chapter 1 Introduction

Chapter gives brief idea about the extended RC circuit theory stating a way to improve the efficiency of typical RC loop providing new SCA topologies. Applications of SCA techniques were described in short. Chapter also explains the objective of the thesis and presents structure of the thesis.

Chapter 2 Background

Chapter gives the brief idea about solar cell and solar PV module along with the equivalent circuit of solar cell explained with the help of one diode modelling. Concept of DC microgrid is covered in this chapter along with its application. Basic introduction of the SCALED and a theory behind it is presented in this chapter along with LED characteristics explaining its function as a useful load in SCALED.

Chapter 3 Overview of surge

Chapter explains the concept of surge protection in a detailed manner along with different types of DC and AC line fluctuations with two different modes of transients. Lightning surge simulator with its internal circuit is introduced along with the combination surge waveforms specified by IEC 61000-4-5 standards. Further, different transient suppression devices are explained with their specifications and properties. Chapter also gives an idea about the design concepts that could be used for surge protection purposes.

Chapter 4 Use of supercapacitors in surge protectors and in SCALED system

Chapter starts with introducing supercapacitors with their specifications and use of SC as a circuit element. Theoretical analysis is provided in a detailed manner along with the practical experimentation to explain surge absorption property of SC. Later part of the chapter explains working principle of SCALED along with the block diagram with each block explained in brief. Normal working operation of SCALED is demonstrated with practical data.

Chapter 5 Effect of surges on SCALED

Chapter starts with demonstrating the effect of surges on solar PV panel as it performs small but important role for protection of SCALED against high voltage transients. Surge withstand capability of the SCALED is verified by subjecting it to high voltage transients in the absence of any external surge suppressors. Observing the response of a system towards these high energy surges, protective measures were taken into account to avoid failure of the system. Modification to

the current system is made by changing the size of supercapacitor modules in order to observe the effect of surges on SCALED.

Chapter 6 Conclusion and Future development

Response of SCALED system towards high energy transients was studied. There is a small circuit block in the overall system which gets affected due to surges even after connecting external protective components. This sub-circuit could be improved for better overall performance and better reliability of the system. Chapter summarizes reasons for SCALED's surge absorbing property towards few surges.

Chapter 2

Background

2.1 Overview

Solar energy is the most abundant renewable energy source in the world. Tapping into this renewable energy and making use of the emerging supercapacitor-based energy storage technique can provide a way to boost the usage of solar power. Making use of supercapacitors as energy storage elements is expected to radically increase the efficiency of solar PV systems. Losses across other components in the PV system, such as the power converters reduce end-to-end efficiency of the system. Majority of the household appliances work on DC; therefore, these intermediate converters are eliminated and replaced by SCALED converter providing DC to the load directly, increasing the overall efficiency of system.

Photovoltaic (PV) system directly converts sunlight into electricity. The basic element of a PV system is PV cell. Cells can be grouped to form panels or arrays. Sophisticated applications require electronic converters to process the electricity from the PV device. These converters may be used to regulate the voltage and current at the load to control the power flow in grid-connected systems and mainly to track the maximum power point (MPP) of the device. Figure 2.1 reflects the construction of solar PV array.

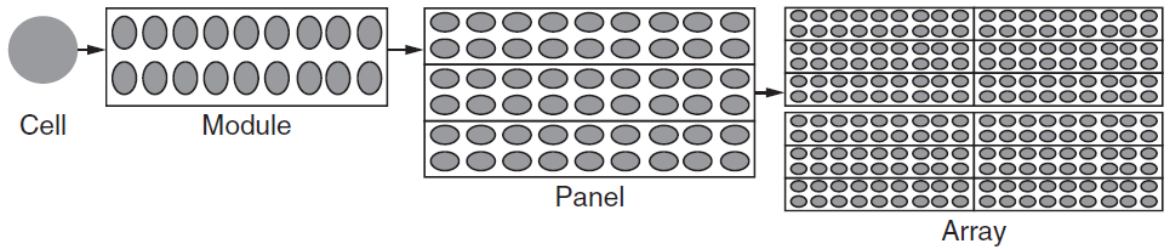

Fig 2.1 PV system [10]

2.2 Solar Cell

Solar cells are made up of semiconductor materials and come in different shapes and sizes. The silicon solar cell is made up of N-type and P-type semiconducting layers, with two conductor plates at the top and at the bottom as shown in Figure 2.2. When a photon strikes the PV cell, electrons from the N-type layer are knocked off and travel to the P-type layer, creating an electron hole pair in the region. Typically, a PV cell generates very low voltage depending on the semiconductor and the built-up technology. This voltage is low enough as it

cannot be of any use. Therefore, these modules can be interconnected in series and/or in parallel to form a PV panel. When modules are connected in series, same current flows through them adding up the voltages. However, when they are connected in parallel, their currents are added while the voltage is same.

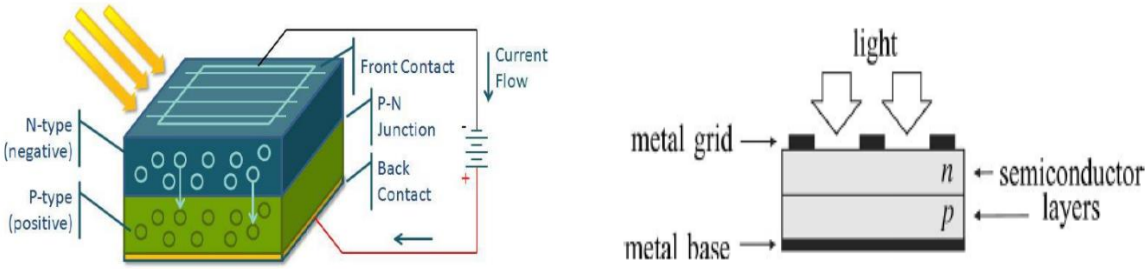

Fig 2.2 Physical structure of PV cell [13] [15]

2.3 Equivalent circuit of solar PV cell

Working principle behind the Photovoltaic cells is similar to photo-electric effect. PV cells are basically a PN junction diode. An ideal solar cell can be represented by an equivalent electrical circuit with a single diode in parallel with a current source as shown in Figure 2.3(a) and Figure 2.3(b). The three parameters are,

I_{ph} - Photo generated current
I_D - Diode equivalent current
V_{oc} - Open circuit voltage

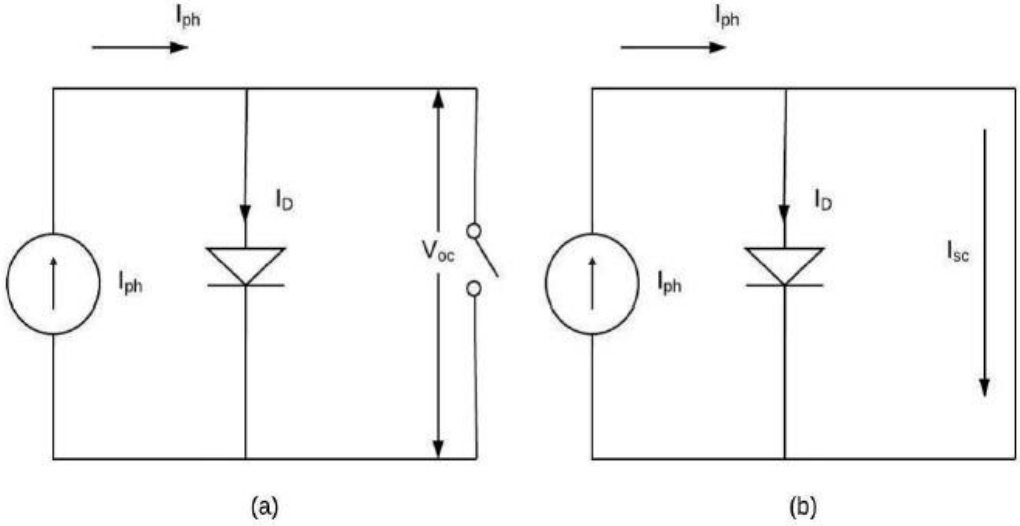

Fig 2.3 Electrical equivalent circuit of solar cell (a) open circuit voltage (b) short circuit current

In practice, none of the solar cells are ideal as the generation of electricity depends on many factors such as the flux of incident light, the temperature of the PV cell,

the bandgap energy of the cell, the reflectance of the surface, and the electron-hole recombination rate [14]. Therefore, the non-ideal PV cell can be represented as an extended equivalent circuit from that shown in Figure 2.3 with the addition of a series resistance R_s and the shunt resistance R_{sh} shown in Figure 2.4.

The practical PV device presents a hybrid behaviour, which may be of current or voltage source, depending on the operating point. The practical PV device has a series resistance R_s whose influence is stronger when the device operates in the voltage source region, and a parallel resistance R_{sh} has a stronger influence in the current source region of operation [15]. The R_s resistance is the sum of several structural resistances of the device. R_s basically depends on the contact resistance of the metal base with the *p* semiconductor layer, the resistances of the *p* and *n* bodies, the contact resistance of the *n* layer with the top metal grid, and the resistance of the grid [15]. The R_{sh} resistance exists mainly due to the leakage current of the *p–n* junction and depends on the fabrication method of the PV cell [15]. The value of R_{sh} is generally high and R_s has a very low resistance.

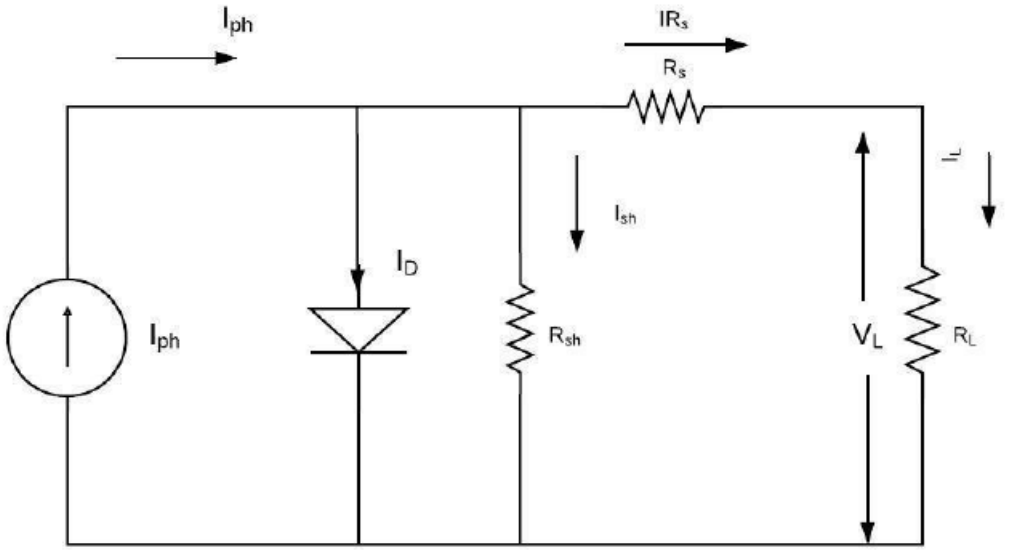

Fig 2.4 Equivalent circuit for practical PV cell

R_s represents the resistance of the bulk material and also the resistance between the bulk material and the metal conductor.

R_{sh} represents the recombination of the electron hole pair before reaching the load.

Ignoring I_{sh}, as this has minimal effect on the photo generated current.

I_{ph} is directly proportional to the solar radiation, therefore the voltage and current relationship seen by the load will be given by,

$$I_{ph} - I_D = I_L \quad (2.1)$$

$$I_D = I_o\,(e^{qV_D/NkT} - 1) \quad (2.2)$$

Where
I_o – reverse saturation current
q – charge of electron
k – Boltzmann constant
T – cell temperature in Kelvin
n – ideality factor

Substituting Equation (2.2) in Equation (2.1)

$$I_{ph} - I_o\left(e^{qV_D/NkT} - 1\right) = I_L$$

$$I_{ph} - I_o\left(e^{q(R_S I_L + V_L)/NkT} - 1\right) = I_L$$

$$\ln\left(\frac{I_{ph} - I_L}{I_o} + 1\right) = \frac{q\,(R_S I_L + V_L)}{NkT}$$

$$(R_S I_L + V_L) = \frac{NkT}{q}\ln\left(\frac{I_{ph} - I_L}{I_o} + 1\right)$$

$$V_L = \frac{NkT}{q}\ln\left(\frac{I_{ph} - I_L}{I_o} + 1\right) - R_S I_L \quad (2.3)$$

For open circuit I_L=0,

$$V_{oc} = \frac{NkT}{q}\ln\left(\frac{I_{ph}}{I_o} + 1\right) \quad (2.4)$$

Open circuit voltage will not reduce much as it is directly proportional to the logarithm of I_{ph} as shown in the Equation (2.4)

Taking the case with shunt resistance R_{sh}, the complete equation for a PV cell relating V_L and I_L can be represented as,

$$I_{ph} - I_D - I_{sh} = I_L \quad (2.5)$$

$$I_{ph} - I_o\left(e^{qV_D/NkT} - 1\right) - \frac{V_D}{R_{sh}} = I_L$$

$$I_{ph} - I_o\left(e^{q(R_S I_L + V_L)/NkT} - 1\right) - \frac{(R_S I_L + V_L)}{R_{sh}} = I_L \quad (2.6)$$

The current-voltage (I-V) and power-voltage (P-V) characteristics of the PV panel is shown in Figure 2.5. These characteristic curves depend on the series and shunt resistances (R_s, R_{sh}) of the panel along with the external factors such as solar irradiance and temperature. Output of the PV panel is non-linear in nature with the maximum power point varying with irradiance and temperature. As

depicted in Figure 2.5, PV panel curves can be divided into three different regions; (i) constant current region where PV panel acts as a current source (A-B) (ii) maximum power point (MPP) range of operation (B-C) (iii) typical voltage source like operation (C-D). With increasing irradiance level short circuit current (I_{SC}) and open circuit voltage (V_{OC}) of the PV panel increases shifting maximum power point.

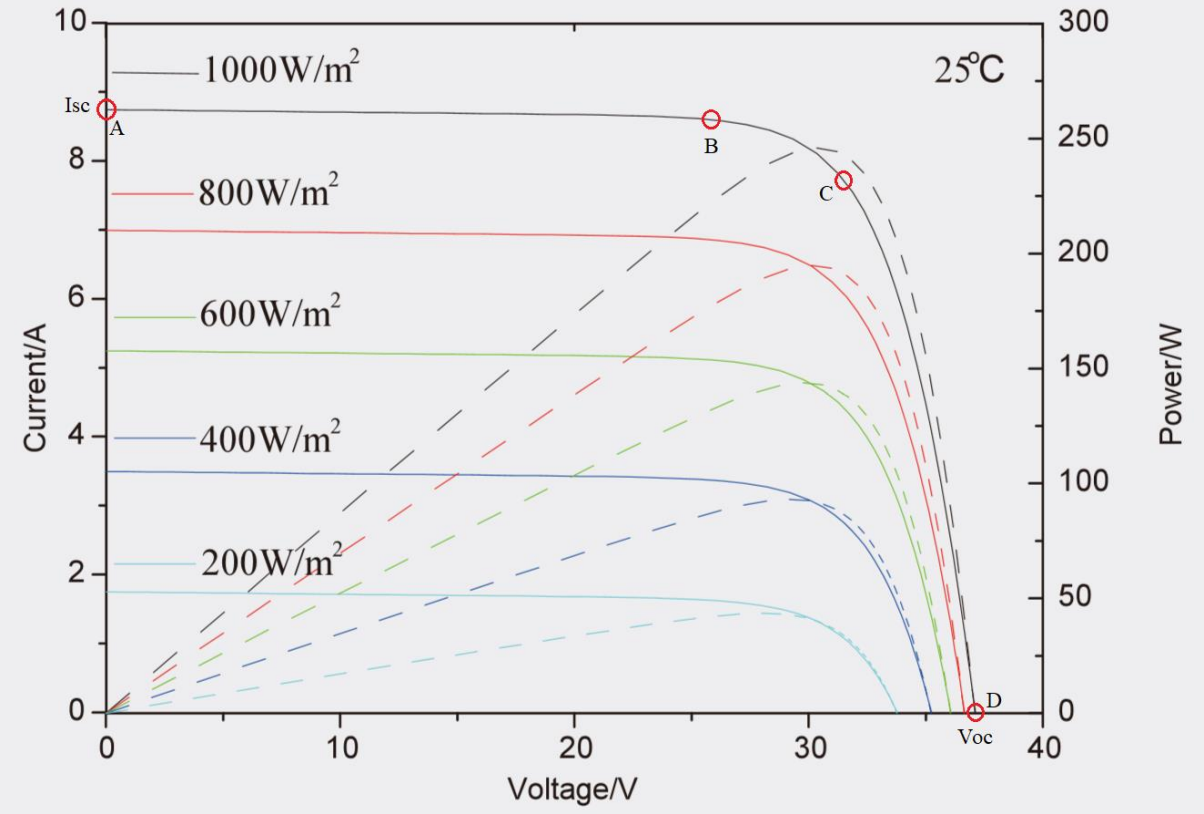

Fig 2.5 Characteristics of PV panel [16]

2.4 DC Microgrid

To mitigate the effects of climate change, DC microgrid is seen as promising technology to increase the renewable energy contribution to power markets. A DC microgrid is analogous to a conventional AC grid system but with only DC power flowing throughout the entire grid. This will easily integrate locally generated power such as solar and wind energy. With proper design and installation, a DC microgrid will be more reliable and flexible, with every component localized. The DC microgrid consist of a renewable energy source, microgrid loads, power converters and energy storage devices as shown in Figure 2.6. In remote or rural areas, by making use of natural resources like solar energy, DC microgrid generates, stores and distributes electrical energy.

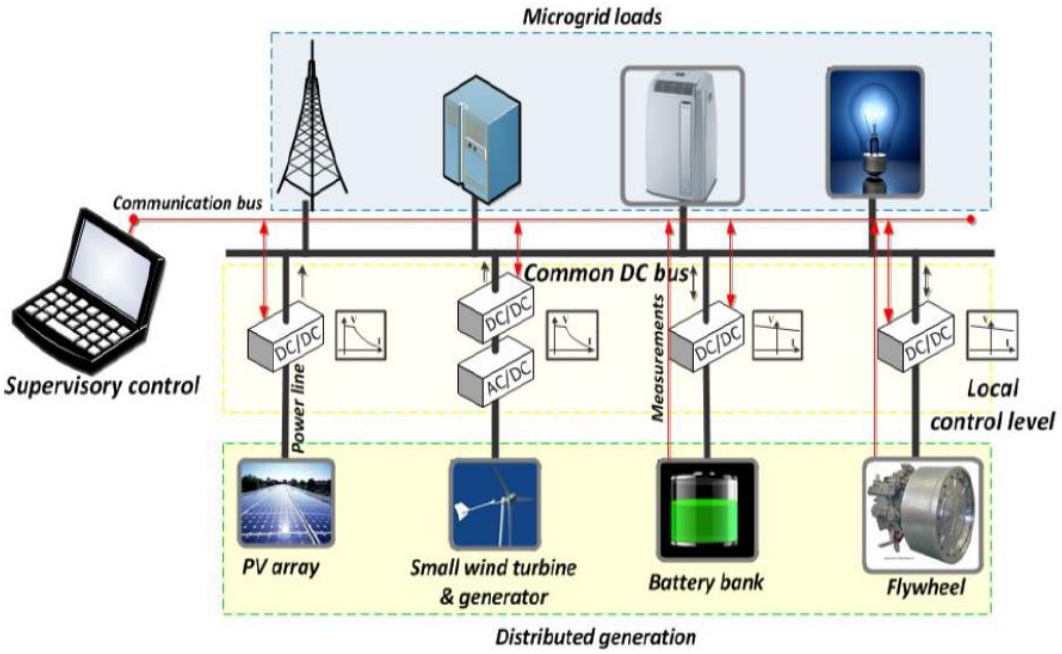

Fig 2.6 DC microgrid configuration [13]

2.5 DC microgrid application

The conventional application of DC microgrid is in distributed power systems, telecommunications, data centres and vehicular power systems [13]. New applications include high efficiency households, renewable energy packs, hybrid energy storage systems and EV charging stations [13], as shown in Figure 2.7. Lately, the efficiency of household appliances has become of more interest to many people who are aiming to reduce their electricity costs.

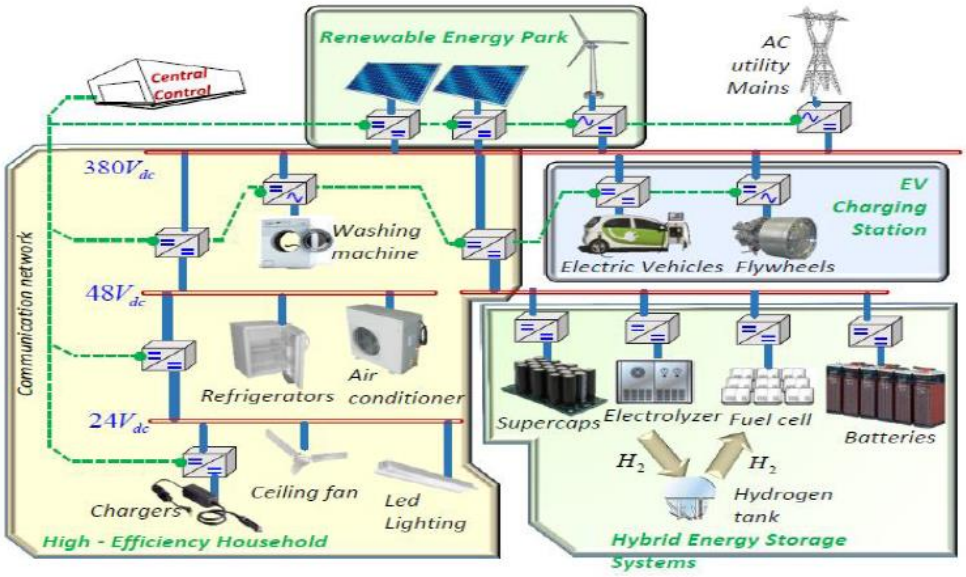

Fig 2.7 DC microgrid application [12]

Adopting DC microgrid will help to create highly energy-efficient households by eliminating the losses that occur in the AC-DC converters. The installation of common modern appliances is shown in Figure 2.8(a). Low voltage appliances use power adapters, where power losses occur. However, with the system shown in Figure 2.8(b), all low voltage appliances are connected to a single interface device, which is directly connected to the DC bus. In low voltage applications, DC microgrids will help to improve efficiency by eliminating power converters.

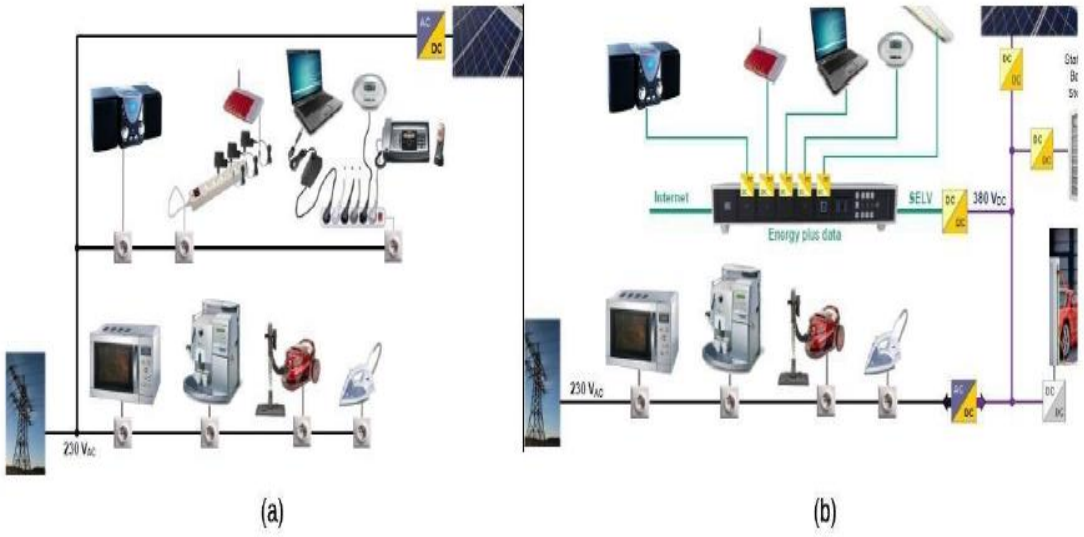

Fig 2.8 (a) Installation and appliances today (b) Installation and appliances in future using DC microgrid [13]

2.6 Introduction of SCALED

Figure 2.9(a) depicts the condition where capacitor is directly charged from constant DC voltage source V_s. Energy stored by the capacitor during the process is $E_C = \frac{1}{2}CV_S^2$. Inserting a resistive load R_L (such as LED lamps, heater) in the series with capacitor as shown in Figure 2.9(b) utilizes part of the wasted energy in useful manner making the capacitor charging circuit more energy efficient. SC assisted topologies were developed at University of Waikato by combining this loss circumvention principle [13] with SC bank, extending the time constant of the circuit by several orders of magnitude.

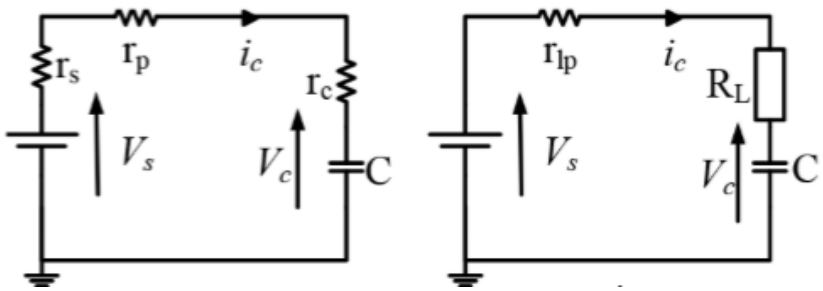

(a) (b)

Fig 2.9 (a) Basic RC charging loop (b) modified RC charging loop ($r_{lp} = r_s+r_p+r_c$) [13]

In these SCA techniques, the above theory is extended by operating a circuit with higher DC source voltage based on multiplication factor (m>1) with SC of rated voltage V_W ($<V_S$) and initial voltage of kV_W ($k<1$) [13]. For this case, charging process efficiency can be given by $\eta = (1+k)/2m$[13]. Figure 2.10 demonstrates the variation in charging efficiency with respect to k and m.

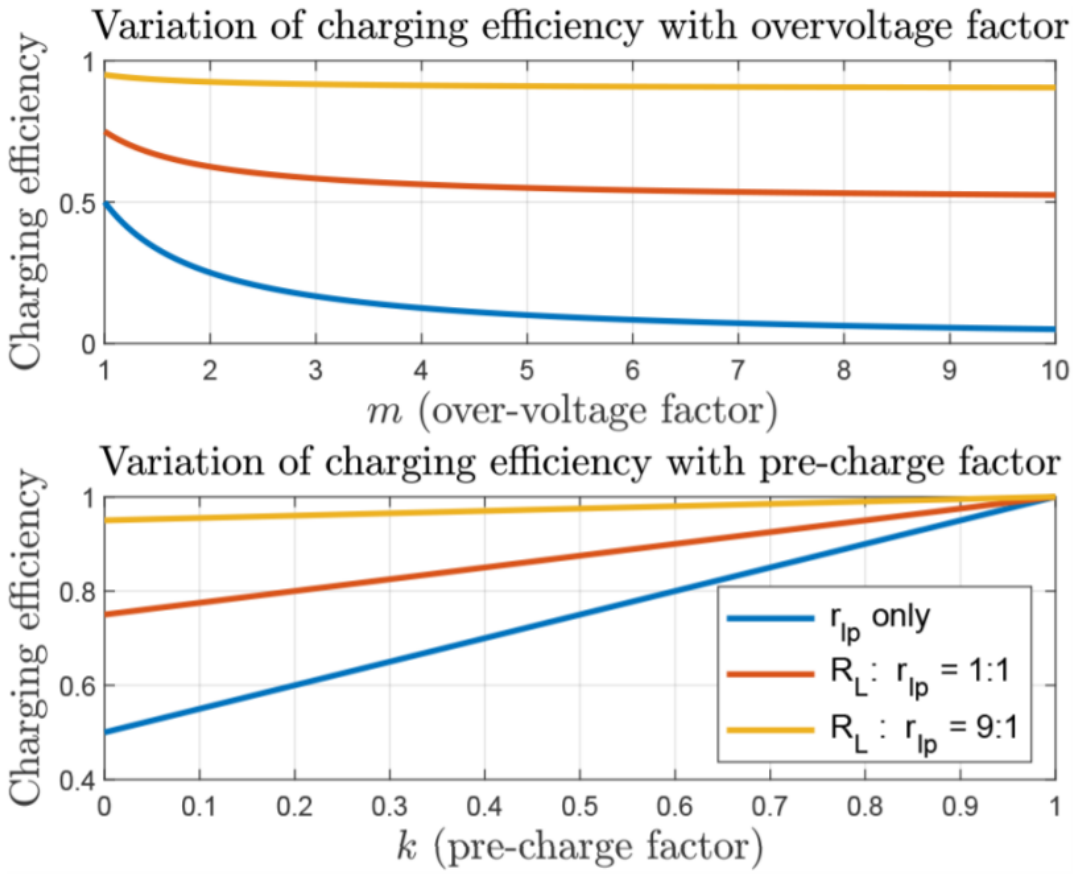

Fig 2.10 Variation of charging efficiency with k and m [13]

The concept of recovering significant amount of energy loss by using a useful load like LED in a capacitor charging loop as depicted in Figure 2.11 is the unique application, where the SC acts as a lossless voltage dropper in the circuit. Switch

protects LED and SC bank from getting exposed any voltage higher than the maximum limit of operational voltage region of SC and LED. One early example of this is SCALDO, where SC is placed in series with the input of a low dropout voltage regulator, producing a substantial improvement in ETEE. This same concept is applied to SCALED in building an efficient SC-assisted low voltage LED lighting system powered by solar energy.

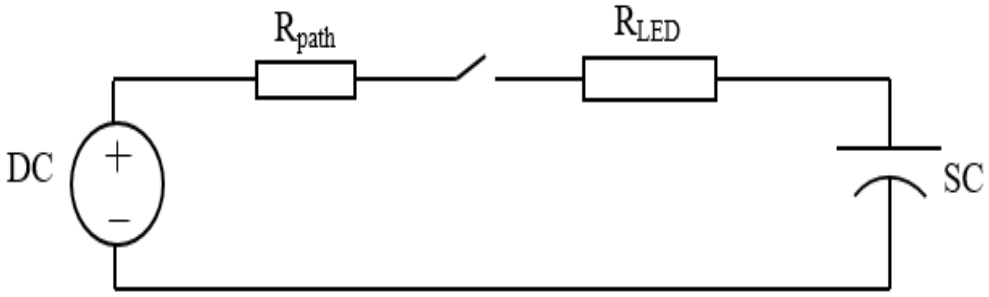

Fig 2.11 LED as a useful load with SC

The existing solar PV based LED lighting system consist of a DC-DC converter and an inverter as shown in Figure 2.12(a). The ETTE is determined by the product of the individual efficiencies of each block. Replacing these intermediate stages with one single SCALED converter increases the efficiency of the system significantly. The main advantage of a supercapacitor is that it can provide a quick burst of power with its fast charging and discharging capability, which enables it to handle peak power demands. In addition, supercapacitors are very reliable and have a lifespan of millions of cycles.

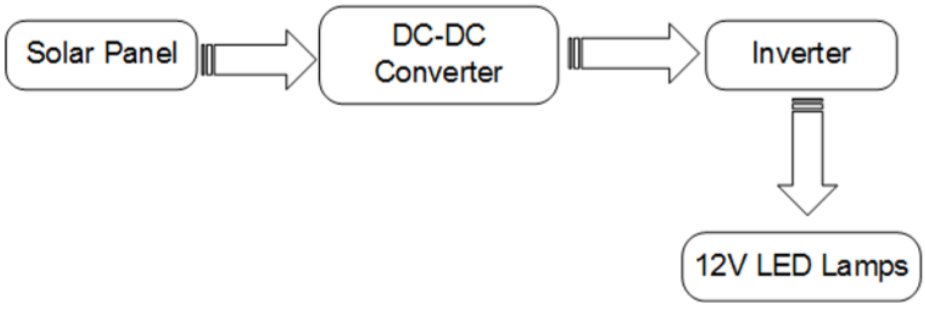

(a)

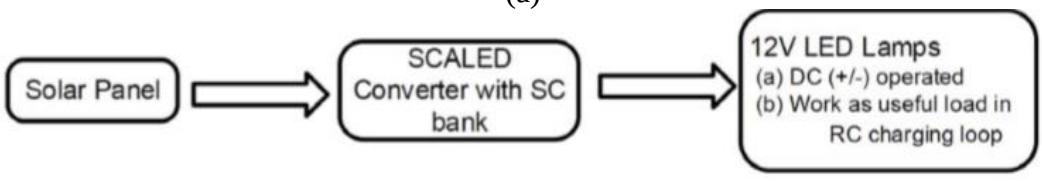

(b)

Fig 2.12 (a) existing solar panel based LED lighting system block diagram (b) Basic block diagram of SCALED [6]

2.7 LED characteristics

Commercially available low voltage LED lamps can operate over a wide range of positive as well as negative DC voltages with constant brightness. Within a constant brightness region, LED dissipates approximately constant power. A set of experiment was performed to understand and verify this behaviour where illuminance and current drawn were recorded. Figure 2.13 reflects the test setup used for the experiment and Figure 2.14 reflects the characteristic properties of the LED observed during this experiment.

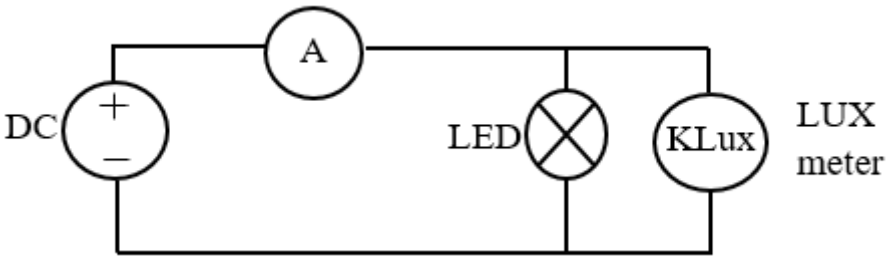

Fig 2.13 Test circuit for the experiment

Tests performed conclude that LED lamps have following features:

(i) Ability to operate over a wide range of DC voltages with constant brightness
(ii) Ability to operate with positive and negative voltages
(iii) Ability to operate as constant power load in constant brightness region

These properties make LED as useful load in SCALED circuit.

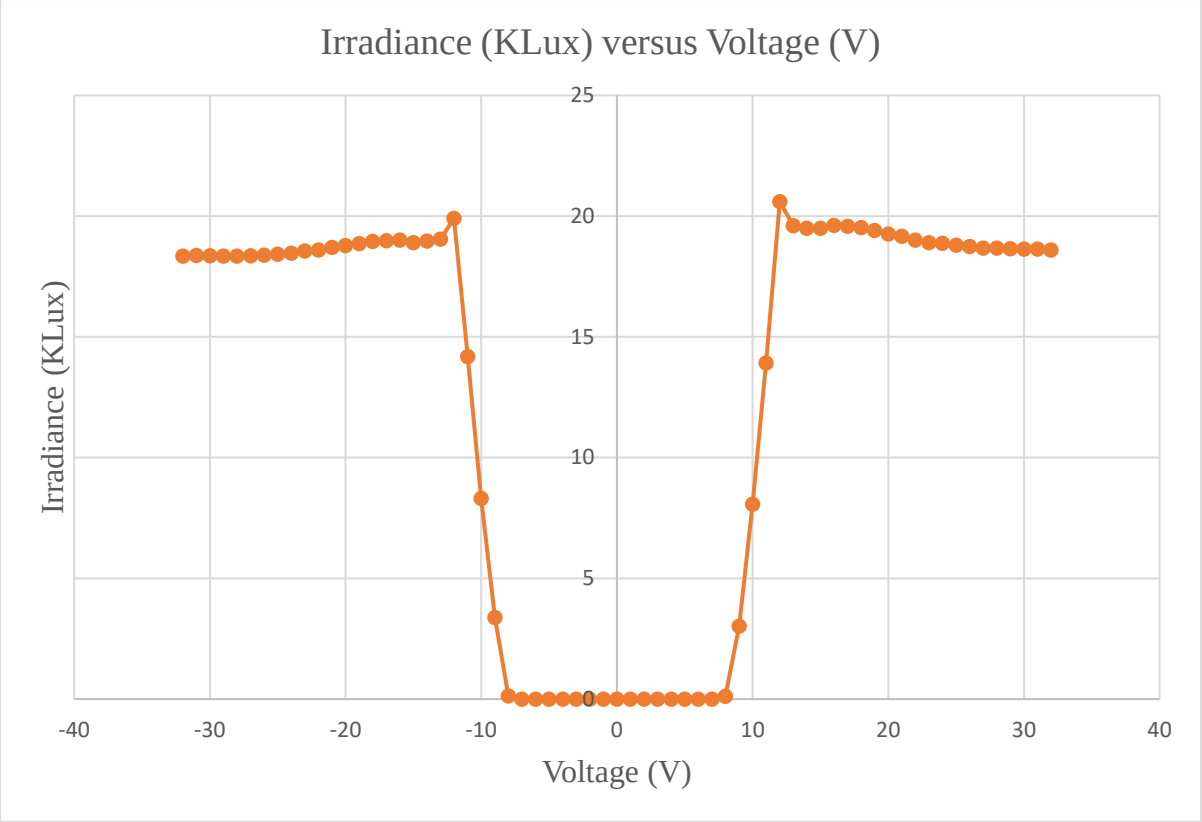
Irradiance (KLux) versus Voltage (V)
Irradiance (KLux)
25
20
15
10
5
0
-40
-30
-20
-10
0
10
20
30
40
Voltage (V)

(a)

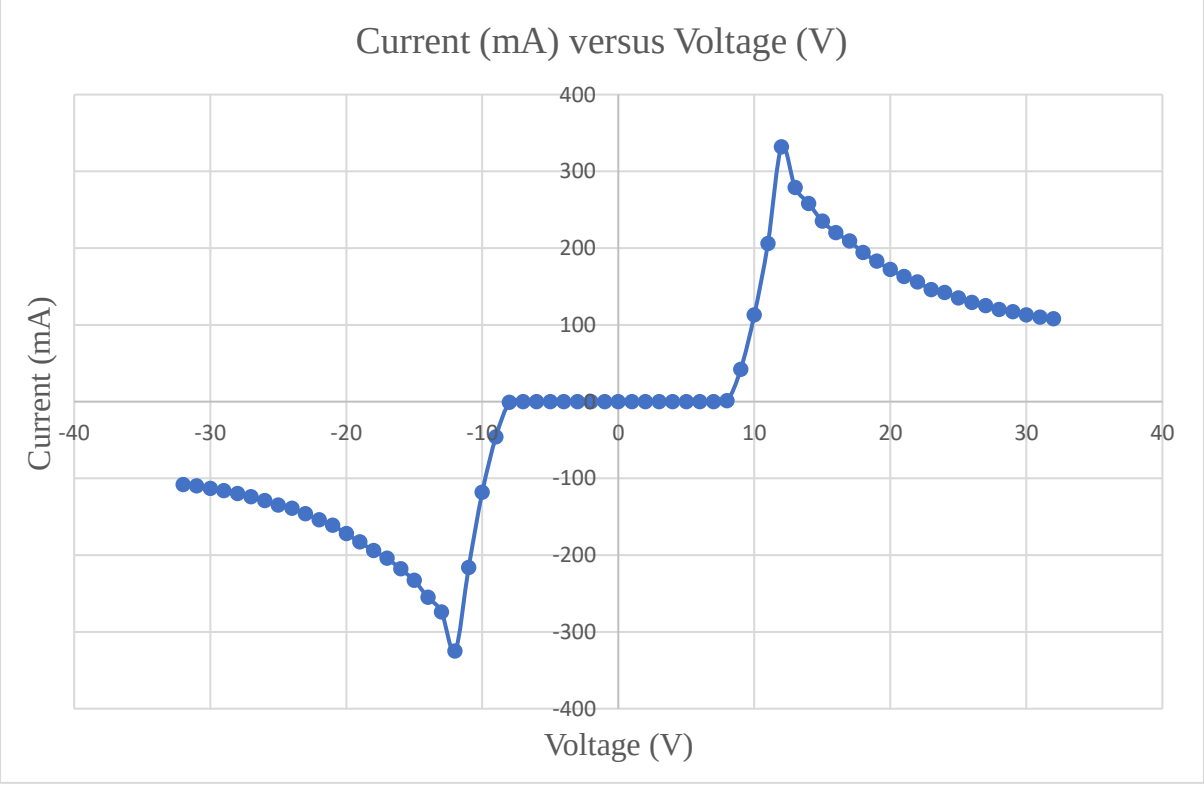
Current (mA) versus Voltage (V)
Current (mA)
400
300
200
100
0
-100
-200
-300
-400
-40
-30
-20
-10
0
10
20
30
40
Voltage (V)

(b)

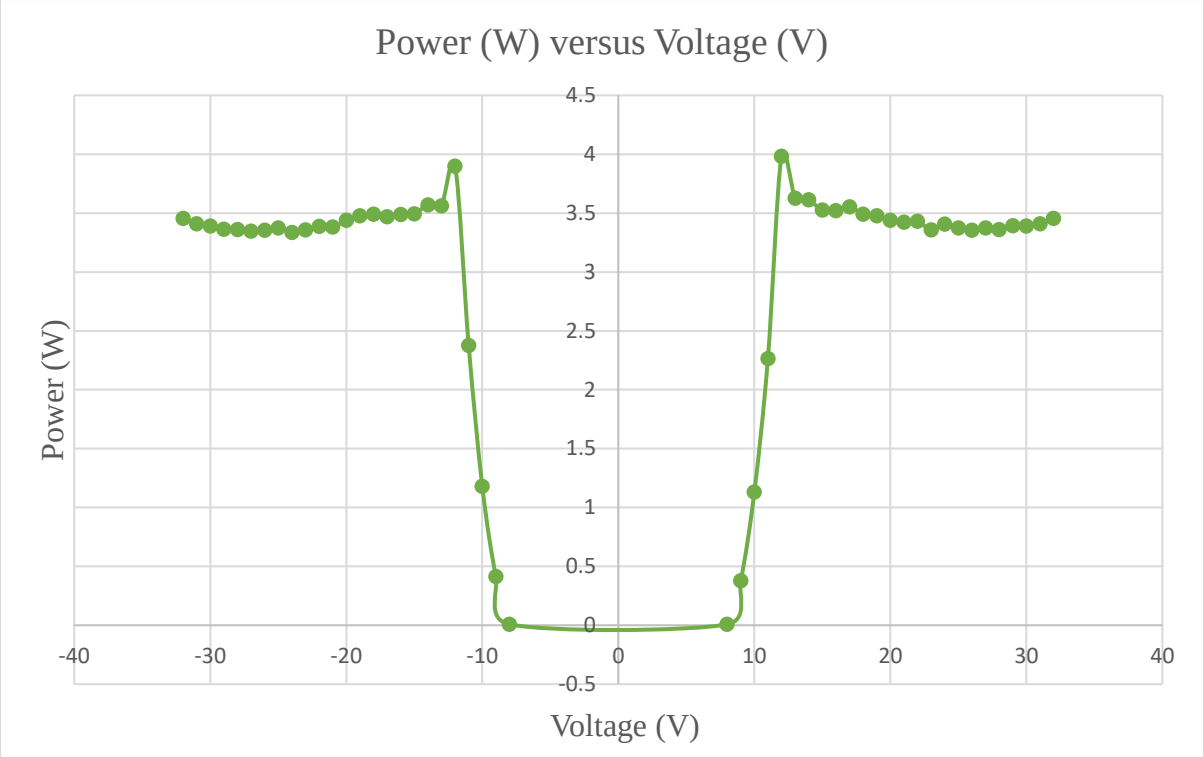

(c)

Fig 2.14 LED characteristics (a) variation of Lux level with voltage (b) current- voltage characteristic (c) power dissipation with changing voltage

Chapter 3

Overview of Surge

3.1 Introduction

Significant increase in the voltage above the normal operating DC/AC level, boosting the electrical charge in power lines can be termed as the surge voltage. This causes an increase in the electric potential energy increasing the current flowing through the circuit. Surge voltages can be extremely damaging to electronic systems, and can take two major forms, switching-induced or lightning-induced [20].

Switching-induced surges/transients are associated with [20]:

(a) major power system switching disturbances such as capacitor bank switching or inductive load switching
(b) minor switching activity near the instrumentation or load
(c) resonating circuits associated with switching devices
(d) system faults, such as short circuits and arcing to the local earthing system

Mechanisms by which lightning induces surge voltage [20]:

(a) direct lightning strike to an external (outdoor) circuit, injecting high current
(b) indirect lightning strike that induces voltages/currents on the conductors outside and/or inside the building

Surge is superimposed on the power line irrespective of the type of supply, AC or DC. In case of the DC supply, surge could be termed as the high energy transient or a single high voltage spike superimposed on the normal operating DC line. On the other hand, AC power line disturbances can be classified into different forms explained in Section 3.2. Figure 3.1 depicts AC and DC power line surges.

3.2 Voltage surge/overvoltage, Voltage sag/undervoltage, Transients

3.2.1 Voltage surge/voltage swell and overvoltage

Increments in the normal operating voltage level that typically last from about one cycle to one-half of a second are termed as voltage surges. Surges are commonly caused by the switching of heavy loads and power network switching. Surges do not reach the magnitudes of sharp spikes, but generally exceed the nominal line voltage by about 20%. A surge that lasts for more than 2 seconds is

typically referred to as an overvoltage. Voltage surges or overvoltage can cause equipment damage, and erroneous readings in monitoring systems [19].

3.2.2 Voltage sag and undervoltage

Decrements in the normal operating voltage level that typically last from about one cycle to one-half of a second are termed as voltage sags. Sags often fall to 20% below nominal voltage and are caused when large loads are connected to the power line. Undervoltage is the condition when voltage sag lasts for more than 2 seconds. Sags can cause computer data loss, alteration of data in progress, and equipment shutdown [19].

3.2.3 Transient

Voltage transients are sharp, very brief increases in the supply waveform. These spikes are commonly caused by the on and off switching of heavy inductive loads such as air conditioners, electric power tools, machinery, and elevators. Lightning can cause even larger spikes ranging in the range of few thousands of volts. Although these lightning surges usually last typically in the order of tens of microseconds, spikes can be dangerous to unprotected equipment. This high magnitude of sudden voltage variations can wipe out stored data, alter data in progress, and cause electronic-hardware damage. In general, the higher the energy content carried into the circuit by the superimposed transient surge, the higher is the potential for damage [19].

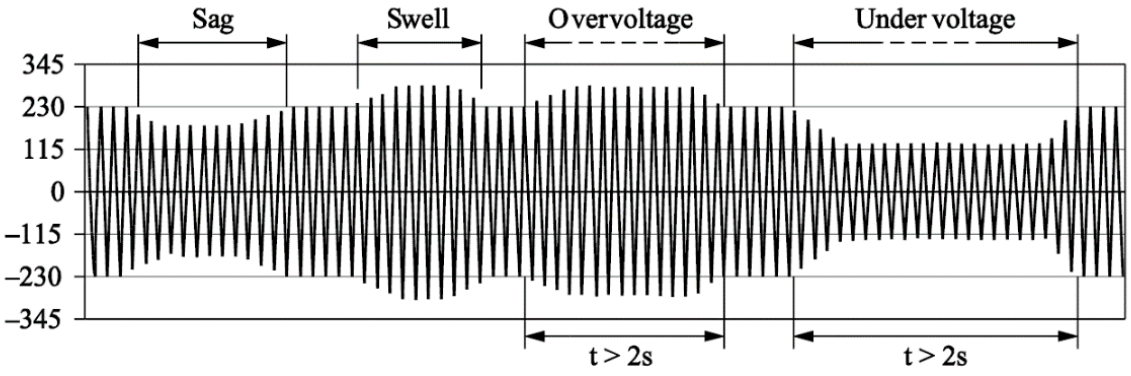

(a)

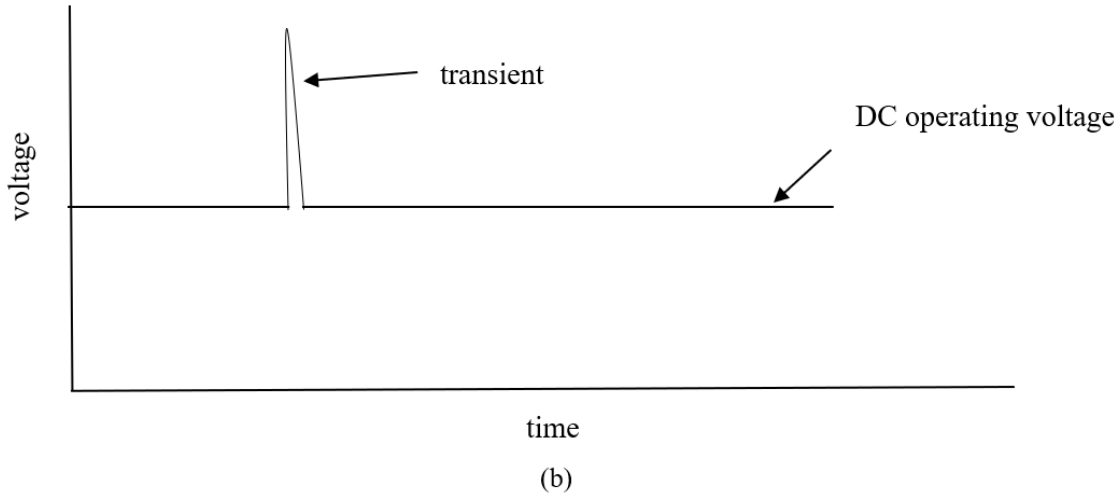

(b)

Fig 3.1 (a) AC Voltage fluctuations [19] (b) Surge superimposed on the DC line

3.3 Modes of Transients

The noise and transients superimposed on the utility voltage can be divided in two different forms, namely common mode and differential mode as shown in Figure 3.2. Differential mode is sometimes also referred to as normal mode or transverse mode.

3.3.1 Differential mode (Normal mode or Transverse mode)

In the case of a DC power supply, differential mode (DM) signal appears between the positive or negative rail and its return current path. For a case of AC supply line, DM signal appears between live wire and accompanying neutral line. These two lines represent the normal path of power through the electric circuits, which gives any normal-mode signal a route into sensitive components [20].

3.3.2 Common mode

Voltage differentials that appear between the ground and either of the two supply lines can be termed as the common-mode (CM) signals. Digital logic or analogue signals are either directly or capacitively tied to the safety ground as a zero-voltage data reference point for semiconductors. Transient CM voltage differences as small as 0.5V can cause that reference point to shift momentarily causing malfunctioning of the semiconductor chips. Hence common-mode transients are most often the cause of disruption [20].

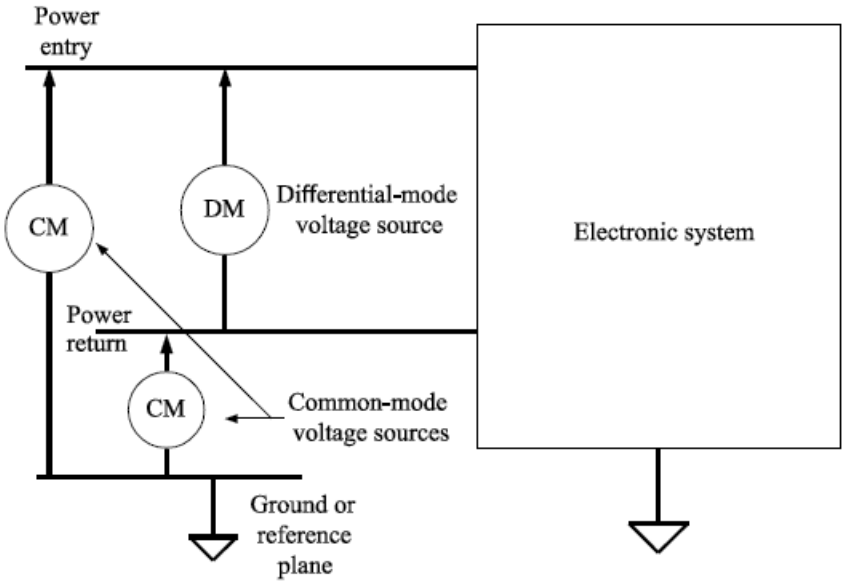

Fig 3.2 Common mode and Differential mode surges [20]

3.4 Lightning Surge Simulator

All surges supplied during the project were generated by Noiseken LSS-6110 lightning surge simulator. Like any other power supply it has a very low internal resistance, approximately 2Ω and can generate high voltage transients up to 6.6 kilovolts with maximum current up to 3.3 kiloamperes. Surge simulator takes 20 seconds time interval between two consecutive surges. This time interval is the time taken to charge the capacitor completely which is internal to LSS. Appendix B shows the MATLAB code written to estimate the open circuit voltage waveform and short circuit current waveform along with average and maximum energy generated by the LSS. Figure 3.3 is the image of Noiseken LSS-6110 lightning surge simulator.

Fig 3.3 Lightning Surge Simulator

3.4.1 Equivalent Circuit of Lightning Surge Simulator

Capacitor C_1 in the LSS can be charged to any value from 100V to 6.6kV in 100 volts steps with time interval of 20 seconds. When switch S_1, a mercury relay discharge switch, is closed, the capacitor C_1 discharges through the wave-shaping circuit to produce the required open-circuit voltage across R_3. Figure 3.4 shows the equivalent circuit of the Noiseken LSS – 6110 surge impulse generator.

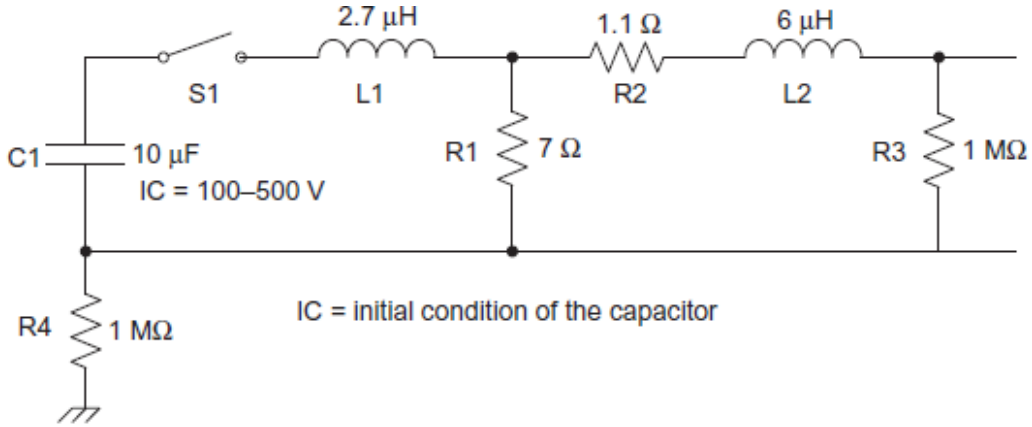

Fig 3.4 Equivalent circuit of the Noiseken LSS – 6110 Impulse generator [21]

3.5 Surge Waveforms (1.2/50 μs voltage and 8/20 μs current)

The IEC 61000-4-5 standard specifies a combination wave consisting of two waveforms, open circuit voltage waveform and short circuit current waveform. These impulse waveforms are defined by their rise time and half amplitude duration. 8/20 μs current waveform has 8 μs rise time from 10% of the peak current to 90% of the peak current. The 20 μs decay time is measured between half amplitude points [21].

An open circuit voltage waveform and a short circuit current waveform combination is defined as the standard waveform to represent high energy transients.

Figure 3.5 represents open circuit voltage waveform which has a rise time, T_r, of 1.2 μs and the decaying curve reaches 50% of the peak voltage in 50 μs. The T_r is measured using the 30 % to 90 % of peak voltage rise time, t_1, as in Figure 3.5; t_1 should be multiplied by 1.67 to get the total rise time, 1.2 μs [21].

Open circuit voltage waveform can be represented mathematically

$$V(t) = A_V V_P (1 - e^{-t/\tau_1}) e^{-t/\tau_2} \quad (3.1)$$

Where $A_V = 1.037(\mu s)^{-3}$; $\tau_1 = 0.4074$ μs; $\tau_2 = 68.22$ μs and V_p is the peak voltage

When the voltage waveform is short circuited, it creates a current waveform as in Figure 3.6. The rise time of the current waveform is 1.25 times (t_{90} - t_{10}) which is 8 μs. The line passing through the 10% and 90% current points cuts the zero current axis at t_0 which is the virtual origin. The decaying curve reaches 50% of the peak current at time t_{50}. The difference (t_{50}-t_0) of the standard current waveform is 20 μs. This waveform is called 8/20 μs combination current waveform because of the 8 μs virtual front time and the 20 μs time to half value [21].

The mathematical representation of the standard short circuit current is given by,

$$I(t) = A_I I_P t^3 e^{-t/\tau} \quad (3.2)$$

Where $A_I = 0.01243\ \mu s^{-3}$, $\tau = 3.911$ μs and I_p is the peak current

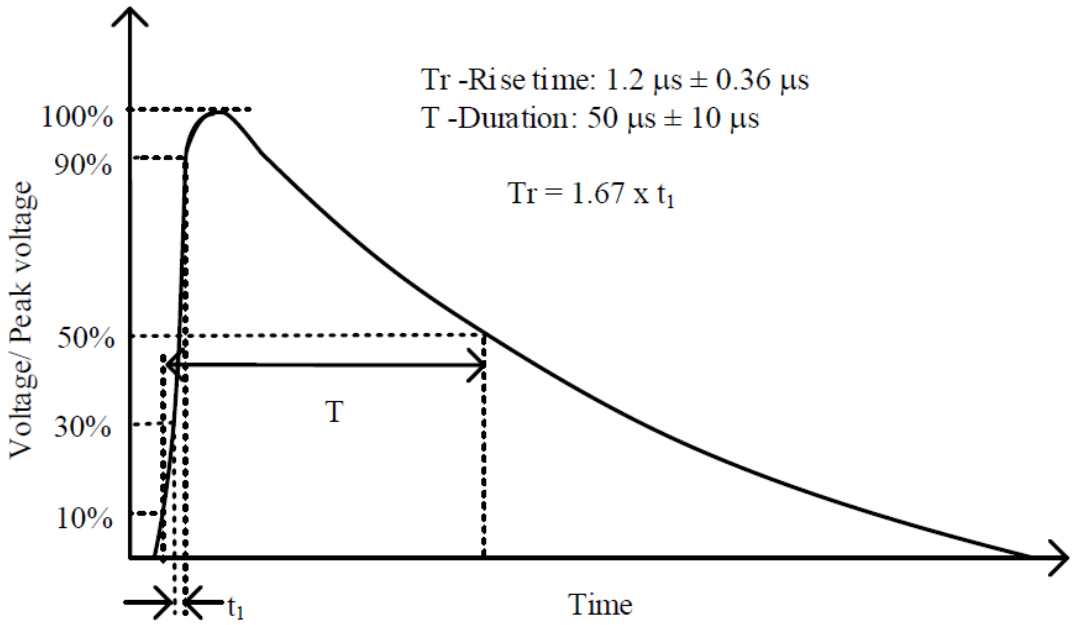

Fig 3.5 Open circuit voltage waveform [21]

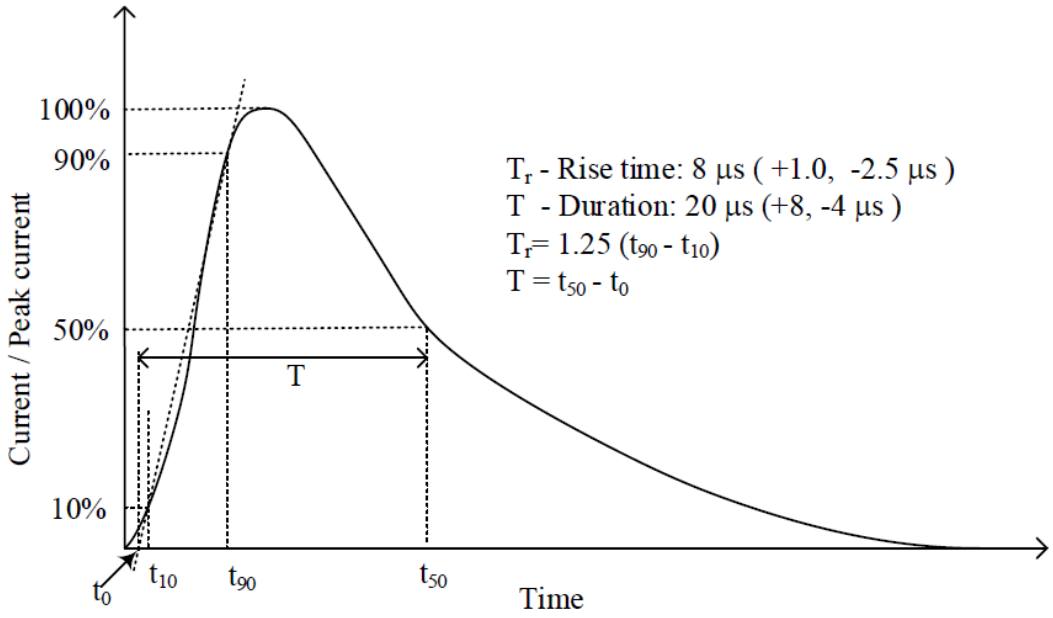

Fig 3.6 Short circuit current waveform [21]

The above-mentioned waveforms do not exactly match with the waveforms generated by the laboratory lightning surge simulator (LSS). This is due to the tolerances of components in pulse generating circuits and parasitic inductances and capacitances in the components of both the LSS and the test units.

When a surge test is performed, the voltage and the current waveforms change with the equipment under test (EUT). Due to this reason, the combination wave

open circuit voltage waveform and combination wave short circuit current waveform parameters were not defined with the EUT.

3.6 Traditional Transient Suppression Devices

Transient Voltage Surge Suppressors (TVSSs) or Surge Protection Devices (SPDs) are designed to protect electronic equipment from high voltage surges. Transients cause the system failure and hence transient suppression plays an essential role in electronic system protection. In most surge protectors, nonlinear electronic components divert the extra energy associated with high voltage transients. Two different technologies based on the type of operation are commonly used: “crowbar type” SPD and “clamping type” SPD. When a transient surge occurs, crowbar type device offers a short circuit path diverting the large surge current to ground and forcing a voltage nearly equal to zero volts. Crowbar action will automatically return to normal operation when overvoltage condition is passed. These devices behave in breakdown region and have only two states, high impedance state and low impedance state. Clamping type devices have variable impedance depending on current flowing through device or voltage across its terminal in the moment of surge. Clamping devices start conducting when surge voltage exceeds their breakdown voltage allowing most of the surge current to pass through, maintaining the clamping voltage across the terminals. Surge absorbing components of SPD have a highly variable nonlinear resistance. These non-linear devices offer very high resistance typically in the order of GΩ in no-surge scenario and the in case of surge their resistance drops down to few ohms typically in the range of 1-10 Ω. Crowbar and clamping action with respect to surge voltage is demonstrated in Figure 3.7.

There are two basic types of transient suppressor:

(a) those that attenuate transients and block the propagation to the critical device
(b) those that divert the transient away from the sensitive load while limiting the residual voltage

Low pass filter is inserted in series with the critical load to attenuate the high frequency transients and allow the low frequency power flow without any disruption. Selection of these TVSS devices depend on the location, clamping voltage and the response time.

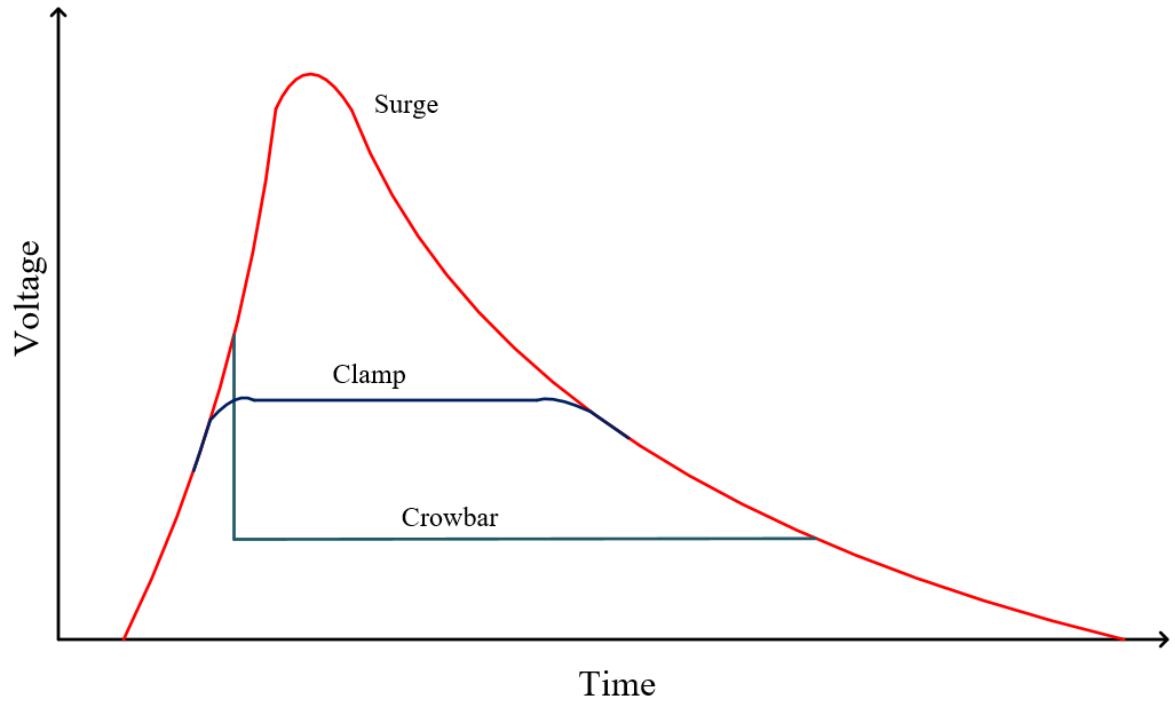

Fig 3.7 Crowbar and Clamping action

The most common nonlinear devices used are metal oxide varistors (MOVs), TVS thyristors and avalanche-type back-to-back TVS diodes. MOVs and avalanche type back-to-back TVS diodes are voltage-clamping devices whereas thyristors and gas discharge tubes are classified as “crowbar” devices.

Each of these TVSS elements has its own strengths and weaknesses:

(a) The GDT can handle very large surge voltages and currents but has relatively slow response time and has high firing voltage. Lifetime of GDT is very limited.

(b) The MOV has high current handling capability with broad voltage and current spectrum. Gradual degradation in lifetime is observed with surges.

(c) TVS diode has low clamping voltage, fast response time and broad voltage spectrum. It has very long lifetime. Limited surge current rating is main disadvantage of these surge arrestors.

(d) TVS thyristors has high current handling capability and fast response time but narrow voltage range. It has long lifetime but is non-restoring under DC.

(e) Other combinational products may use resistors, capacitors, inductors and/or SCRs in conjunction with these TVSS elements, which make them prone to the respective failure characteristics.

(f) Choke coils are inductors designed to block higher frequencies in an electrical transmission line. They use their property of self-inductance to

attenuate electromagnetic interference and radio frequency interference from power supply lines.

Fig 3.8 Transient surge suppression devices

3.6.1 Metal Oxide Varistor

Varistors are voltage dependent, nonlinear devices primarily composed of Zinc Oxide and dissipate very high levels of transient energy. Therefore, MOVs are typically used for the suppression of lightning and other high energy transients [19]. Figure 3.9 shows the typical V-I characteristic curve of MOV. When exposed to high voltage transients, the varistor impedance changes from a near open circuit to a highly conductive level, thus clamping the transient voltage to a safe level [19]. Potentially destructive energy of the incoming transient pulse is absorbed by the varistor, thereby protecting vulnerable circuit components. MOVs are designed to protect sensitive circuits against external transients (lightning) and internal transients (inductive load switching, relay switching and capacitor discharges) [21].

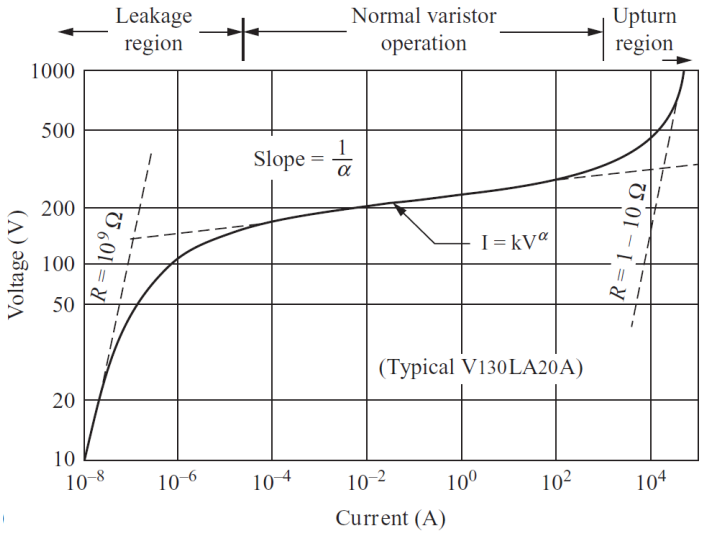

Fig 3.9 Typical I-V characteristics of MOV [19]

3.6.1.1 Equivalent Circuit Model

Figure 3.10 represents the electrical circuit model of the MOV which is useful to explain all the three regions of operation demonstrated in Figure 3.9.

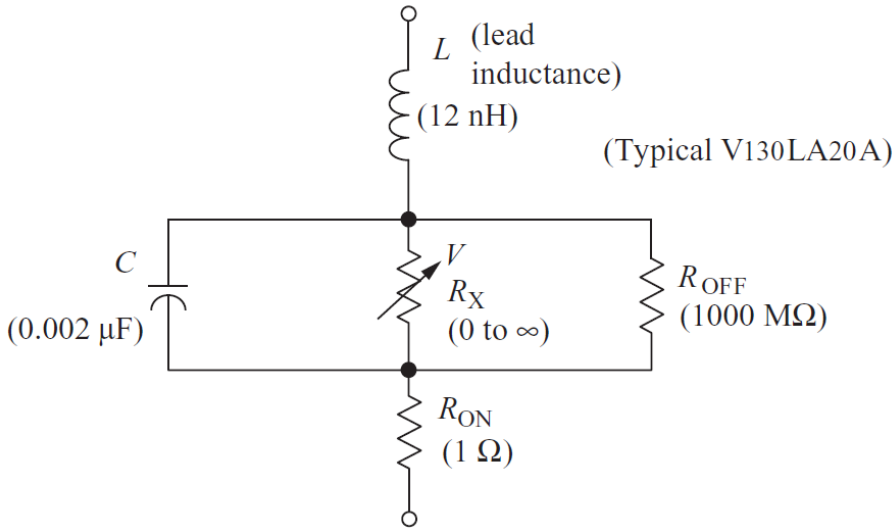

Fig 3.10 Varistor equivalent circuit model [19]

At low currents, the V–I curve approaches a linear ohmic relationship. Under this operating region, MOV is in a very high resistance mode approaching about 1GΩ or higher. Under this near open-circuit condition, nonlinear resistance R_X in Figure 3.10 can be ignored, as R_{OFF} value in parallel will dominate [20]. The resulting equivalent circuit for leakage region is shown in Figure 3.11.

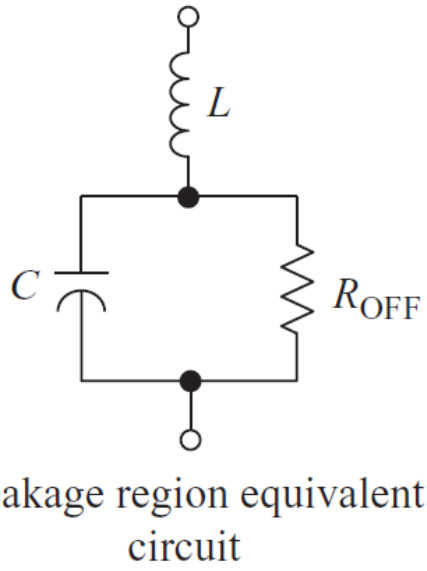

Fig 3.11 MOV in Leakage region [19]

In the normal varistor operation region or in the conduction mode the value of R_X drops down significantly. Due to this effect, now R_X dominates and hence R_{OFF} resistance can be ignored [21]. Equivalent circuit applicable to normal varistor operation is shown in Figure 3.12. At high currents, the nonlinear resistance is in a low-resistance mode approximates to a short circuit. This is represented by R_{ON} which is the bulk resistance of the zinc oxide grains and would be in the range 1–10Ω [19].

High transient energy absorbent capability is achieved by increasing the size of the disc. Typical diameters range from 3 to 20 mm. MOVs turn on in a few nanoseconds and have high clamping voltages. Subjecting a MOV to continuous abnormal voltage conditions, rather than short-duration transients, may cause the MOV to go into thermal runaway, resulting in overheating, smoke, and possible fire. To prevent this condition, many modern MOVs include an internal thermal fuse or a thermal cut-off device [20].

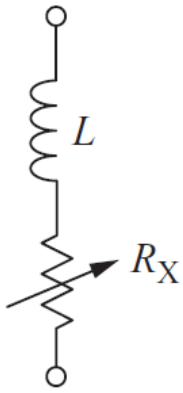

Fig 3.12 MOV in conduction region [19]

3.6.2 TVS diode and Thyristor

Transient voltage suppressor (TVS) diodes and TVS thyristors are the two basic types of solid state surge protection devices. These devices are available as both unidirectional and bidirectional protectors, suitable for protection against positive or negative surges appearing in the power or signal entry inputs. The TVS diode is a clamping device, which suppresses all voltages above its breakdown voltage whereas the TVS thyristor is a crowbar device which switches on when overvoltage rise up to the break-over voltage. A TVS diode behaves similar to a Zener diode but the Zener is designed to regulate a steady-state voltage and the TVS diode is designed to clamp a transient surge voltage [21].

The surge power and surge current capabilities of a TVS is proportional to the cross-sectional area of the p-n junction [20]. A higher cross section allows high-transient currents. Clamping voltage ranges from a few volts to a few hundred volts, depending on the breakdown voltage of the device. Like all clamping devices, it automatically resets when the transient drops below the breakdown voltage, but absorbs much more of the transient energy internally than a similarly rated TVS thyristor [20].

When individual excessive surges occur beyond the rating of the TVS diode, it can fail like any other stressed semiconductor component. For the TVS diode, this primarily involves peak pulse power (P_{PP}) and/or peak pulse current (I_{PP}) [20]. The basic form of failure mechanism is attributable to excessive heat in the active p–n junction of the silicon element. TVS thyristors are solid-state crowbar devices constructed with four alternating layers of p- type and n-type material [20]. The resulting device is capable of handling very high pulse currents. Figure 3.13 demonstrates typical current-voltage characteristics of TVS diode.

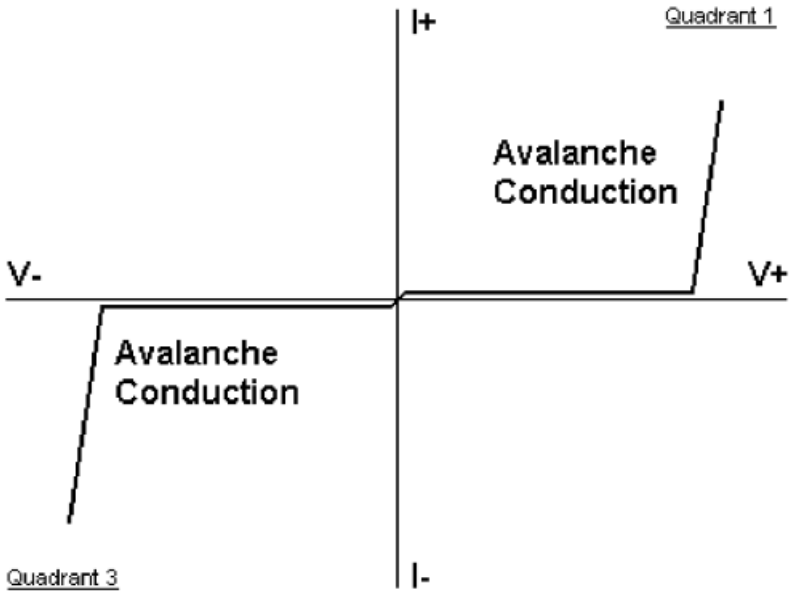

Fig 3.13 I-V characteristics of Bidirectional TVS diode [21]

3.6.3 Gas Discharge Tube

Gas discharge tubes (GDTs) are devices that use inert gases like argon, krypton, neon, or easily ionisable gases in a sealed chamber to ionize and conduct during a transient event [19]. The internal gas requires time to ionize. Gas tubes can take several microseconds to turn on or fire. The reaction time and firing voltage are dependent on the rising slope of the transient [20]. Table 3.1 illustrates and compares characteristics of commonly used surge suppressor devices.

Table 3.1 Comparison of TVS devices [20]

Suppression Element	Advantages	Disadvantages	Expected Life
Gas Discharge Tubes	Very high current handling capability Low capacitance High insulation resistance	Very high firing voltage Non-restoring under DC Slow response time	Limited
Metal Oxide Varistor	High current handling capability Broad current spectrum Broad Voltage Spectrum	High clamping voltage High capacitance Gradual degradation	Degrades over time
TVS diode	Low clamping voltage Broad voltage spectrum Does not degrade Fast response time	Limited surge current ratings High capacitance for low voltage types	Long
TVS thyristor	Fast response time High current handling capability Does not degrade	Does not restore under DC Narrow voltage range Turn-off delay time	Long

3.6.4 LC filter

Practically all typical SPDs have LC filters combined with NLDs such as MOVs and bipolar breakdown devices (BBDs) to more effectively divert and absorb the

surge energy. If a surge is considered to be a 5–100 μs transient event having shapes discussed in Section 3.5 then the transient can be termed as a combination of sinusoids of frequencies in the range of 10–200 kHz with their higher-order harmonics [19]. Impedance of an inductor is given by $2\pi fL$ and the impedance of a capacitor is $1/2\pi fC$ which together filters out the high frequency harmonics present in the transient surge waveforms along with more series impedance offered by an inductor with capacitor providing a path of less impedance to high voltage transient. For example, a 10 μH inductor will provide an impedance of 3.14 mΩ at 50 Hz compared with an impedance of 6.28 Ω at 100 kHz. Similarly capacitor of 100 μF will offer an impedance of 31.84 Ω at 50 Hz compared to impedance of 15.92 mΩ at 100 kHz.

3.7 Selection of surge protecting components

Given below are some criterions that should be taken into consideration while selecting TVSS component.

(a) What voltage levels of TVSS are expected?
(b) What current levels of TVSS are expected?
(c) What is the maximum energy rating of the TVSS component?

While selecting the surge protecting component following properties has to be considered.

3.7.1 Reverse standoff voltage (V_R)

This voltage should be equal to or greater than the peak operating level of the circuit to be protected. This is to ensure that the SPD does not clip the circuit drive voltage.

In the case of a uni-directional TVS diode, this is the maximum peak voltage that may be applied in the 'blocking direction' with no significant current flow. In the case of a bi-directional transient, it applies in either direction.

3.7.2 Breakdown voltage (V_{BR})

Voltage at which device starts conducting heavily is termed as breakdown voltage. Device offers very low resistance when fired and hence absorbs most of the surge energy protecting the circuit from surge destruction.

3.7.3 Clamping voltage (V_C)

This is the peak voltage which will appear across the device once fired and once subjected to peak pulse current. In the presence of surge, device starts conducting heavily providing a near constant voltage across its terminal. This voltage is

termed as the clamping voltage of the device. Lower clamping voltage provides better protection.

3.7.4 Peak pulse current (I_{PP})

Maximum current allowed to pass without any damage to the suppressor for a single standard test impulse. Surge currents exceeding that value will be passed to the protected equipment.

3.7.5 Energy rating/absorption

This rating, in joules, indicates the amount of energy the device can absorb before it fails. A higher number indicates better protection.

3.7.6 Response time

Surge protectors do not function immediately when subjected to a transient surge. The time required to turn 'ON' the SPD and conduct current through the voltage clamping device when exposed to a transient is known as response time. Surge protection devices with longer response times pass the transient voltage to the critical load connected to the power line and will be exposed to the surge for a greater amount of time.

3.7.7 Lifetime

Number of transients of specified voltage, rise time, and duration that the SPD can survive before the threshold voltage changes by more than a specified amount is defined as the lifetime of SPD.

3.8 Design Concept for Surge Protection

High voltage power line transients can be generated due to lightning, electrostatic discharge (ESD), switching transients, inductive kickback, short circuits and faults in power lines. A high voltage transient can be of either positive or negative polarity and can be additive or subtractive from the normal power line waveform. Despite the short duration (in microseconds) of the surge, it can damage equipment or other loads connected to power lines. Surge protection device (SPD) limits the surge energy passing to the protected load, to a minimum level, such that the load is not damaged [21].

In developing surge protection circuits, the designer has to ensure that;

(a) surge arrestor stages do not alter the normal operation of the power conversion circuit

(b) components used for surge absorption, diversion, or attenuation should be able withstand the surge

Reliability of the surge protection system is also important, because a very high-level surge might destroy the surge arrestor components.

All SPD circuits basically work as voltage dividers. Figure 3.14 illustrates this principal with a series impedance, Z_S, and a load impedance, Z_L. The series impedance, Z_S, represents path resistance i.e. resistance due to wirings and internal resistance of the transient source. When there is no protection as in Figure 3.14(a), the input surge voltage gets divided among the two impedances Z_S and Z_L. Z_L is very much greater than Z_S, hence a higher voltage is developed across the load which causes the damage. As depicted in Figure 3.14(b), a blocking device with impedance Z_{block} is inserted in series. With increasing frequency, impedance of this blocking element increases developing a voltage across Z_{block} and hence the voltage at load reduces. When a shunting SPD component is used as per Figure 3.14(c), it decreases its impedance, Z_{shunt}, during the event of a high-voltage transient; short circuiting the surge current and dissipating the surge energy [19].

An ideal SPD must limit the surge energy passed to the load to a minimum level such that the load as well as the SPD are not damaged. The energy passing to the load can be found using the integral of the surge voltage and current, $\int v\, i\, dt$. A practical SPD should develop a lower instantaneous voltage across the load (clamping voltage) to limit the current passing to the load [19].

It is important that series blocking device should offer more impedance and shunting device should offer less impedance with increasing frequency components to absorb maximum surge energy. Hence inductor is connected in series and capacitor is connected in parallel, combination of which acts as a low pass filter and blocks high frequency components.

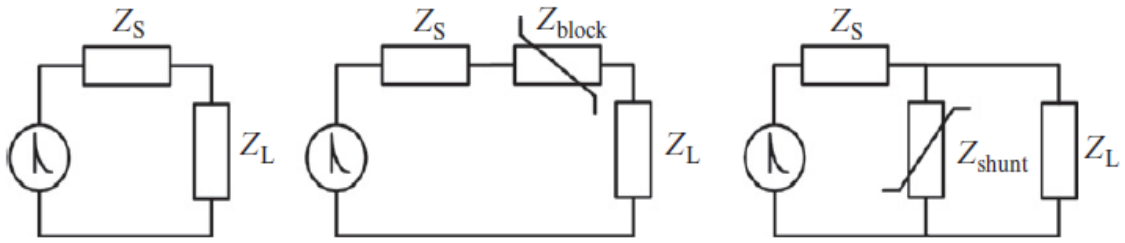

(a) (b) (c)

Fig 3.14 Voltage division with transient surge protector (a) without any protection (b) with series blocking device (c) with shunting device [19]

Transient surges are usually unpredictable and statistical in nature. It is not possible to stop them totally but, in planning engineering facilities, every effort must be made to minimize their effects. Transients that either get induced or enter directly can cause disastrous effects on various end user circuits. Protection of circuits against transients is based on two main principles: (a) limiting the amplitude of the surge at each component to a safe value, and (b) diverting the surge currents through protection-specific components.

In general, practical circuits developed for surge protection are based on three basic concepts: (1) design the protection circuit separately as an add-on block to the base circuit; (2) attenuate the incoming transient using passive series connected high impedances, or shunt the surge currents via passive low impedance circuits (which act as filters for high-frequency components of the surge); (3) use nonlinear devices such as gas discharge tubes, MOVs, transient voltage suppressor (TVS) diodes or TVS thyristors to divert the surge currents and absorb the transient energy [19].

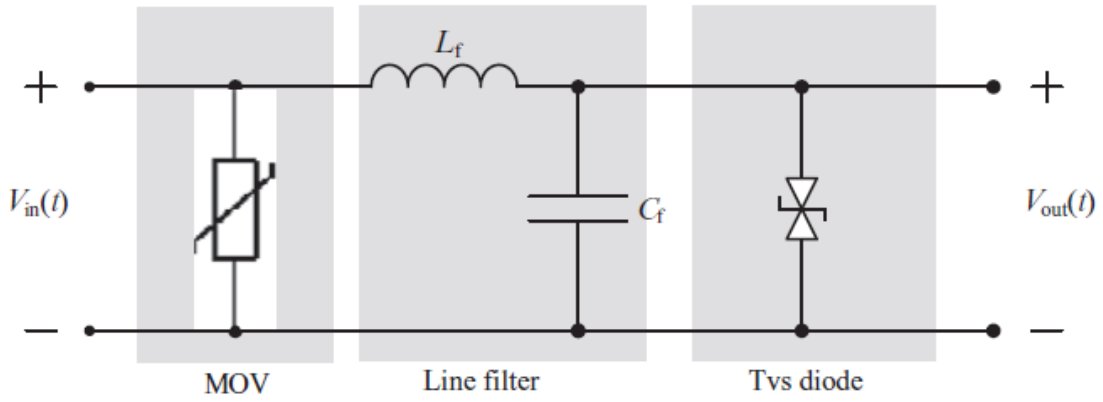

Fig 3.15 Surge protection unit with two level of protection [19]

This circuit in Figure 3.15 uses a MOV for the first level of protection and a TVS diode as the second level of protection. L_f and capacitor C_f form the line filter connected in series for extra safety. The MOV will enter in its firing or conducting state when the transient voltage exceeds break-down voltage thus providing the first level of protection. For very short lived high-voltage transients, the clamping action of the varistors, together with the voltage dropped across the series inductance, holds off the majority of the transient voltage from the output. For more extended stress conditions, the current in L_f will increase to the point where the output capacitor C_f is charged to a voltage at which the TVS diode is brought into conduction. This diode prevents the output voltage from exceeding its rated clamp value for all stress currents up to the failure point of the diode.

Chapter 4

Use of supercapacitors in surge protection and in SCALED system

4.1 Supercapacitors

Supercapacitors are also referred as ultracapacitors or electrical double layer capacitors whose capacitance is million times larger than the normal conventional capacitors and have high power densities with limited energy density compared to conventional batteries. Energy density is the amount of energy stored per unit mass and power density is maximum amount of power that can be delivered per unit mass. DC voltage rating of these capacitors is very low and have very low ESR. More interestingly, ESR of SCs reduces as the capacitance value increases. Their ESR remains relatively constant over the discharge period and throughout the life span. Figure 4.1 shows supercapacitors with same voltage rating but different capacitances of Maxwell family. Figure 4.2 depicts the comparison between the internal resistance of Eclipse 6V battery and ESR of 3.3F supercapacitor with depth of discharge. Supercapacitors can be charged and discharged at much higher currents. Theoretical maximum output current can be given by V_{rated}/ESR. According to Ohm's law, an electric current flowing through the circuit causes a voltage drop across resistive components in the circuit; energy is lost by dissipation of power across these components which is usually in the form of heat. Power dissipation across the ESR warms up the SCs. Overheating of SCs can lead to increased ESR, gas generation, decreased lifetime, leakage and rupture. Based on the formula $E = \frac{1}{2}CV^2$, supercapacitors' extremely high capacitance values theoretically allow them to absorb large amounts of energy.

Fig 4.1 Different Super Capacitors of Maxwell Family [30]

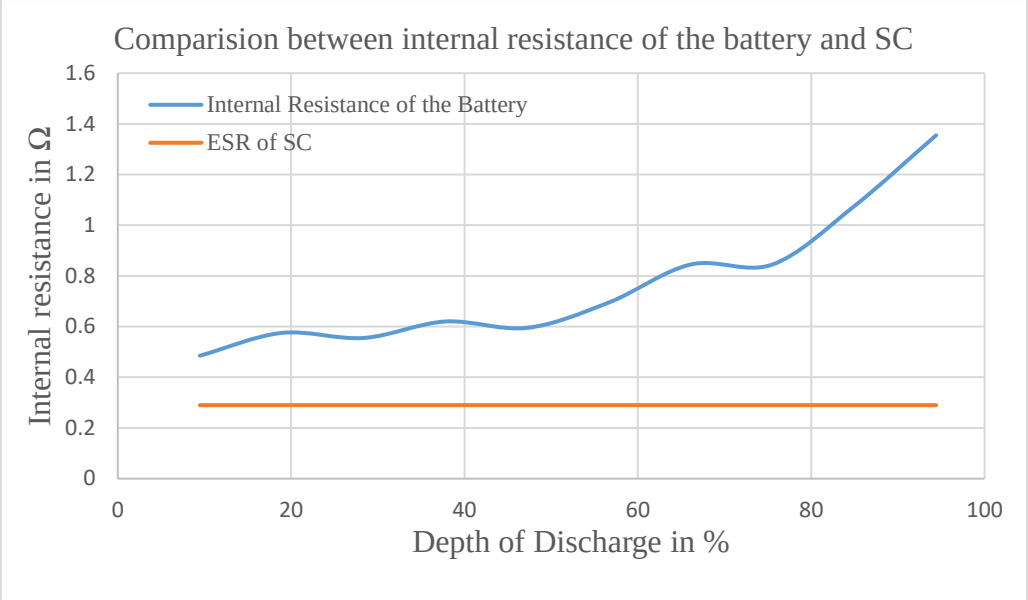

Fig 4.2 Internal resistance of non-rechargeable carbon zinc Eclipse 6V lantern battery and SC with Depth of Discharge

The comparison between energy density in Watthours per kg (Wh/kg) and power density in Watts per kg (W/kg) explains exactly where each ESDs stands on the graphical plot commonly known as a Ragone plot, as shown in Figure 4.3. SCs are in the middle of the Ragone plot demonstrating that their energy and power density values lie between those of batteries and electrolytic capacitors.

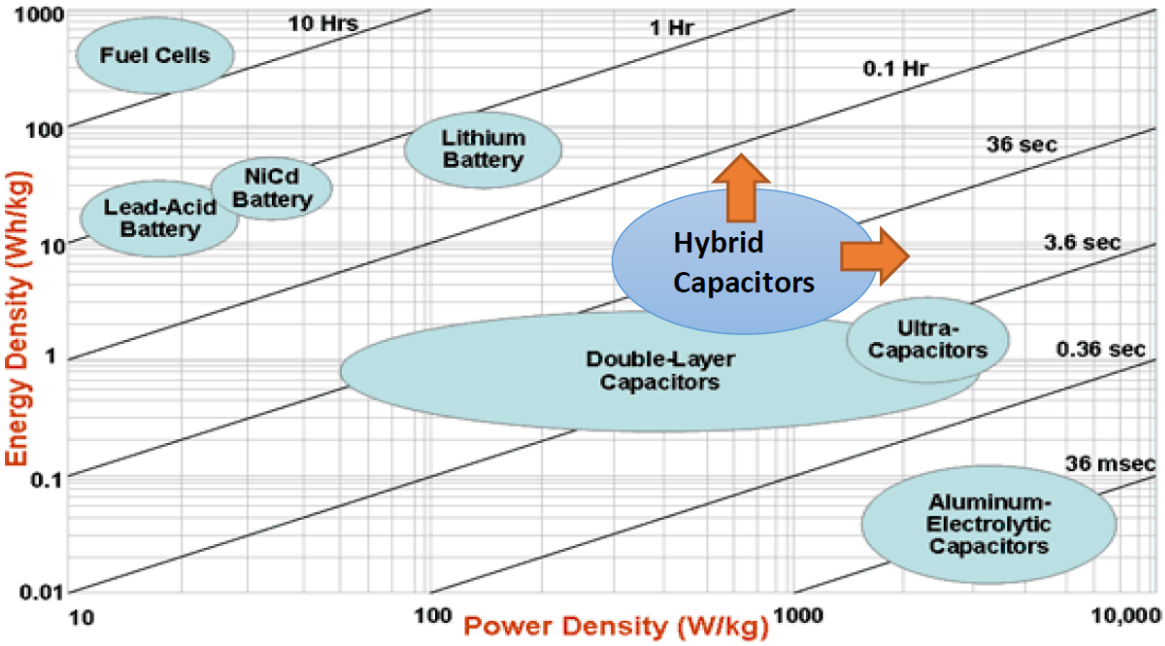

Fig 4.3 Ragone plot for various energy storage devices [35]

4.2 Specifications of SC

Given below are the technical specifications and ratings to be considered before selecting a supercapacitor.

4.2.1 Capacitance

Measurement of energy storage capacity in Joules. Capacitance values for commercial capacitors are specified as "rated capacitance C_R". This is the value for which the capacitor has been designed. The value for an actual component must be within the limits given by the specified tolerance.

4.2.2 Voltage Rating

Maximum operating voltage of the capacitor specified by the manufacturer. Voltage beyond this rating could cause serious damage to SC.

4.2.3 Equivalent Series Resistance

Resistance corresponding to all resistive components within SC. It is comprised of contact resistance, resistance due to electrode, electrolyte and material.

4.2.4 Short circuit current

Maximum current that can be delivered by the SC if its terminals are short circuited.

4.2.5 Leakage current

Stable parasitic current that is expected when SC is held indefinitely on charge at its rated voltage.

4.2.6 Thermal Resistance

This may be used to determine the heat generation within SC at any given current load and duty cycle. This value is based on free convection and would be considered for the worst case scenario. Forced convection would improve the thermal resistance.

4.2.7 Operating Temperature Range

Temperature range specified by the manufacturer within which supercapacitor operates. While a device might technically work between the given minimum and maximum operating temperatures, its efficiency may be greatly reduced at the lower and higher end of the operating temperature range.

4.2.8 Storage Temperature Range

Represents the safe storage temperature without affecting ultracapacitor performance when no voltage is applied to the ultracapacitor.

4.2.9 Endurance Capacitance

The maximum capacitance change expected when the SC is held at rated voltage for a specified life-time and temperature, which is intended to be considered as the upper operational limit.

4.2.10 Endurance Resistance

The maximum resistance change expected if the SC is held at rated voltage for a specified life-time and temperature, which is intended to be taken as the upper operational limit.

4.2.11 Maximum Energy Rating

Energy that could be absorbed by SC when it is charged to its rated voltage from completely discharged state.

4.2.12 Peak Power Density

Measurement of the instantaneous power from full rated voltage V_R to $V_R^2/4R_{AC}$ where R_{AC} is the AC resistance. This value does not represent the sustainable power.

4.2.13 Power density

Gravimetric power density calculated between the ranges of a 20% to 40% reduction in voltage from the rated voltage of SC.

4.2.14 Life Time

Capacitance reductions of over 30% or internal resistance exceeding four times its data sheet specifications are considered "wear-out failures", implying that the component has reached end-of-life. The capacitors are operable, but with reduced capabilities.

4.2.15 Cycle Life

Expected performance change after cycling half to one million times from rated voltage to half the rated voltage. Cycling is to be performed at a duty cycle resulting in no heating of the super capacitor with the SC maintained at 25°C.

4.3 Supercapacitor as circuit element

Figure 4.4 represents circuit schematic of first-order model for a supercapacitor and demonstrates frequency response of the impedance of series RLC circuit. It is comprised of four ideal circuit elements, which include a capacitance C, a series resistor R_S, a parallel resistor R_P, and a series inductor L. R_S is called the equivalent series resistance (ESR) and contribute to energy loss during capacitor charging and discharging. R_P simulates the energy loss due to capacitor self-discharge. It is often referred to as the leakage current resistance. Inductor L results primarily from the physical construction of capacitor and is usually small. Resistor R_P is always much higher than R_S in practical capacitors. Thus it can often be neglected, particularly in high-power applications. In that case, the impedance of the first-order circuit model *Z* is:

$$Z = \sqrt{R_S^2 + (X_L - X_C)^2} = \sqrt{R_S^2 + \left[2\pi fL - \left({}^{1}/_{2\pi fC}\right)\right]^2}$$

Frequency at which impedance of the circuit is purely resistive is termed as resonance frequency given by formula $f = \frac{1}{2\pi\sqrt{LC}}$.

Impedance is purely resistive when $2\pi fL - \frac{1}{2\pi fC} = 0$.

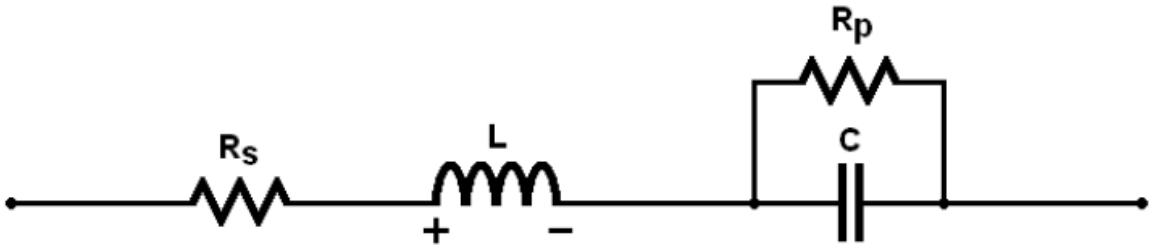

(a)

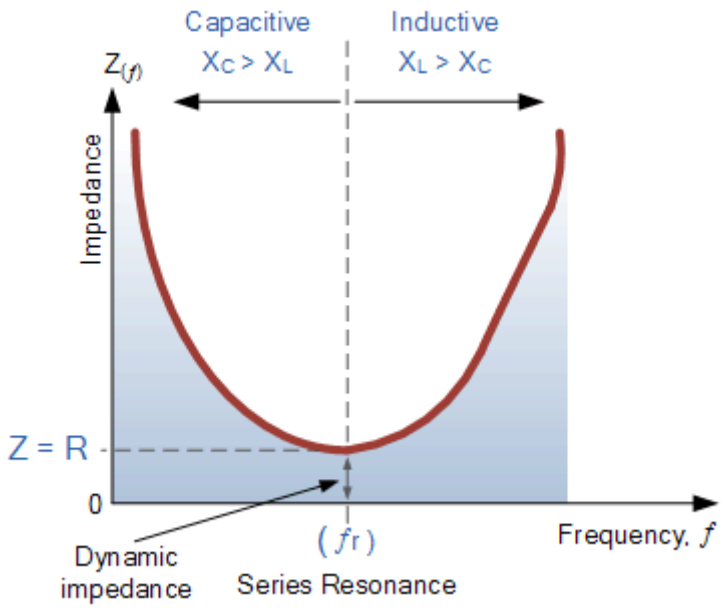

(b)

Fig 4.4 (a) First order circuit model of supercapacitor (b) Impedance vs Frequency graph [36]

4.4 Supercapacitor for surge absorption phenomenon

1 Ω resistor connected in series with the 10 µF capacitor gives the time constant of the 10 µs. When a step DC voltage source is applied to the circuit, capacitor will reach source voltage within approximately five time constants. However, if the DC voltage source lasts for a much shorter time than the circuit time constant then the capacitor will not reach the source voltage and most of the energy flowing through the circuit will be wasted in loop resistance.

Supercapacitors are capable of storing energy in the range of fractional joules to several thousands of joules despite their lower DC voltage ratings. Farad-order capacitances combined with milliohm-order equivalent series resistances provide time constants ranging from fractional seconds to seconds. Time constants of supercapacitors are in the range of 100mS to tens of seconds compared to the time durations of power line transients, which are usually within a few hundred microseconds. Therefore, supercapacitors should be able to withstand short duration high energy surges as these capacitors do not charge fully by the high voltage transients.

Figure 4.5 demonstrates step voltage source connected to RC circuit along with applied step waveform and voltage developed across the SC in the event of surge.

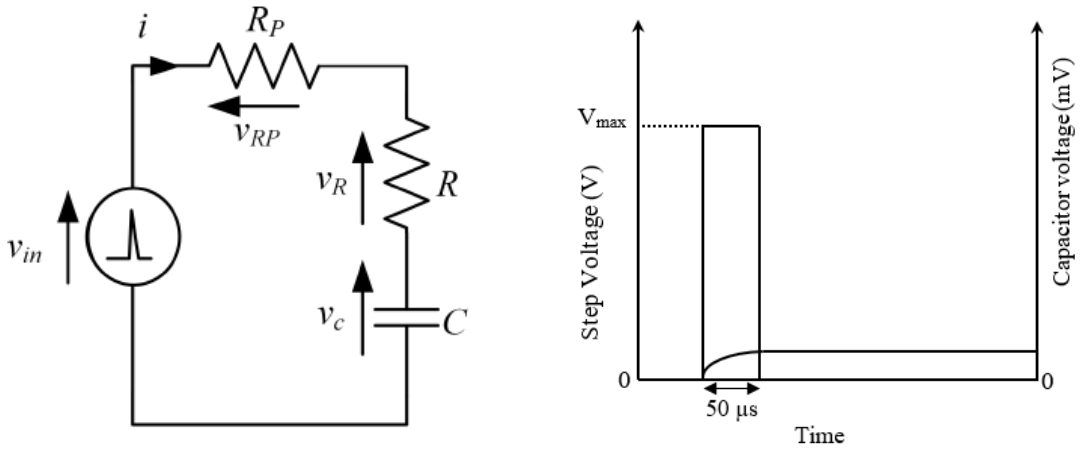

(a) (b)

Fig 4.5 (a) Step voltage applied to RC circuit [19] (b) Step voltage and resulting voltage waveform for supercapacitor

4.4.1 RC loop analysis

To analyse the SC voltage rise, stored energy in SC and energy dissipation across ESR in the occurrence of surge, an experiment was conducted where SC was connected to LSS directly and subjected to high voltage transients. Surges with increasing magnitude were applied to different supercapacitors. Consider Figure 4.5 where high voltage rectangular pulse with voltage V_{SG} is applied to simple RC network for duration T, starting from $t = 0$. Input source voltage, V_{in}, with path resistance, R_p, is connected to capacitor, C, with internal resistance, R. Approximate time constants for capacitor charging will be always much higher than the case of $\tau = RC$ because internal resistance of source and path resistance adds up with ESR of SC. Approximate estimations of the worst-case voltage build up across the capacitor due to a step voltage can be given as,

$$V_C(t) = V_{SG}\,(1 - e^{-t/CR_T}) \tag{4.1}$$

Current flowing through the capacitor can be given as,

$$i_c(t) = \frac{V_{SG}}{R_T}\,(e^{-t/CR_T}) \tag{4.2}$$

Where $R_T = R_P + R$ and V_{SG} is the step pulse voltage.

By applying Kirchhoff's Voltage Law,

$$V_{in} = iR_T + \frac{1}{C}\int_0^T i\,dt \tag{4.3}$$

$$V_{SG} = iR_p + iR + \frac{1}{C}\int_0^T i\,dt$$

Now, the energy dissipated in the ESR is given as,

$$E_R = \int_0^T i^2 \, R \, dt \tag{4.4}$$

Substituting eq^n (4.2) in eq^n (4.4)

$$E_R = \int_0^T \frac{V_{SG}^2}{R_T^2} \left(e^{-2t/CR_T}\right) R \, dt$$

$$E_R = \frac{V_{SG}^2}{R_T^2} \, R \left[\frac{e^{-2t/CR_T}}{-2/CR_T}\right]_0^T$$

$$E_R = \frac{V_{SG}^2 \, C \, R \, R_T}{-2 \, R_T^2} \left(e^{-2T/CR_T} - 1\right)$$

$$E_R = \frac{V_{SG}^2 \, C \, R}{2R_T} \left(1 - e^{-2T/CR_T}\right) \tag{4.5}$$

Energy dissipated across the capacitor is,

$$E_C = \frac{1}{2} \, C \, V_C^2 \tag{4.6}$$

Substituting eq^n (4.1) in eq^n (4.6)

$$E_C = \frac{1}{2} \, C \, V_{SG}^2 \left(1 - e^{-T/CR_T}\right)^2 \tag{4.7}$$

To compare how much energy is dissipated in the capacitor ESR compared to the energy stored in the capacitor, (E_R/E_C) ratio is considered.

$$\frac{E_R}{E_C} = \frac{\frac{V_{SG}^2 \, C \, R}{2R_T} \left(1 - e^{-2T/CR_T}\right)}{\frac{1}{2} C \, V_{SG}^2 \left(1 - e^{-T/CR_T}\right)^2} = \frac{R}{R_T} \frac{\left(1 + e^{-T/CR_T}\right)}{\left(1 - e^{-T/CR_T}\right)}$$

Consider a practical example of an uncharged 3.3F SC with 290mΩ ESR, connected to a 1kV step voltage source for 50µs. Path resistance is 2Ω. Hence the final capacitor terminal voltage, V_C will be,

$$V_C = 1 \, KV \left[1 - \exp \frac{-50 \, \mu s}{(2 + 0.29)\Omega * 3.3 \, F}\right] = 6.61 \, mV$$

During this short duration of 50 µs, the energy stored in the SC is will be

$$E_C = \frac{1}{2} \, 3.3F * (6.61 \, mV)^2 = 72 \, \mu \, \text{J}$$

The energy lost in capacitor ESR

$$E_R = \frac{(1 \, kV)^2 \, (3.3 \, F) \, (290 \, m\Omega)}{2 \, (2.29 \, \Omega)} \left[1 - \exp \frac{-2 * 50 \, \mu s}{2.29 \, \Omega * 3.3 \, F}\right] = 2.76 \, J$$

Energy ratio E_R/E_C is

$$\frac{E_R}{E_C} = \frac{2.76\ J}{72\ \mu J} = 3.833\ \text{X}\ 10^4$$

This shows that a very small voltage is building up on the capacitor while storing small amount of energy during the short duration of the high-voltage rectangular pulse input.

4.4.2 Surges on supercapacitor

Two different capacitors 1F and 3.3F are subjected to increasing surge voltages as per IEEE C62.4X standards from 1kV till 4kV and voltage developed across the capacitor is measured after every 10 surges. Figure 4.6(a) and (b) shows the voltage developed across the capacitor with number of surges. It has been clearly observed that even though the surge voltage is in kilovolts; voltage developed across the supercapacitor is in the range of few millivolts at the end of the surge duration.

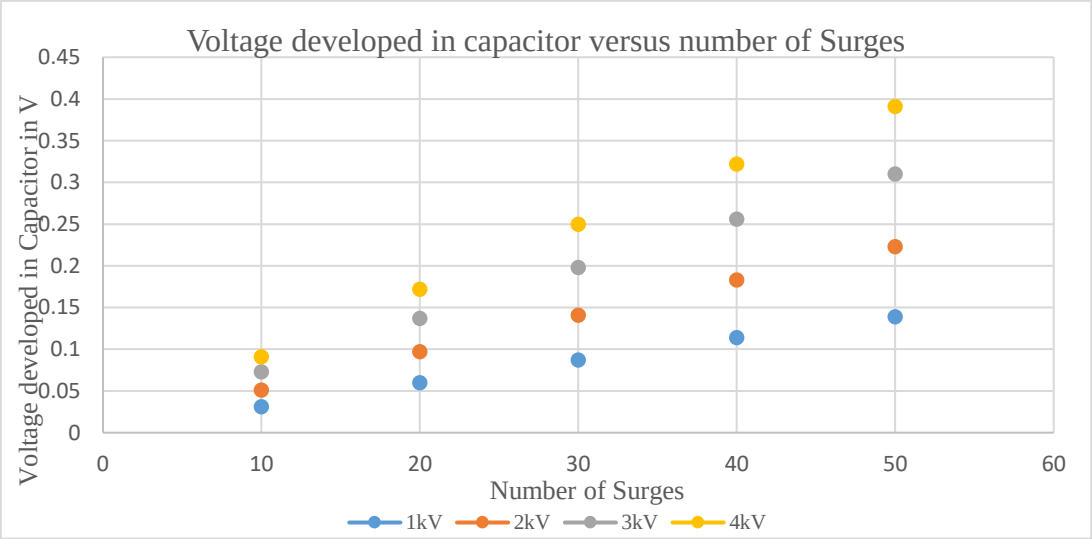

(a)

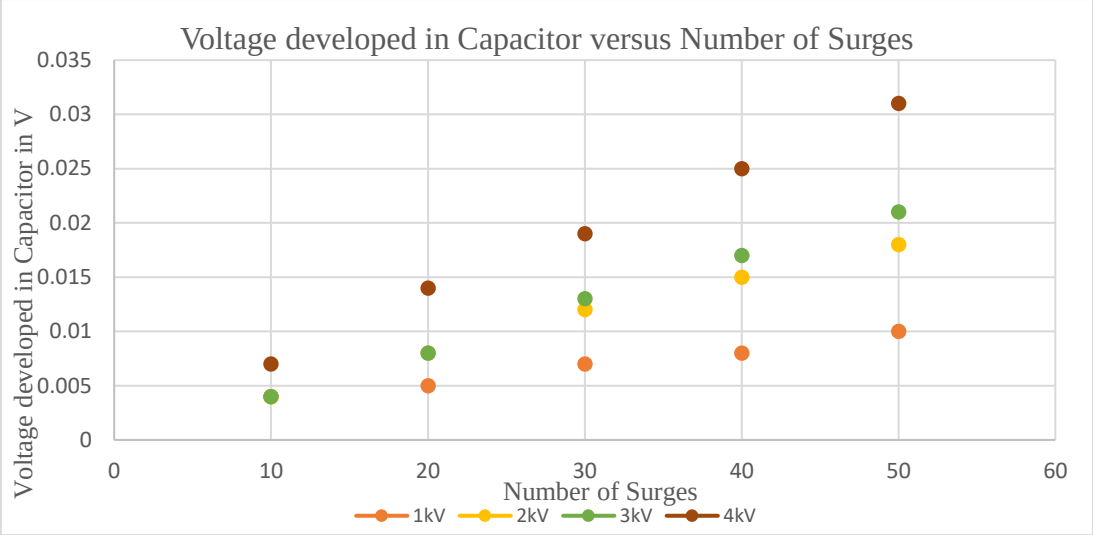

(b)

Fig 4.6 Voltage developed across capacitor with increasing surge voltages (a) 1 F capacitor under surges (b) 3.3 F capacitor under Surges

4.4.3 Surges on Buffer SC bank used in SCALED

It is important to connect energy storage devices such as batteries or supercapacitors to the system which depends on solar energy. This is due to the intermittent nature of this renewable energy resource. SCALED uses solar energy as the primary source of power and therefore to buffer the temporary input energy fluctuations and to provide stable input voltage, SC bank is connected in parallel to the system. In the absence of adequate irradiance, this SC bank keeps the SCALED converter running for short duration (in order of minutes), hence termed as “buffer SC bank”.

LS supercapacitor energy storage devices are positioned between conventional electrolytic capacitors and rechargeable batteries. These are optimized for the highest performance with the lowest resistance possible. LS 16.8V 58F ultracapacitor module has high energy performance and low ESR (22mΩ) to meet energy storage and power delivery requirements. This single SC module is a series connection of various supercapacitor cells for higher DC voltage rating and more energy storage capability.

Figure 4.7 demonstrates a single module of the buffer supercapacitor bank. Four such modules were connected in series comprising total capacitance of 14.5F with total ESR of 88mΩ.

Fig 4.7 58F 16.8V Supercapacitor from LS Mtron [31]

This buffer SC bank is subjected to high energy transients and voltage developed across the bank is calculated from Equation 4.1 where path resistance is 2Ω and ESR of the SC bank is 88mΩ. Figure 4.8 demonstrates the voltage developed across buffer SC bank with increasing surge voltage.

Table 4.1: Readings for surges on Buffer SC bank

V_{surge} (V)	I_{surge} (A)	V_{buffer_SC} (mV)
34.4	36.8	0.5
76	78.4	1.1
118	124	1.7
156	168	2.2
200	212	2.8
240	252	3.4
288	304	4.1
328	344	4.6
376	400	5.3
416	440	5.9
640	720	9
860	960	12.1
1080	1120	15.2
1300	1360	18.3
2160	2400	30.4
2480	2560	35
2640	2720	37.2
2880	2960	40.6

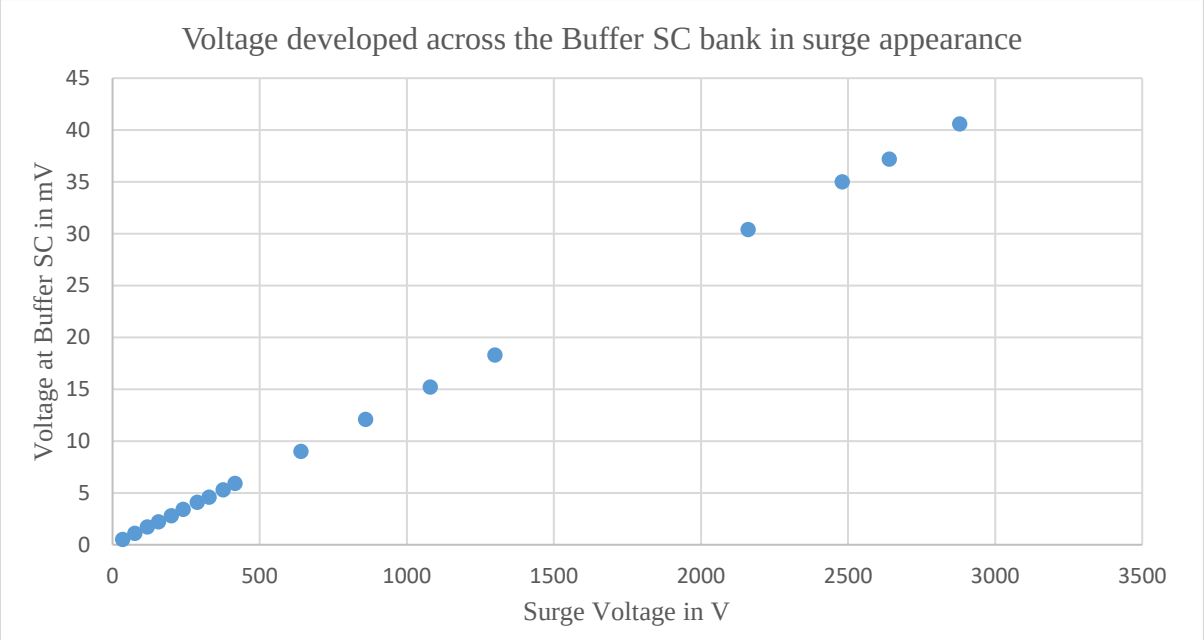

Fig 4.8 Voltage developed across buffer SC in surge condition

From above mathematical analysis and experimental tests performed, it can be said that supercapacitors can be used for surge absorption phenomenon. One good example which makes use of this characteristic property of SC is the patented Supercapacitor Assisted Surge Absorber (SCASA) technique [21]. This unique technique is developed by power electronics research team of University of Waikato.

4.4.4 SCASA Technique

Commercial surge protectors are designed using metal oxide varistors or bidirectional break over diodes combined with inductor-capacitor filters. These devices are rated for short term energy absorption. Figure 4.9 depicts few commercial surge protectors available for inexpensive prices.

Fig 4.9 Commercial surge protectors available in market [37-39]

In many situations of internal transients, worst case conditions can be estimated and the product can be optimized for providing better protection. However in the situation of external transients, peak amplitude and the frequency of the transient cannot be predicted and this makes it difficult to develop a reliable SPD. These

surge suppressors fail frequently due to repeated high voltage surges, when transient energy dissipated exceeds the threshold limit of surge suppressors. Failure of these devices occurs mainly due to the gradual heat-up and damage to the MOVs and other semiconductor type devices used in the circuit. In general, traditional surge protectors are unable to reduce transient load voltage lower than the clamping voltage of the surge suppressor device [21].

SCASA was developed to minimize these issues of surge protector circuits by using [21],

- SC to absorb part of the transient energy superimposed on normal 230 V, 50 Hz AC supply
- Coupled-inductor to transfer part of the transient energy into the SC by which it lowers the transient load voltage

During the event of high voltage surge, a varistor is fired into conduction and triggers the coupled inductor circuit. Part of surge energy is stored in coupled inductor circuit and SC is used to absorb this energy. Figure 4.10 shows the circuit configuration of SCASA technique [21].

Inductors are connected in surge protection circuits mainly in series to the load. An inductor placed in series with the surge absorber, acts as a filter by opposing the quick rise of current (i) through the circuit and drops voltage proportional to di/dt. Therefore a typical surge protector circuit cannot reduce the load voltage below the varistor clamping voltage. Further the energy stored in the inductor can cause oscillations, affecting the load power quality [21].

In the SCASA technique, the coupled-inductor-secondary winding, polarity and placement is arranged in such a way that the instantaneous load voltage is lower than the varistor clamping voltage. By the inductor placement and polarity arrangement of the coupled inductor, as shown in Figure 4.10, it is possible to [21],

- trigger the coupled inductor circuit only at the event of a high voltage transient surge
- reduce the load voltage during the event of a high voltage transient surge
- store a part of the surge energy in the coupled inductor

During the event of surge, part of surge energy gets stored in two inductors of this coupled inductor circuit. To avoid this stored energy propagating towards load side, a closed loop is formed by connecting these two coils through RC sub-circuit [21] as shown in Figure 4.10.

It was proven that SCASA can reduce the transient clamping voltage of a surge protection device designed for 230 V, 50 Hz AC system, by at least 150 V when an IEEE Standard combined surge up to 6.6 kV was repeatedly applied. This increases the life of the SPD by more than 300%. More details on SCASA technique can be found out in references [19, 21].

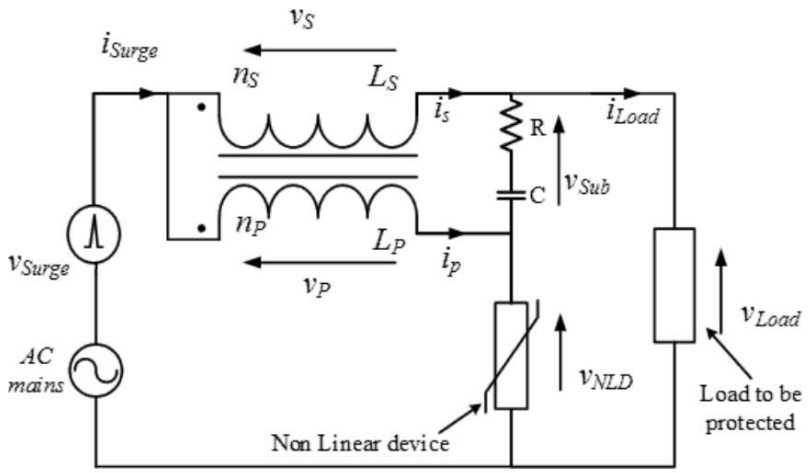

Fig 4.10 SCASA circuit developed at University of Waikato [21]

Figure 4.11 is the image of commercial surge protector “Smart TViQ” built on SCASA concept by “THOR Technologies”.

Fig. 4.11 Commercial product launched in Australian market in 2014 [19]

As a result it can be said that SCASA is a completely new unique technique in the field of surge absorption with its own commercial product. This surge absorber is a part of Supercapacitor Assisted (SCA) techniques which is a family of new SC applications done by power electronics research team at University of Waikato.

4.5 Supercapacitor Assisted LED lighting (SCALED)

Super Capacitor Assisted Light Emitting Diode (SCALED) is one of the SCA techniques developed at University of Waikato, which has led to another novel application in DC microgrid technology. As many domestic electrical appliances operate internally on DC, a locally operated DC microgrid using a renewable energy source such as solar power is a potential alternative to a traditional electricity supply. The concept of recovering significant amounts of energy loss by using a useful load like LED in a capacitor charging loop is a new application, where the SC acts as a lossless voltage dropper in the circuit.

Figure 4.12 depicts charging and discharging phases of SCs and the basic version of SCALED is shown in Figure 4.13(a). Here, four switches are used to partition the LED lamp load with 50% charging and discharging, ultimately leading to an increased overall efficiency of the circuit. The solar PV panel is represented as a constant DC voltage source. As depicted in Figure 4.13(b), PV panel will charge the supercapacitor bank SC2 powering the LED2 when switch S3 is closed, concurrently the other supercapacitor bank SC1 will discharge into the identical LED1 by closing switch S2. Once SC2 charges, it will switch to discharging phase through switch S4 powering LED2 and allowing SC1 to charge through switch S1 powering LED1 as depicted in Figure 4.13(c). This cycle repeats itself to keep the circuit working continuously. Switches are operated through the PIC microcontroller for monitoring the charging and discharging of the supercapacitor banks.

Table 4.2 Switch position and capacitor phases

S1	S2	S3	S4	SC1	SC2
on	off	off	on	charging	discharging
off	on	on	off	discharging	charging

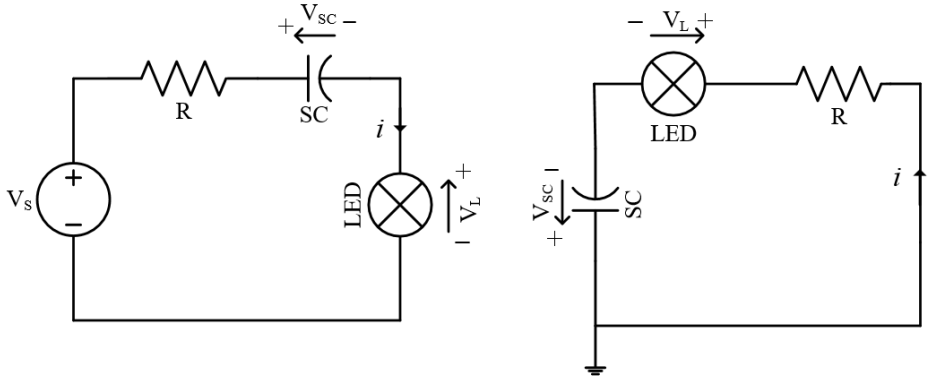

(a) (b)

Fig 4.12 Concept of SCALED system (a) SC charging phase (b) SC discharging phase [18]

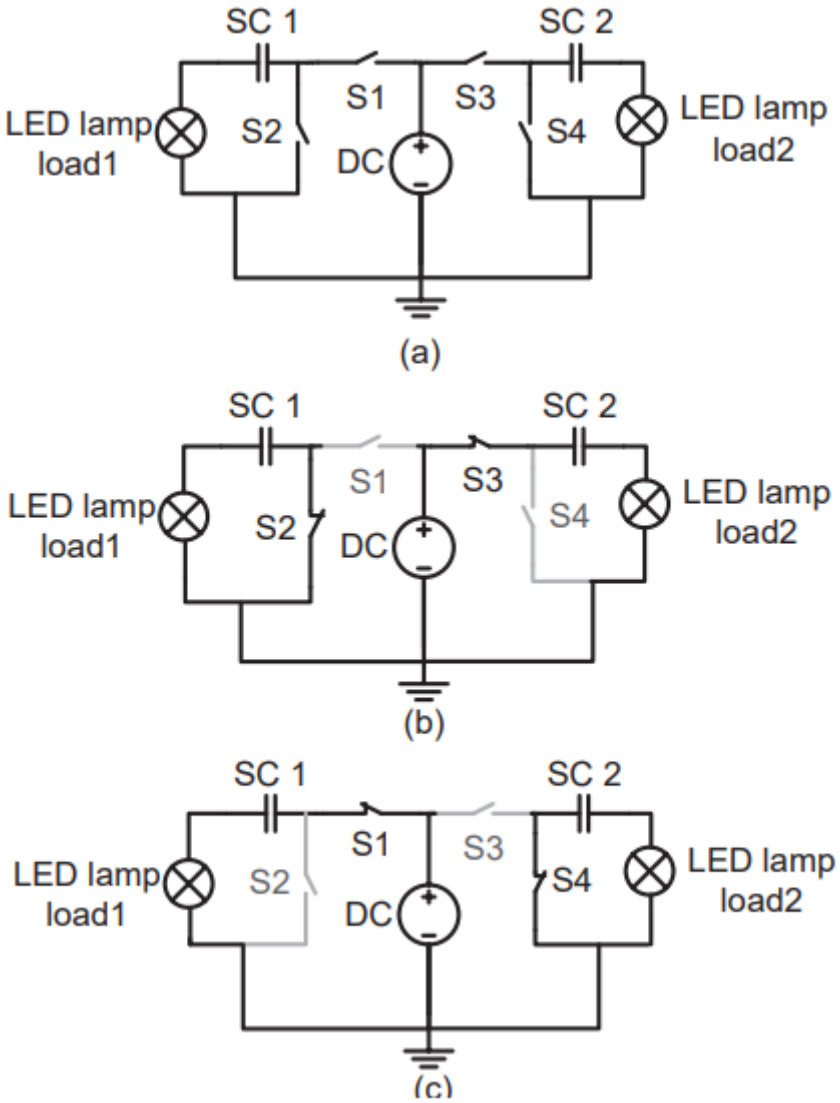

Fig 4.13 (a) Basic version of SCALED (b) Charging phase of SC2 and discharging phase of SC1 (c) Charging phase of SC1 and discharging phase of SC2 [17]

4.6 Block Diagram of SCALED

SCALED mainly consists of two circuit boards namely “Control board” and “Power board”. Control board have different sub-circuits to get the system going smoothly. Power board on the other hand contains switches to control charging and discharging of two supercapacitor banks which power up the LEDs as explained in previous section. These switches are operated by the microcontroller based small circuit on the control board.

Control board is divided into different blocks. Each block along with its function is explained below. Buffer supercapacitor bank is connected in parallel to the PV panel. This buffer SC bank charges initially through PV panel and once charged, circuit is powered by solar panel. Whenever PV panel is not able to supply the required voltage (in cloudy or rainy atmosphere as well as at night times), this

buffer SC bank powers up the circuit. Figure 4.14 demonstrates the overall block diagram of SCALED system and Figure 4.15 depicts insight of start-up and protection block as well as control and feedback network.

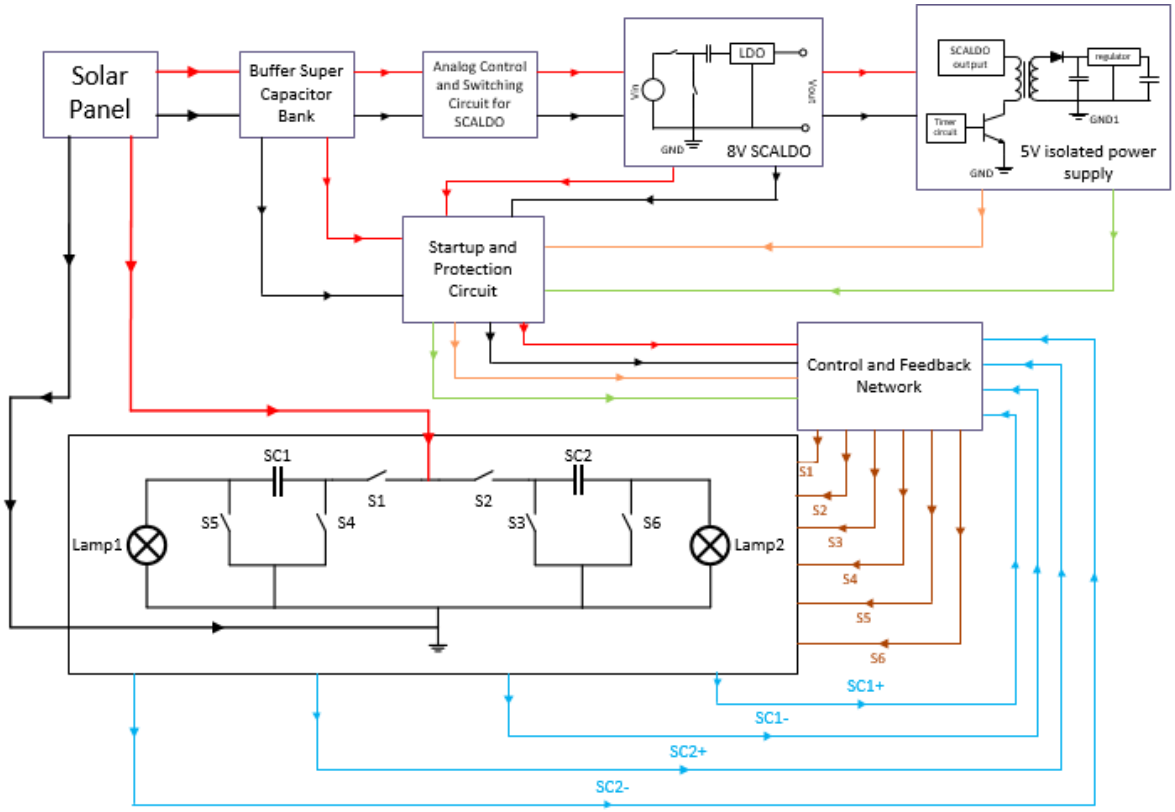

Fig 4.14 SCALED system block diagram

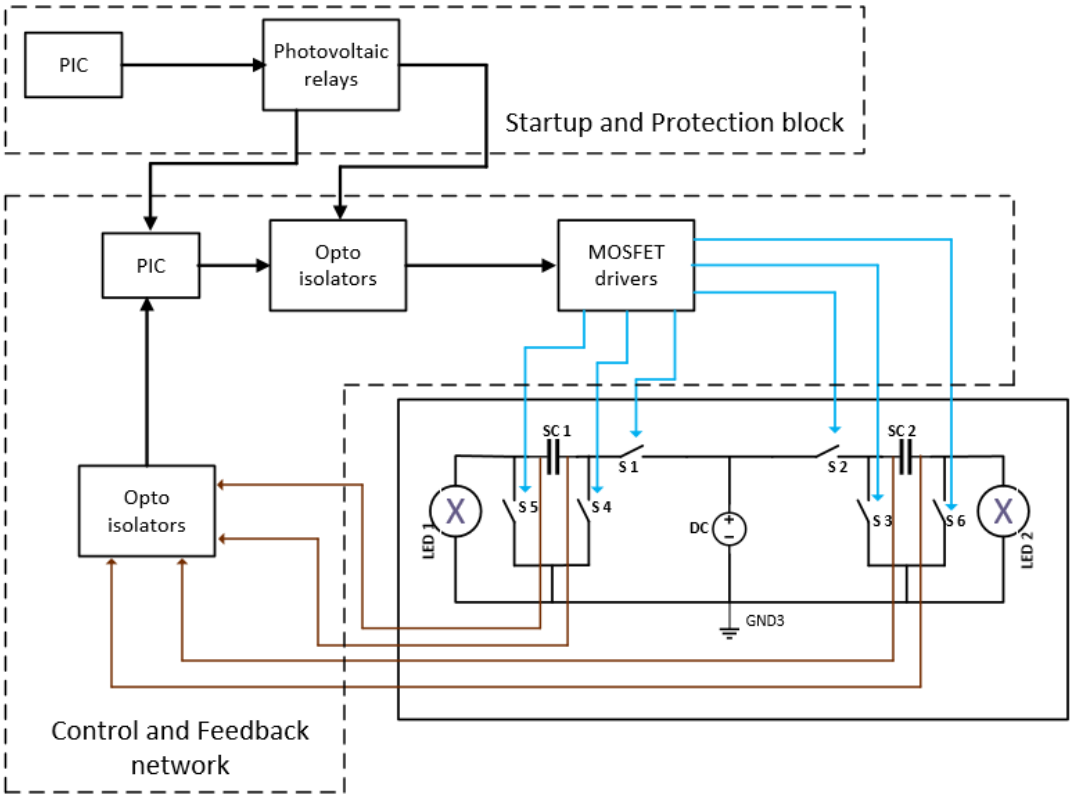

Fig 4.15 Insight of startup and protection block and control and feedback network

4.7 Different blocks in SCALED

4.7.1 Control Board

4.7.1.1 Analog Control and Switching circuit for SCALDO

Block consists of the switching circuitry to monitor the charging and discharging phases of SCALDO. This switching circuit is comprised of photovoltaic relays, operational amplifiers and RS flip-flops.

4.7.1.2 SCALDO

Supercapacitor Assisted Low Dropout Regulator is a technique where SC is placed in series with LDO to increase end to end efficiency of the circuit. Supercapacitor acts as a lossless voltage dropper with LDO acting as useful load, reducing the losses in RC charging loop during the charging phase of the supercapacitor. The energy stored in the SC during the charging phase is reused in discharging phase [18]. Figure 4.16 represents the basic SCALDO technology.

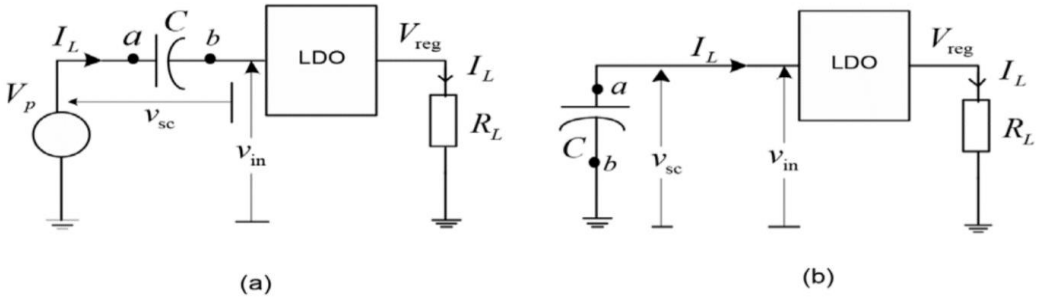

Fig 4.16 Basic concept of SCALDO (a) SC charging phase (b) SC discharging phase [18]

4.7.1.3 5V isolated power supply

Block includes an isolation transformer which provides the secondary Ground; different from the PV panel's ground (primary ground). 555 timer used in Astable mode controls the switching of the transformer through NPN transistor. 5V regulated output is supplied by this block which powers up the PIC controllers in the overall system.

4.7.1.4 Start-up and protection circuit

This block includes a PIC microcontroller which reads the voltage across the buffer SC bank through opto-isolator. It then writes signals to turn on the photovoltaic relays which supply voltages to the another PIC and MOSFET drivers in control and feedback network

4.7.1.5 Control and feedback network

PIC used in this block is different from the previous one. It reads the voltages across the two SC banks connected to power/load board. Depending upon the values read, it controls the switching of these banks through MOSFET switches via MOSFET drivers such that previously charging SC bank will undergo into discharging phase and discharging SC bank will undergo into charging phase.

4.7.2 Power Board

This is a second circuit board of SCALED system to which supercapacitor banks and LED loads are connected. The board has power MOSFETs for switching purposes which controls the charging and discharging phases of these SC banks.

4.8 Operation of SCALED

Two important properties of 12V LED lamps: (i) ability to operate with positive and negative DC voltages, (ii) ability to operate over a wide range of DC voltages

with constant brightness make LED lamps suitable as useful load in SCALED converter as observed in Chapter 2. Initially both the SC banks are charged to 20V and 14V respectively after which normal operation of the SCALED commences where one SC bank keeps charging (SC bank with the voltage of 14V) through LED lamps while the other SC bank discharges (SC bank with the voltage of 20V) to the other LED lamps. When first SC bank is charged to 20V, it will switch to discharging phase while the other bank now switches to charging phase and cycle repeats. Due to the ability of LED lamps to operate within wide range of positive or negative voltages without degradation of brightness, this technique can cope with large fluctuations of solar irradiance. In addition, SC banks are able to provide power to LED lamp loads during low irradiance levels to provide short-term DC-UPS capability. In this converter switches S2 and S4 help to preserve the charge balance of respective SC banks by alternately switching S1 and S3 as a pair. Figure 4.17 (a) and (b) shows voltage waveforms across the SC banks and LED lamps respectively.

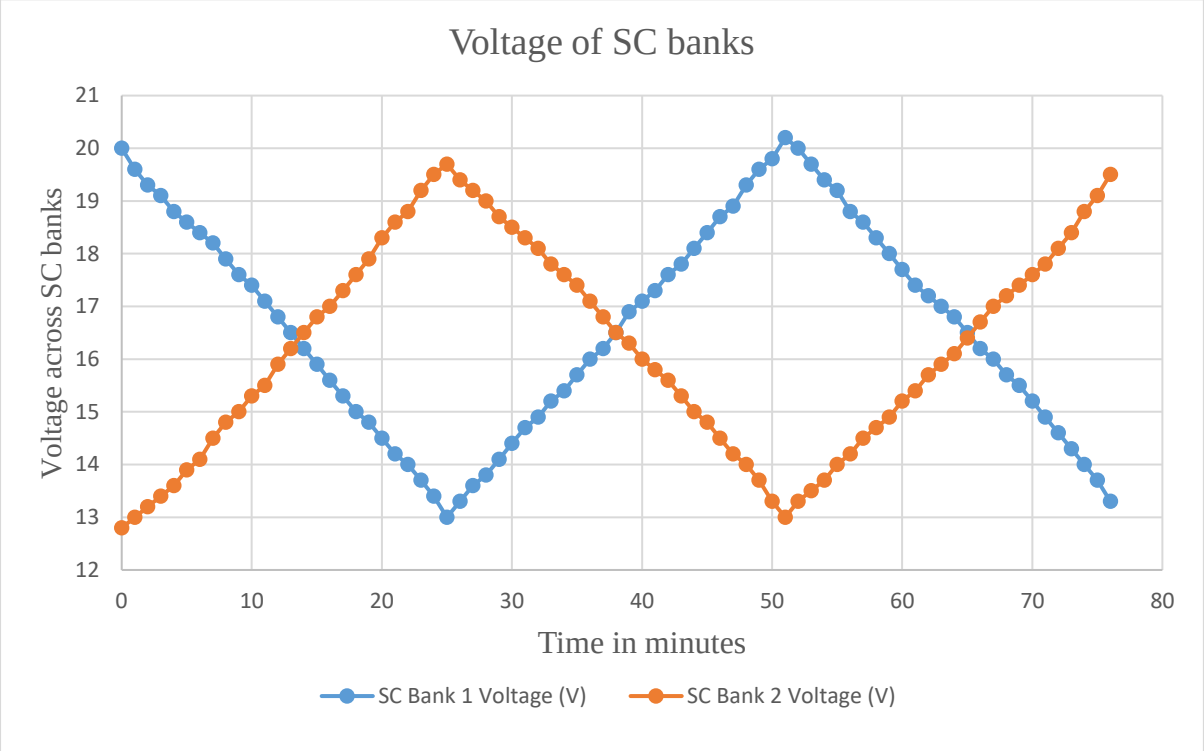

(a)

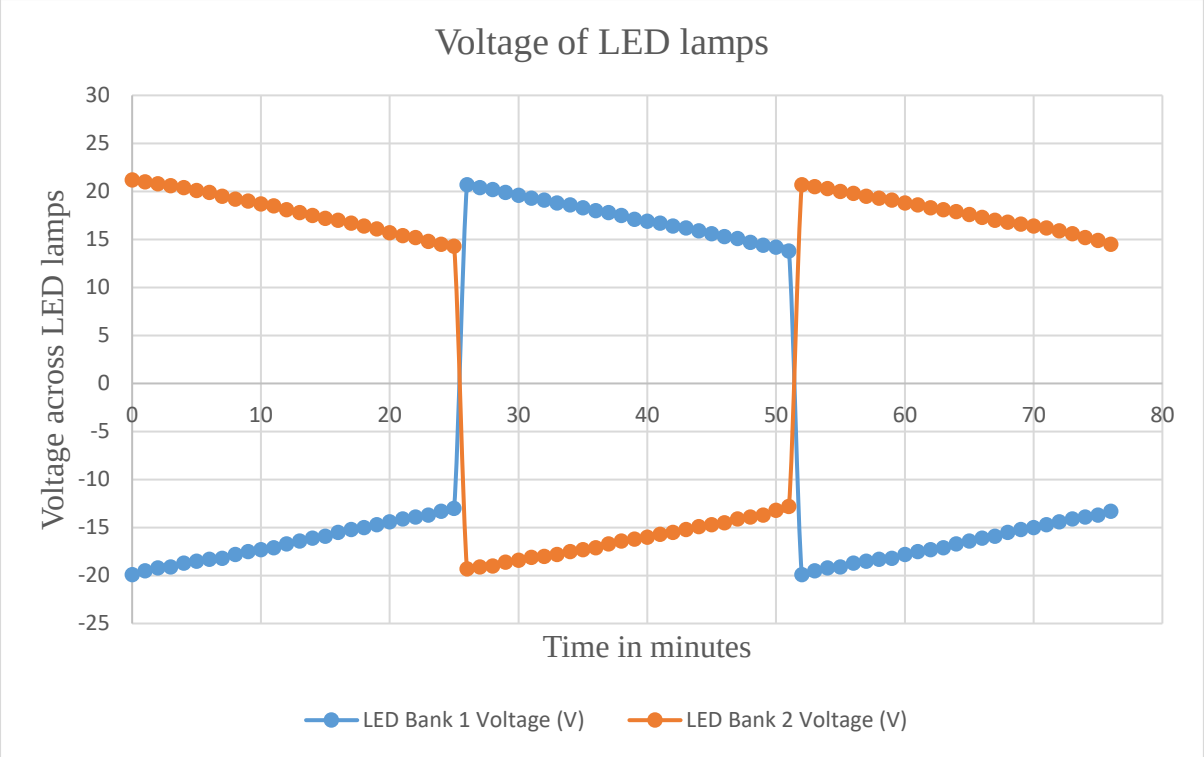

(b)

Fig 4.17 (a) SC bank switching of SCALED converter (b) Voltage across the LED loads

Chapter 5

Effect of surges on SCALED

5.1 Surges on solar PV panel

Before conducting surge testing on SCALED, solar PV panel was subjected to high voltage transients of increasing magnitude. Figure 5.1 depicts the simple connection between LSS and PV panel along with the test circuit diagram.

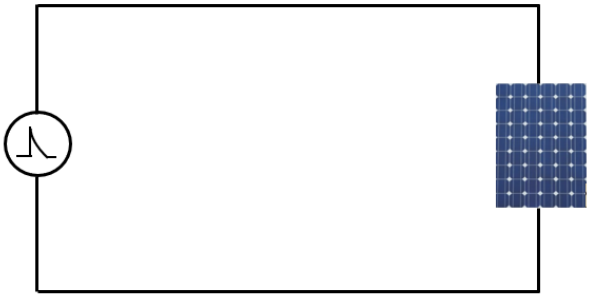

(a)

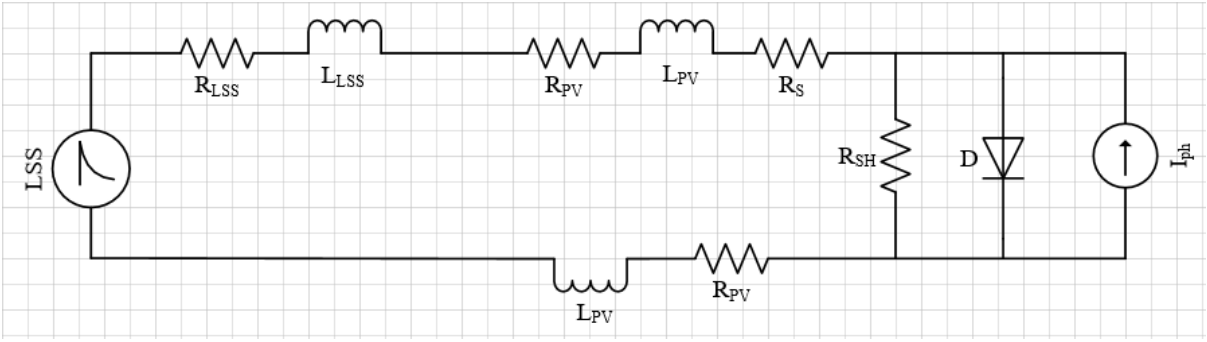

(b)

Fig 5.1 PV panel connected to LSS (a) laboratory test setup (b) circuit connection with PV panel represented by its one diode model along with path inductances and path resistances

Readings for terminal voltage across the PV panel, surge voltage and surge current were recorded. MATLAB code was written to observe the energy sourced by LSS and energy absorbed by PV panel as well as the voltage dropped during the path due to parasitic components was calculated. Appendix C demonstrates readings and the MATLAB code along with the scope images obtained during the experiment and LTspice circuit. Figure 5.2 depicts the transient model of the PV panel. Figure 5.3(a) shows the inductive and resistive voltage drop along the path and Figure 5.3(b) shows energy graphs for LSS and PV panel.

From these graphs it is observed that not all the surge voltage appears across the solar panel as some of it is dropped due to the parasitic components in the path

and surge energy which is not lost during the transmission gets equally distributed over the large surface area of PV panel. Hence even after applying surges, no damage was observed to the solar panel.

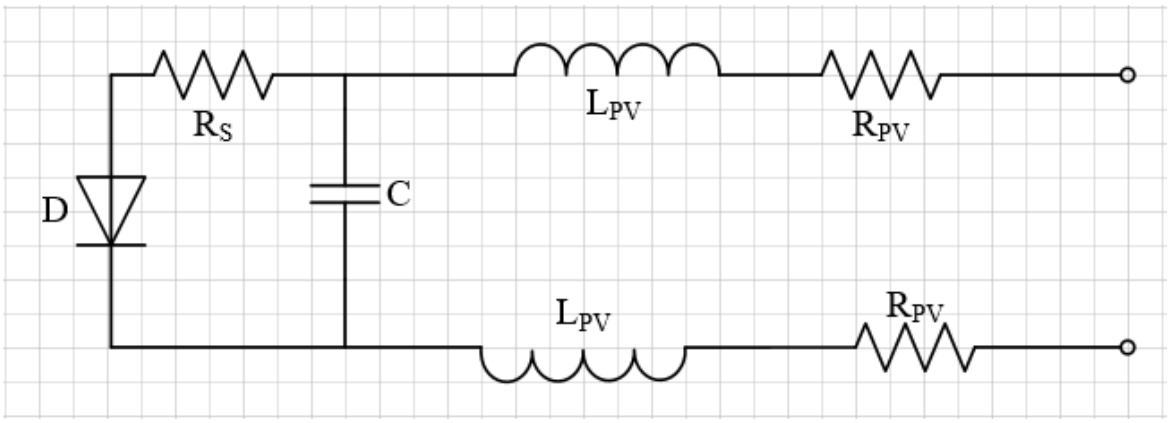

Fig 5.2 Transient model of PV panel

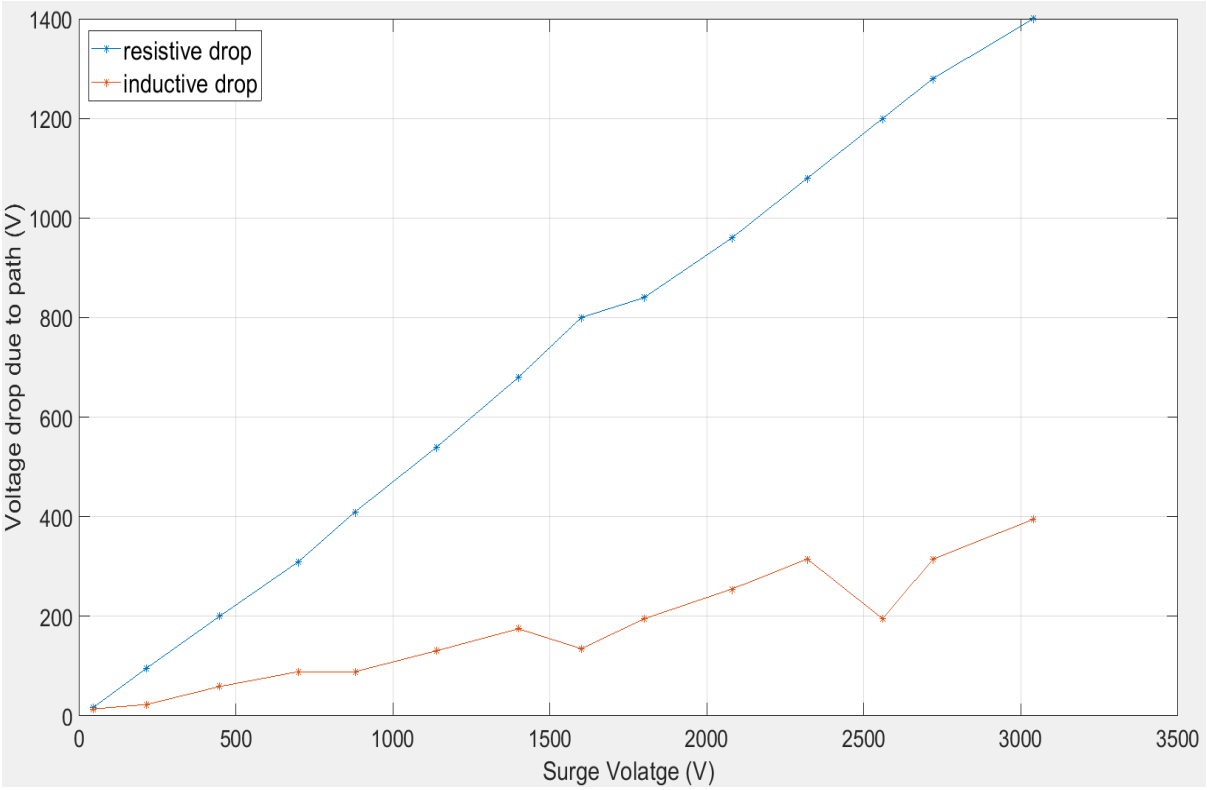

(a)

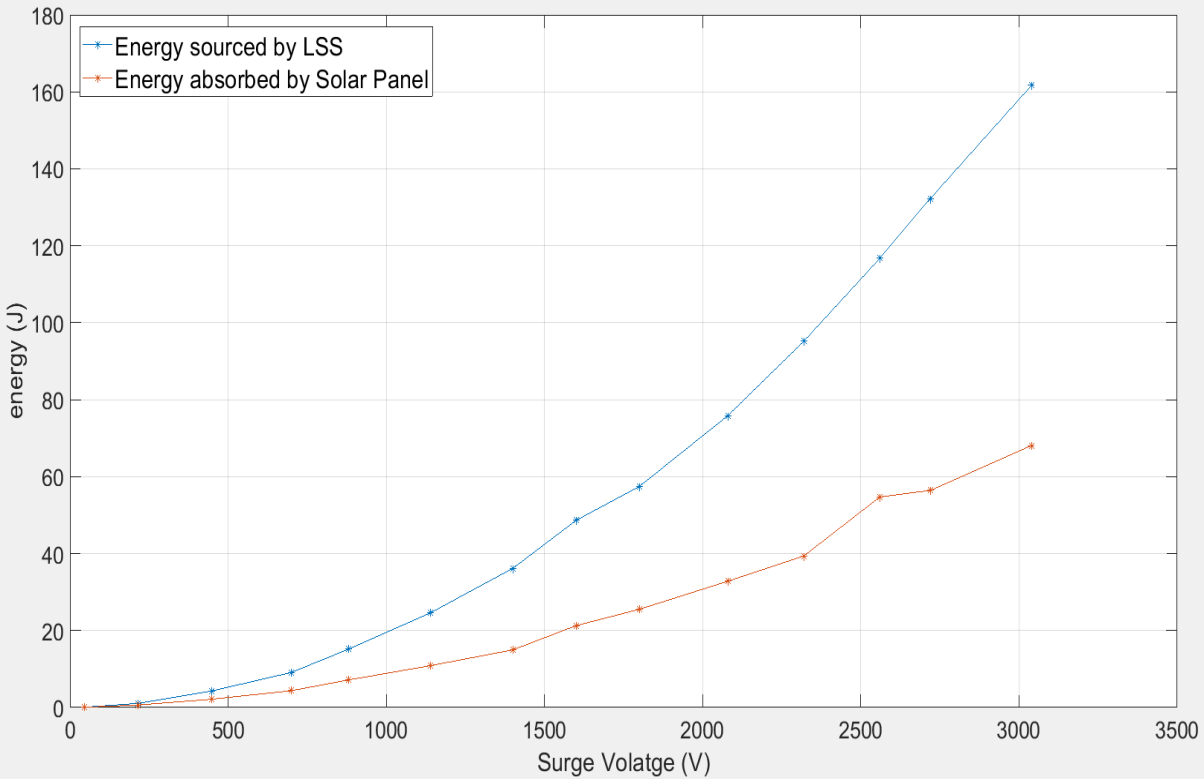

(b)

Fig 5.3 MATLAB graphs for (a) Voltage drop during path (b) Energy graphs for LSS and PV Panel

These high voltage transients do not cause any serious damage to the PV panel but circuit connected to it could fail due to high transient energy. To protect this electronic circuit, it is important to divert the surge energy by introducing first level of protection. Therefore, MOV (V180ZA20P) was connected to the PV panel which conducts heavily providing a clamping action and diverting the high transient energy whenever surge voltage exceeds its breakdown voltage. Figure 5.4 depicts the voltage and energy graphs obtained during the experiment.

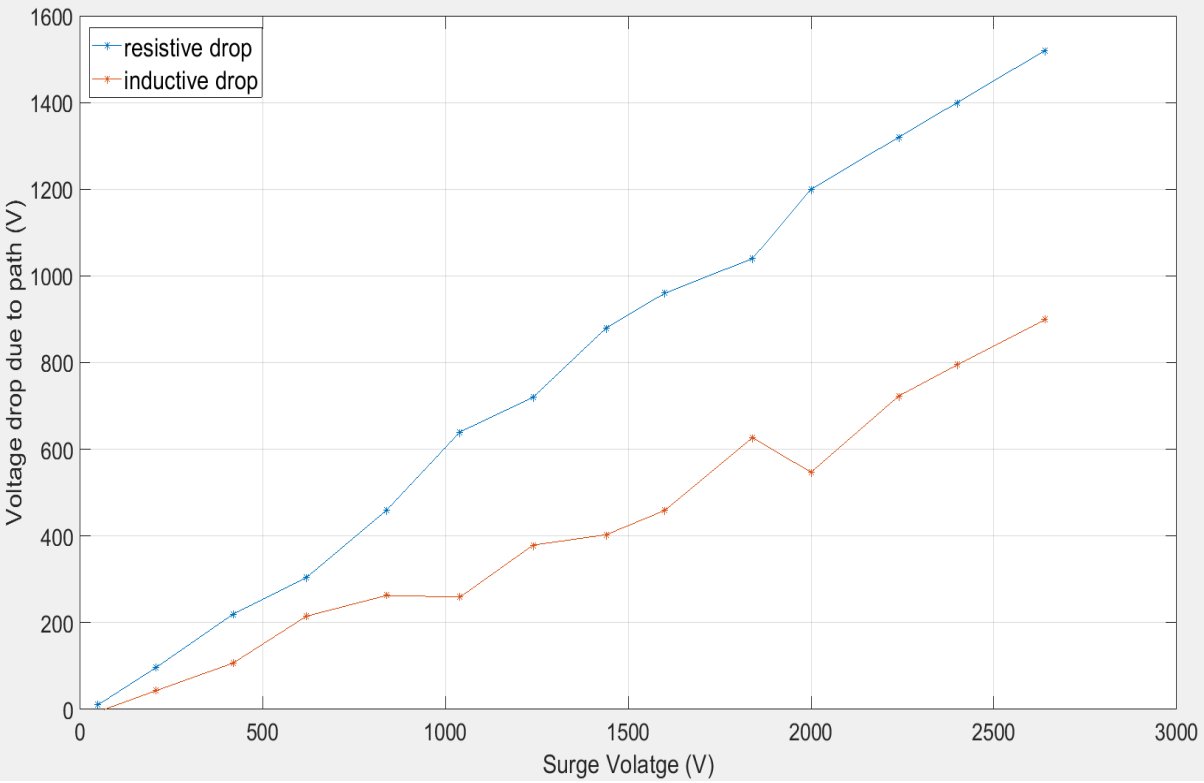

(a)

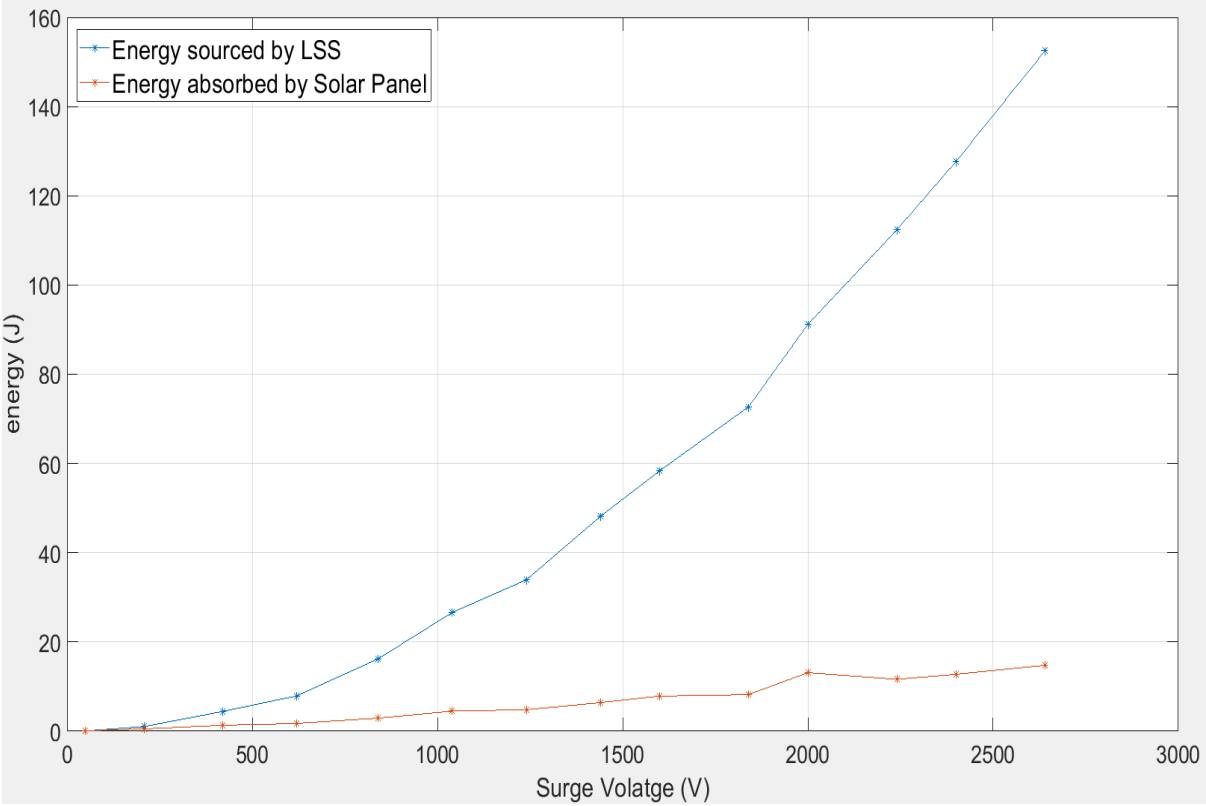

(b)

Fig 5.4 MATLAB graphs with MOV connected as first level of protection (a) Voltage drop during path (b) Energy graphs for LSS and PV Panel

In the absence of MOV, maximum energy appeared across the solar panel due to high voltage transients was observed to be approximately 70 Joules which dropped down to 15 Joules the moment MOV was connected. Hence it can be said that MOV absorbs maximum surge energy as expected and protects the equipment under test.

5.2 Surge testing setup for SCALED converter

In order to observe the surge withstand capability of a system, LSS is connected in parallel with the solar PV panel and SCALED. High voltage transients of increasing magnitude were performed on SCALED in absence of surge suppressors and voltages across the two circuit boards (power/load board and control board) were recorded. Figure 5.5 reflects the block diagram of the test setup connected for this experiment.

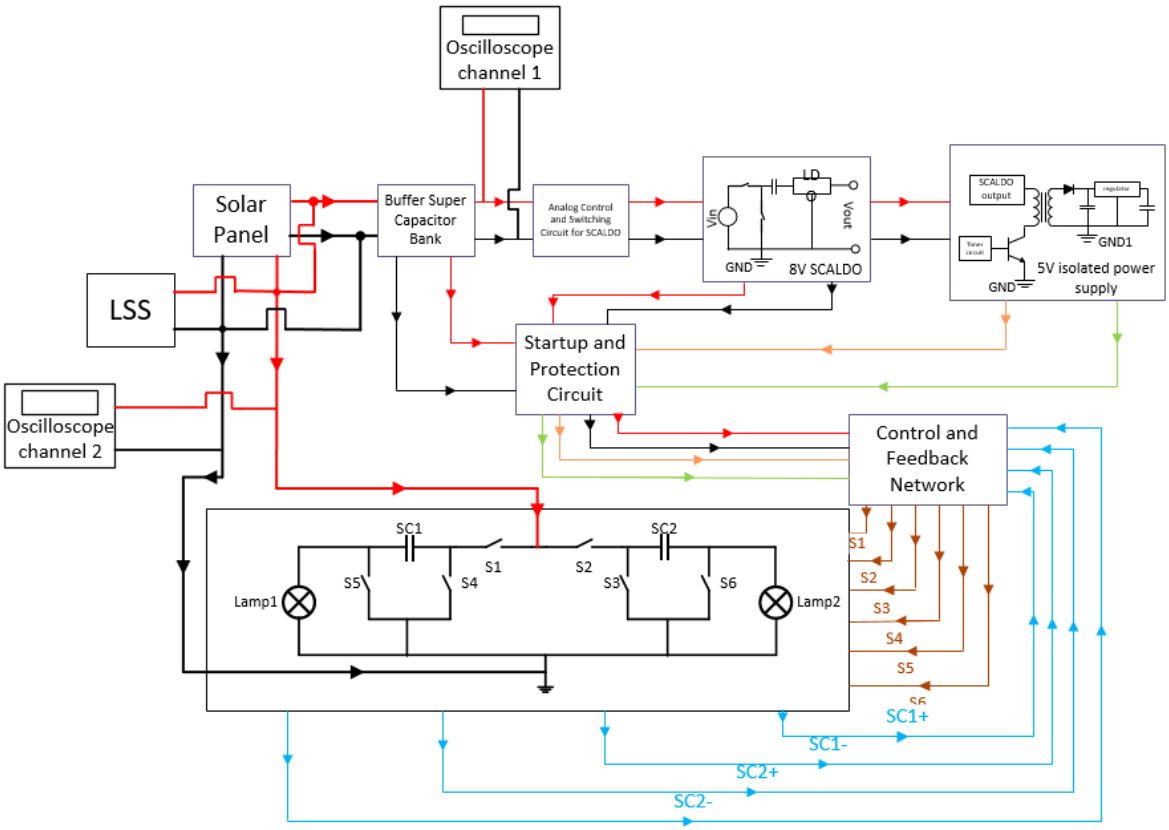

Fig 5.5 Block diagram of the test setup for SCALED under surges

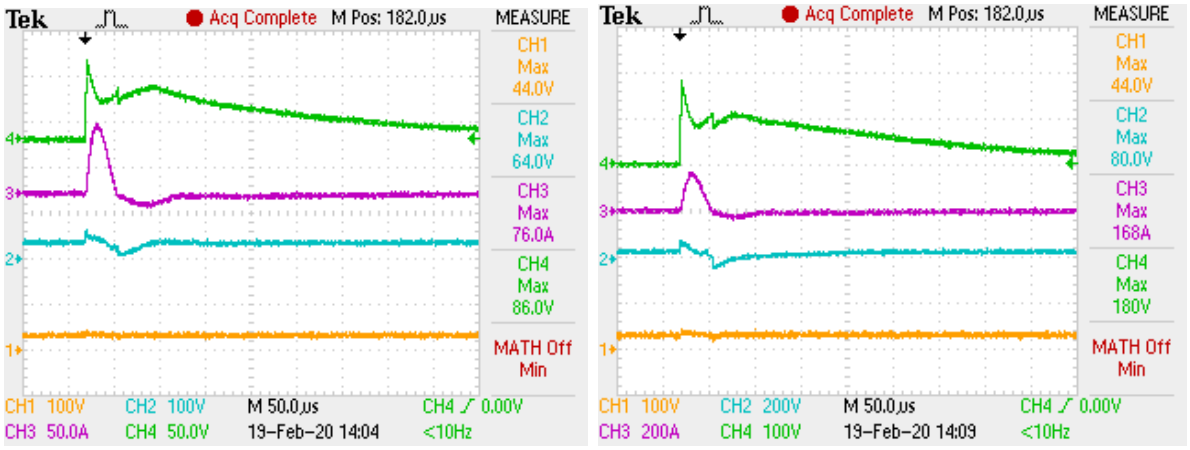

(a) (b)

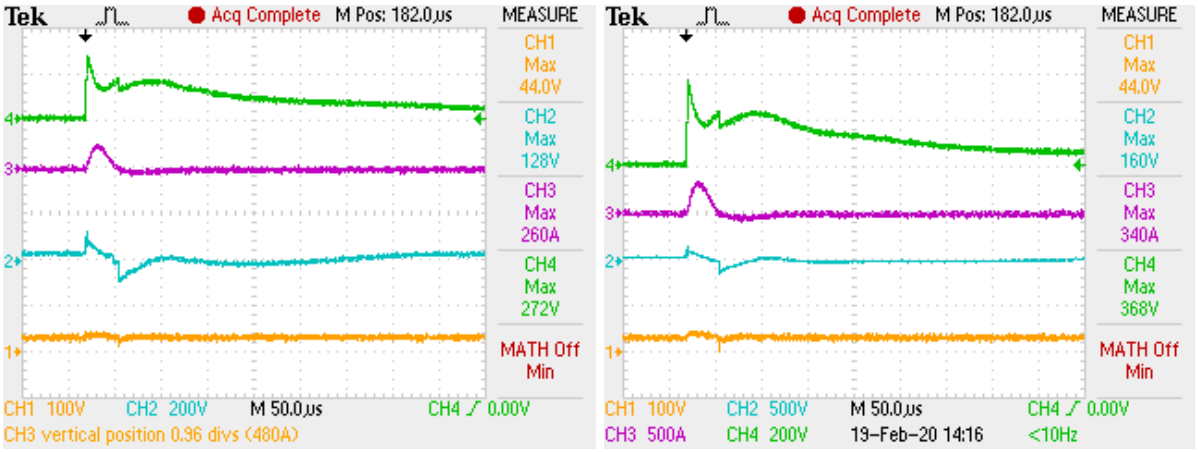

(c) (d)

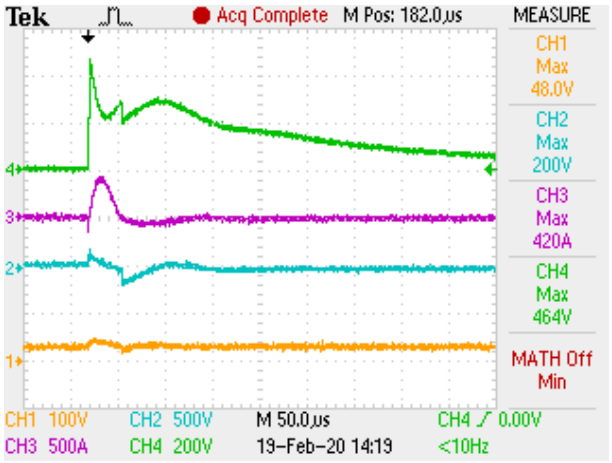

(e)

Channel 4: Surge Voltage waveform Channel 3: Surge Current waveform
Channel 2: Voltage across the power board Channel 1: Voltage across the control board

Fig 5.6 Oscilloscope images for SCALED under surges of (a) 100V (b) 200V (c) 300V (d) 400V (e) 500V

Buffer SC bank is connected in parallel to the control board which functions as an energy storage device in normal operation of SCALED. In the presence of high

voltage transients, this SC bank absorbs most of the surge energy protecting the control board from damage. As a result, maximum voltage across the board in the event of surge is in the range of 44V to 48V as observed in Figure 5.6. However with increasing surge, voltage across the power/load board increases. As no external surge protective component is connected to protect the board from high voltage transients, part of surge current streams through the power board and at the surge of 500V this surge current is strong enough to damage the components on the power board. Figure 5.7 demonstrates the laboratory test setup for the experiment performed.

Not all the surge current travels towards SCALED but part of it streams towards solar panel as well. It can be said that solar panel absorbs part of surge energy and helps in protecting the system. Therefore SCALED is able to withstand surges up to 500V and hence till this point there is no need of any external protection. Protective measures should have been taken into account in order to prevent the damage to the system if surges of more than 500V are encountered. Due to limited equipment availability, it was not possible to observe the current flowing through each individual branches.

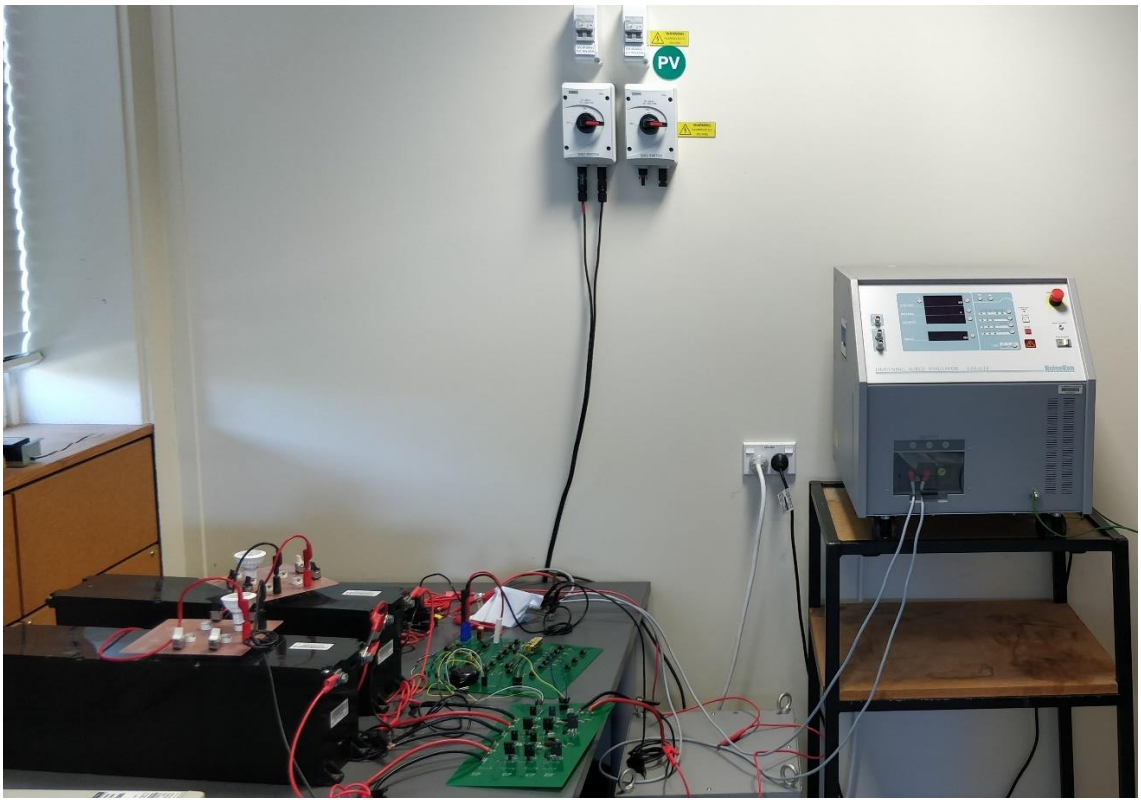

Fig 5.7 Experimental test setup to observe surge withstand capability of SCALED

5.3 Protection against high voltage transients

In order to protect the SCALED from high energy surges, need of an external surge suppressor is necessary. As observed in previous section, protection is

necessary to prevent damage to the power/load board as control board due to buffer SC bank connected to it can withstand surges. Due to its high current handling capability as well as broad current and voltage spectrum, MOV is used as first level of protection.

5.3.1 Selection of MOV

Metal oxide varistors are the most common type of voltage clamping devices and are available for use at a wide range of voltages and currents. MOVs are extremely effective in absorbing short term high voltage transients and have higher energy handling capabilities. Metal oxide varistor starts conduction at a specific voltage called breakdown voltage providing near constant voltage across its terminals termed as clamping voltage and stops conduction when the surge voltage falls below its threshold voltage.

SCALED is able to withstand surges up to 500V in the absence of any external protection therefore MOV with a clamping of less than 400V can be used as first level of protection. V180ZA20P MOV was selected from Littelfuse ZA series, as varistors in this series are designed for the use in the protection of low and medium voltage circuits [33].

5.3.2 Inductor and Capacitor

Connecting MOV in parallel to the PV panel or SCALED input is not enough and hence for extra safety purposes inductor is connected in series with the power board. This series connected inductor with surge absorbing clamping device acts as a filter by opposing quick rise in the current through circuit. During the event of surge when surge current pulse 'i' passes through an inductor, voltage proportional to $\frac{di}{dt}$ will appear across it opposing the source voltage. Assuming worst case scenario that the PV panel connected does not absorb any surge energy and to calculate the inductor value, consider the case where surge voltage of 1kV is applied to the circuit. Internal resistance of the LSS is 2Ω therefore maximum surge current that could be supplied by LSS at 1kV will be 500A.

The moment surge voltage exceeds breakdown voltage of MOV, it switches to its conducting stage by allowing approximate peak pulse current of 100A to flow through. Remaining surge current gets divided into two paths. One path is towards power board and another is towards control board. Control board has buffer SC bank connected to it in parallel and hence total equivalent resistance of this path will be much lower than the power board. Hence most of the remaining surge current flows through this buffer SC bank which is given by Equation 4.2,

$$i_c(t) = \frac{V_{SG}}{R_T}\ (e^{-t/C*R_T})$$

Where R_T is total resistance which is addition of internal resistance of LSS, path resistance and ESR. Internal resistance of LSS is 2Ω, path resistance is considered to be 1 Ω and ESR of SC bank is 88 mΩ. For the surge of 20 µs, current flowing through the buffer SC bank can be determined by,

$$i_c(t) = \frac{3000}{(2+1+0.088)} \exp\left[\frac{-20\mu s}{14.5*3.088}\right] = 323.8\ A \approx 324\ A$$

Current that could flow towards power board can simply be given by Kirchhoff's current law meaning subtracting the current flowing through buffer SC and MOV together from total surge current. Hence it can be said that the peak pulse current that could flow through power board in the occurrence of surge will be 76A. Maximum terminal voltage that power board could withstand without getting damaged is 200V as observed.

Considering the surge current waveform has a period of 20µs, inductor value can be calculated by formula,

$$L = \left(V_{MOV} - V_{power}\right) * \frac{dt}{dI}$$

$$L = (300 - 200) * \frac{20\mu s}{76} = 26\mu H$$

Where V_{MOV} is the clamping voltage of MOV.

V_{power} is the maximum peak pulse voltage that power board could withstand.

Inductor stores energy in the occurrence of surge and this stored energy gets released causing the oscillations across the power board input. To absorb this energy as well as to bypass the peak pulse current of 76A and to protect the current sensitive components on the power board, 100µF 50V rated capacitor is connected in parallel with the power board. Figure 5.8 depicts the simplified as well as detailed block diagram of the SCALED with surge protective measures. With MOV, inductor and capacitor connected to SCALED, surges were performed on the system. Voltage waveforms across the control and power boards were recorded. Figure 5.9 shows the oscilloscope images for the readings recorded.

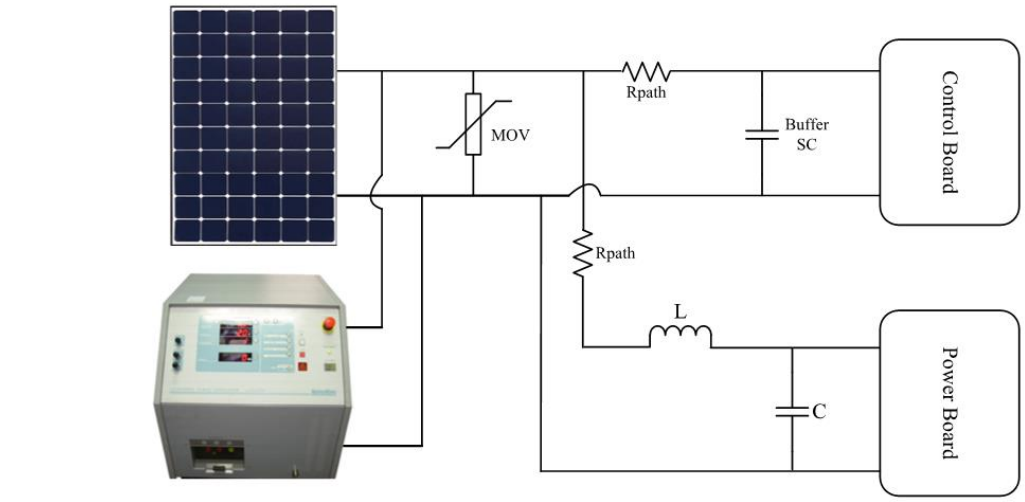

(a)

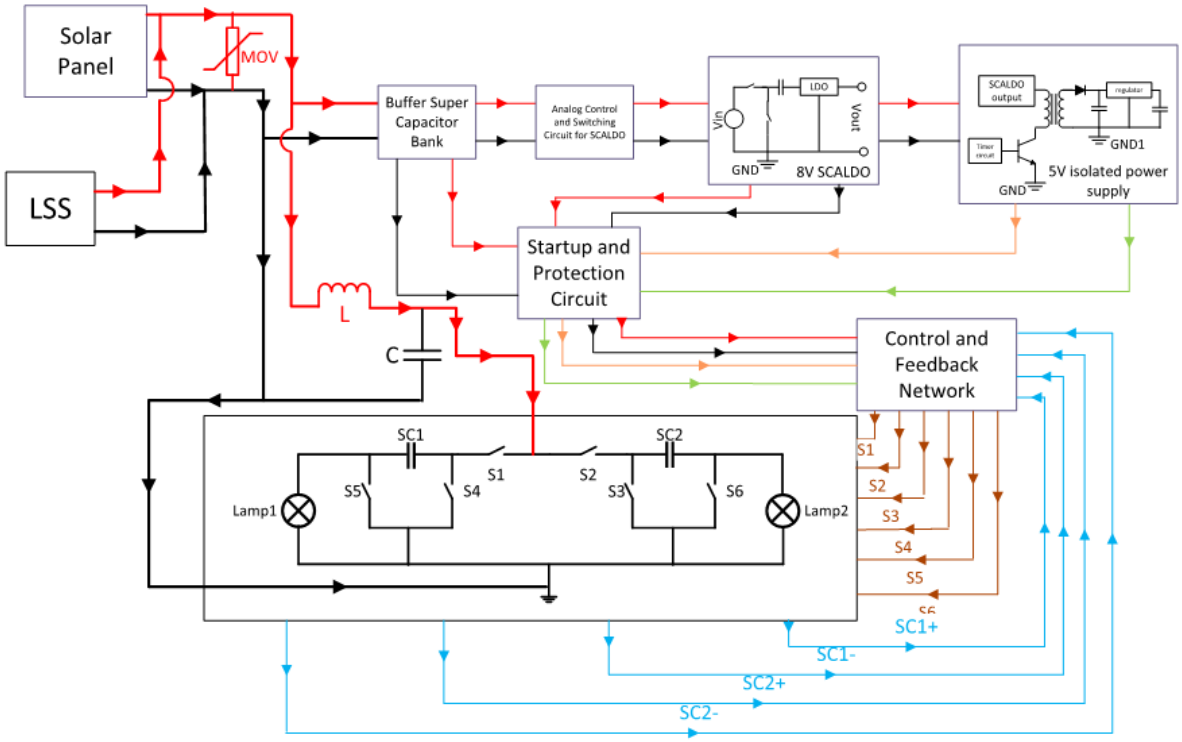

(b)

Fig 5.8 Block diagram of SCALED with surge protective components (a) simplified block diagram with two boards of SCALED (b) detailed block diagram of actual test setup

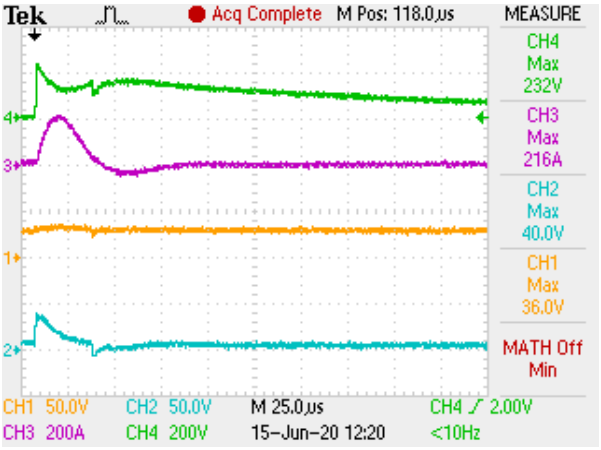

(a) 500V

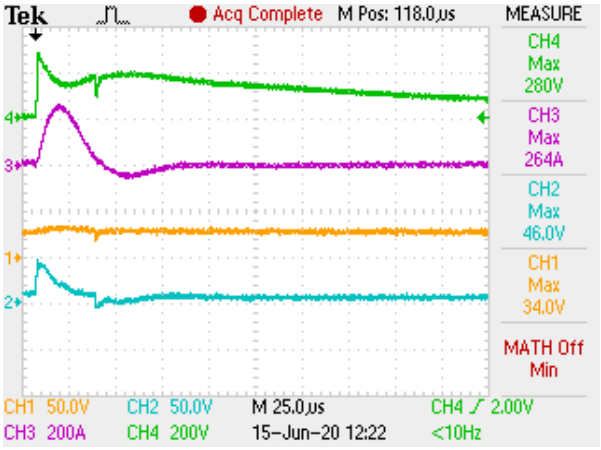

(b) 600V

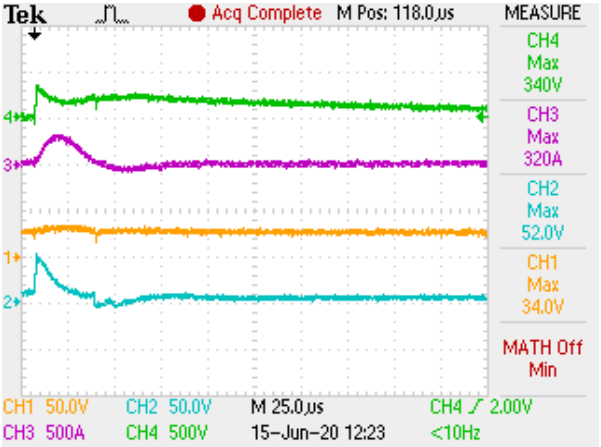

(c) 700V

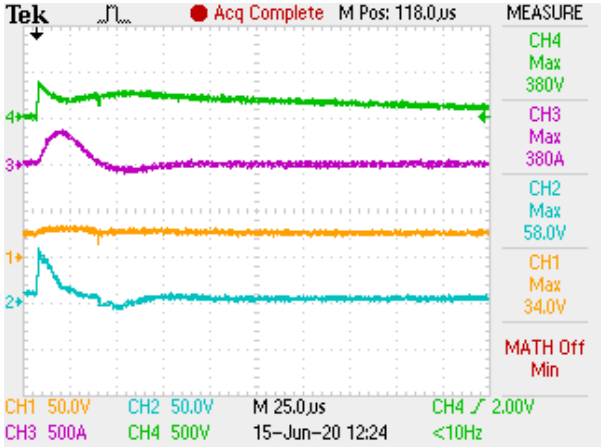

(d) 800V

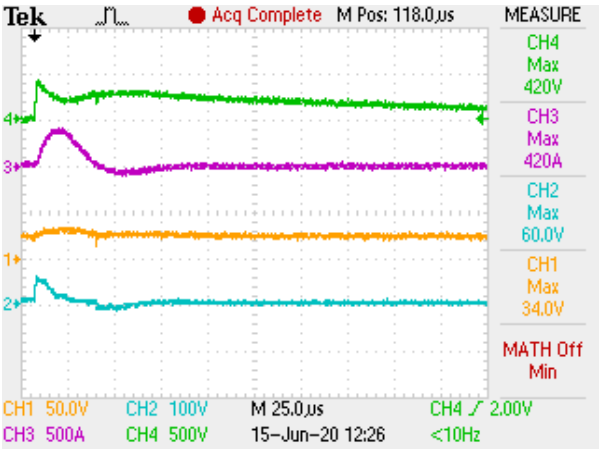

(e) 900 V

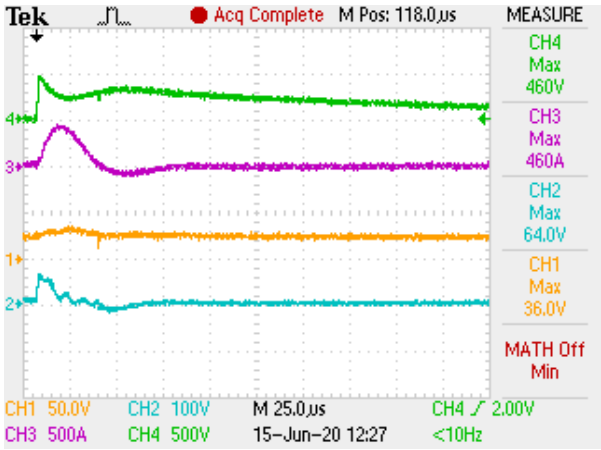

(f) 1kV

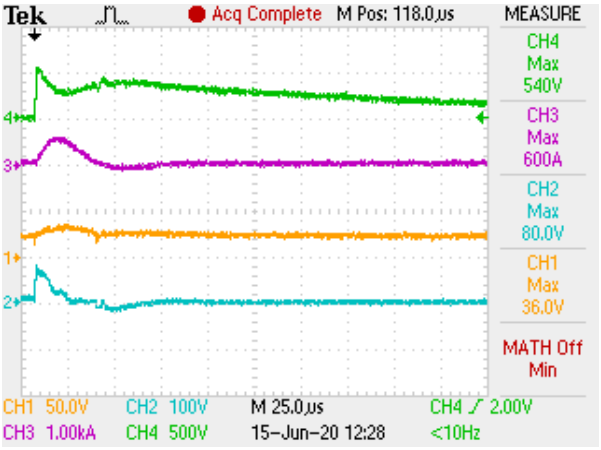

(g) 1.2kV

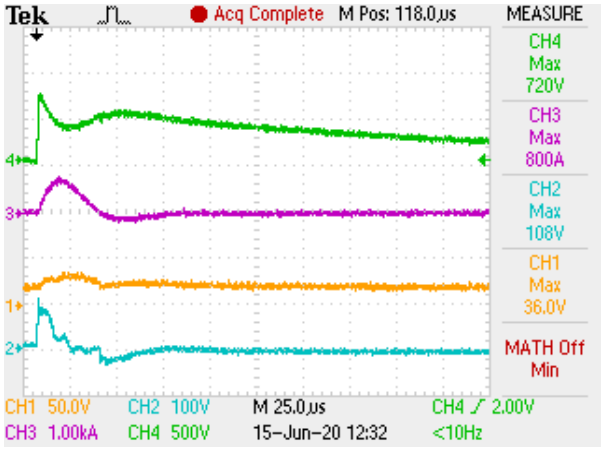

(h) 1.6kV

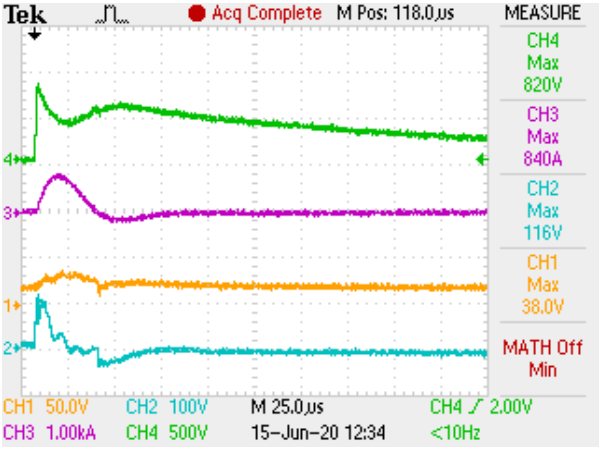

(i) 1.8kV

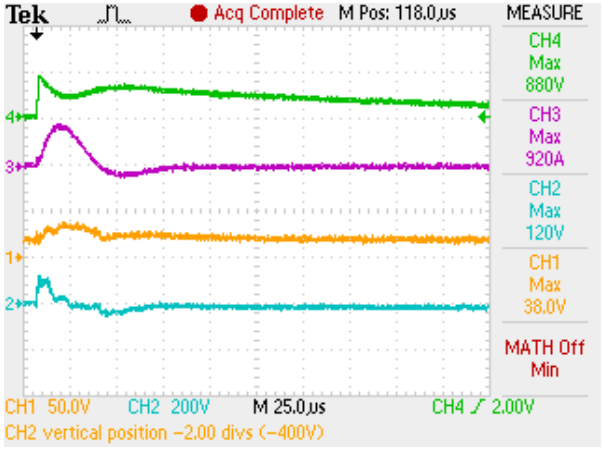

(j) 2kV

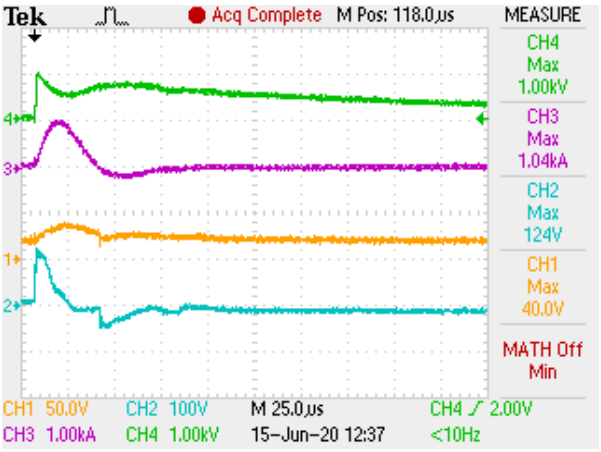

(k) 2.2kV

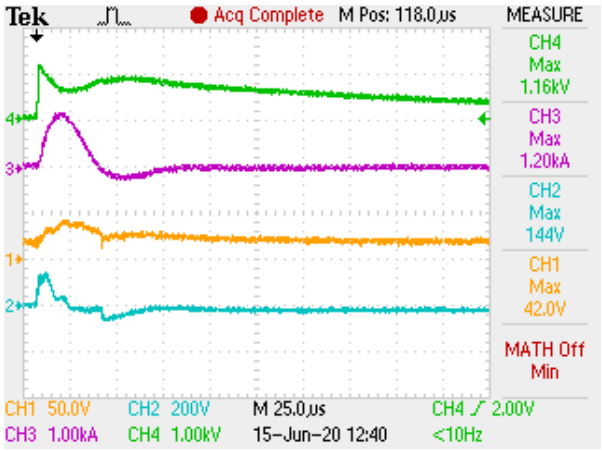

(l) 2.6kV

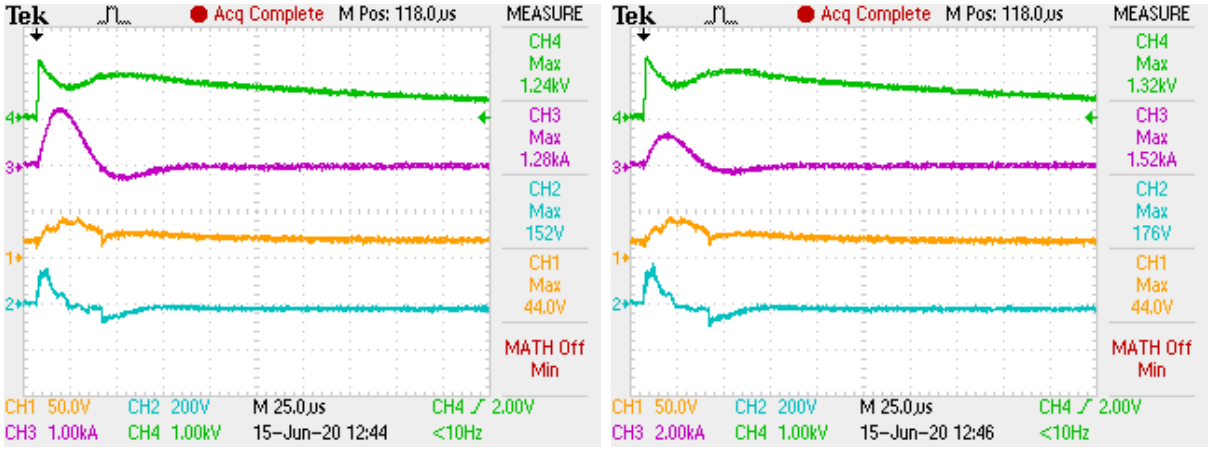

(m) 2.8kV (n) 3kV

Channel 4: Surge Voltage waveform Channel 3: Surge Current waveform
Channel 2: Voltage across the power board Channel 1: Voltage across the control board

Fig 5.9 Observations for surge protected SCALED

Note that even though the maximum voltage set on LSS was till 3kV, observed maximum surge voltage from scope waveforms is 1.32kV. This is because surge voltage and current waveforms changes according to EUT connected to LSS as mentioned in Chapter 3. In addition to this, tolerances and non-ideal nature of the components inside LSS play an important role for this mismatch of the values observed.

5.3.3 Simplified equivalent circuit for LSS

Figure 5.10 depicts simplified version of internal circuitry of LSS. Various internal impedances affect the total loop resistance during the measurements and its voltage monitoring and current monitoring outputs provide electrical isolation for oscilloscope input channels. Total loop impedance is comprised of [19],

- Internal resistance of high voltage source of LSS
- Wave shaping circuit of LSS
- LSS output coupling circuit
- Path resistances and inductances created by the circuit connections
- Input impedance of the EUT

When Live (L) and Neutral (N) terminals of LSS are short circuited, maximum current monitored was 3.42 kA and maximum voltage monitored was 3.8 kV when front panel settings for voltage was set to 6.6 kV [19].

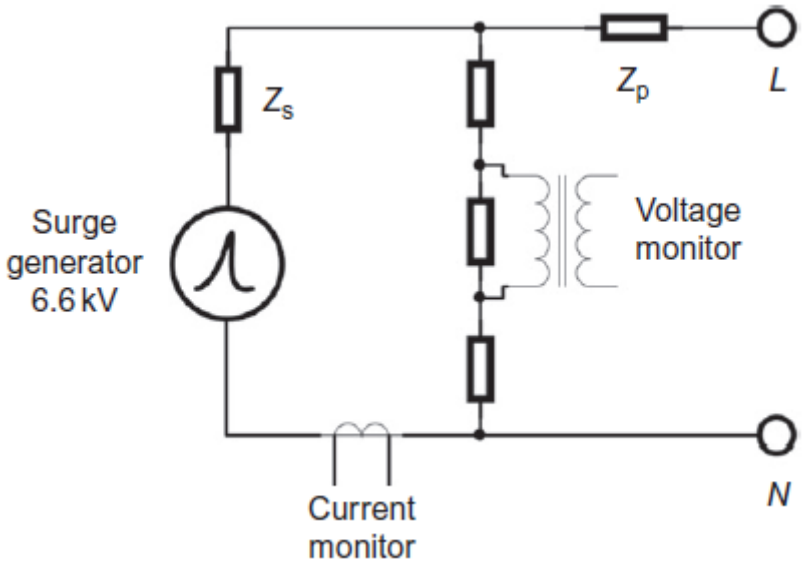

Fig 5.10 LSS internal simplified circuitry (Z_S: internal series impedance Z_P: path series impedance) [19]

5.4 Operational delay due to surge

SCALED is able to withstand surges up to 3kV with protective measures taken into account. No damage to the system is witnessed but a small deviation in the functionality of PIC in startup and protection block of control board is observed. To investigate the reason behind such a behaviour, system was subjected to high voltage transients again and this time output voltage of 8V SCALDO and 5V isolated power supply were recorded.

Small voltage spikes are observed at the output of both these blocks in the event of surge. Voltage of the spike increases with increasing surge voltage. Figure 5.11 depicts the images of the spikes observed at 3kV. Appendix E shows images of spikes observed for rest of the surge voltages.

In normal working operation of SCALED, the above mentioned PIC produces signals continuously without any time delay to drive MOSFET drivers and another PIC. These two components are parts of control and feedback network. But after each surge, the PIC in startup and protection block takes small amount of time to produce these signals. This time delay increases with increasing surge voltage. Table 5.1 demonstrates the time taken by PIC to write signals with increasing surge voltage as well as magnitude of the voltage spike observed at the output of 8V SCALDO and 5V power supply blocks.

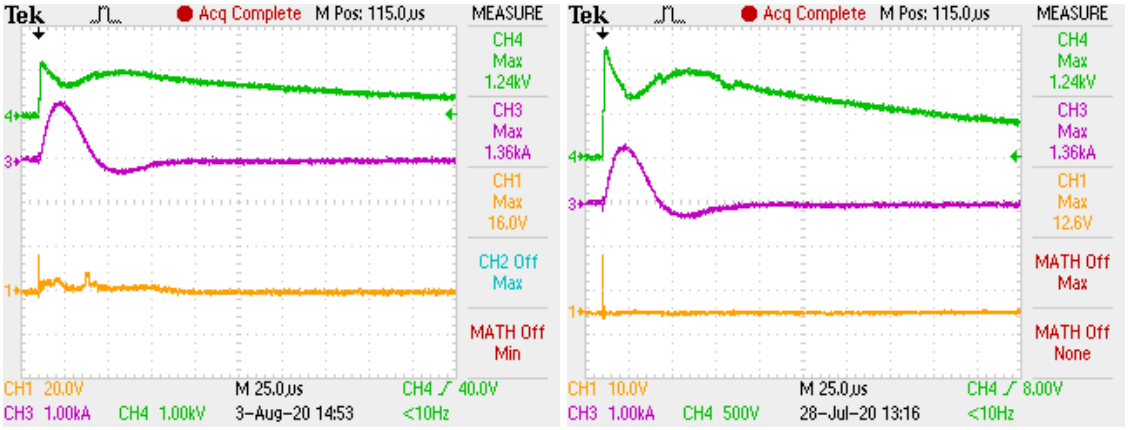

(a) (b)

Fig 5.11 Output Voltage waveform in the event of surge when channel 1 is at (a) 8V SCALDO (b) 5V isolated power supply

Table 5.1 Time delay with respect to surge

V_{surge} (V)	V_{spike} at 8V SCALDO output (V)	V_{spike} at 5V isolated power supply output (V)	Time delay (seconds)
100	9.6	5.4	4
200	9.2	5.4	7
300	10.4	5.6	7
400	11.2	5.4	12
500	12	5.4	10
600	11.2	5.8	10
700	12	9	16
800	10.8	8.8	20
900	14	9.6	23
1000	16	8.2	28
1200	16.8	7.4	30
1400	11.2	11.8	33
1600	15.6	11.8	37
1800	20	11.8	40
2000	18.4	12.2	49
2200	16	10.6	46
2400	12.8	11.2	51
2600	22.4	11.6	52
2800	29.6	11.8	53
3000	16	12.6	53

PIC was expected to fail the moment its supply voltage goes beyond 5V but this effect was not observed. Instead malfunctioning and reduced reliability was witnessed for this PIC. Supply voltage exceeds the normal operating voltage of PIC only for very short duration in the order of nano-seconds and hence this overvoltage condition does not kill the processor.

SC modules in SCALED switches every 25 minutes hence it can be said that switching frequency of the SCALED is 0.66 mHz. Maximum operational delay

observed was of 53 seconds and will have no effect on load side due to large switching time of SC banks. In order to observe the effect of this delay on the normal operation of system, switching time of SCALED could be reduced considerably either by increasing the number of LED lamps or by decreasing the size of SC modules.

5.5 Reduced size SC module

SC modules used in SCALED system which are represented as SC1 and SC2 in the block diagram of SCALED are ultracapacitor modules from LS Mtron with 166F capacitance, 51.3V rated voltage and ESR of 7.8 mΩ. Figure 5.12 is the image of single module of above mentioned ultracapacitor. Below mentioned features make this module suitable for a wide variety of applications because of its high energy rating and wider voltage range.

Fig 5.12 166 F 51.3 V Ultracapacitor from LS Mtron [34]

Features

- High power performance compared to batteries
- High energy performance
- Low ESR and High power
- Environmentally friendly
- Maintenance free

To observe the effect of operational delay on the load side, this 166F SC module has to be reduced in such a way that the switching time reduces approximately to one minute instead of 25 minutes. This can be done by calculating the total energy

consumption of the LED lamps. Average current flowing through SCALED is 200 mA and source input voltage i.e. the voltage of the PV panel is 34V.

5.5.1 Calculation for new SC module

Energy consumed by LED in one minute's time of SC module's charging phase can be given as,

$$E = I(34 - V_{charging})t = 0.2 * (34 - 13) * 60 = 252\,J$$

For discharging phase, LED is powered directly by SC hence energy consumed by LED in discharging phase of SC module is,

$$E = I(V_{discharging})t = 0.2 * (20) * 60 = 240\,J$$

$V_{charging}$ and $V_{discharging}$ represents the lower and upper voltage limits at which SC modules switch themselves. $V_{charging}$ is the point where SC module switches to its charging phase and $V_{discharging}$ is the point where SC module switches to its discharging phase.

Size of the new SC module can be calculated as,

$$E_{average} = \frac{1}{2}C(V_{upper_{switching}} - V_{lower_{switching}})^2$$

$$246 = \frac{1}{2}C(20 - 13)^2$$

$$C = \frac{246*2}{49} = 10F$$

This new SC module should have the voltage rating greater than the maximum voltage till which the SC charges i.e. $V_{rated} > 20V$. As individual SC have very low voltage ratings therefore in order to get the rated voltage of the module greater than 20V, number of SCs need to be connected in series. While doing so it is important to keep track of the capacitance of the module as series connection of these capacitors reduces the net capacitance of the unit. Hence individual capacitors should be selected in such a way that their series connection will keep the balance of these two important parameters.

Maxwell Technology's 100F 2.7V rated supercapacitors were selected for the purpose of series connection. For capacitors connected in series, net capacitance can be determined by,

$$\frac{1}{C_{total}} = \frac{1}{C_1} + \frac{1}{C_2} + \frac{1}{C_3} + \ldots\ldots\ldots + \frac{1}{C_n}$$

For 'n' SC cells of equal voltage rating and equal capacitance connected in series, total capacitance is given by,

$$C_{total} = \frac{C_{individual}}{n}$$

Number of capacitors required to get the net capacitance of 10F with individual capacitors of 100F is,

$$n = \frac{C_{individual}}{C_{total}} = \frac{100}{10} = 10$$

Therefore, 10 such capacitors should be connected in series to form the new SC module. Voltage rating of this new SC module is,

$$V = n * V_{R_{individual}} = 10 * 2.7 = 27\ V$$

Connecting capacitors in series adds up the ESR of each supercapacitor which is 15mΩ and hence the SC module will have total ESR of 150 mΩ.

Table 5.2 Specifications of the newly designed SC module

Parameter	Specification
Manufacturer	Maxwell Technology
Number of capacitors in series	10
Net Capacitance	10 F
Rated voltage of the module	27 V
ESR of the module	150 mΩ

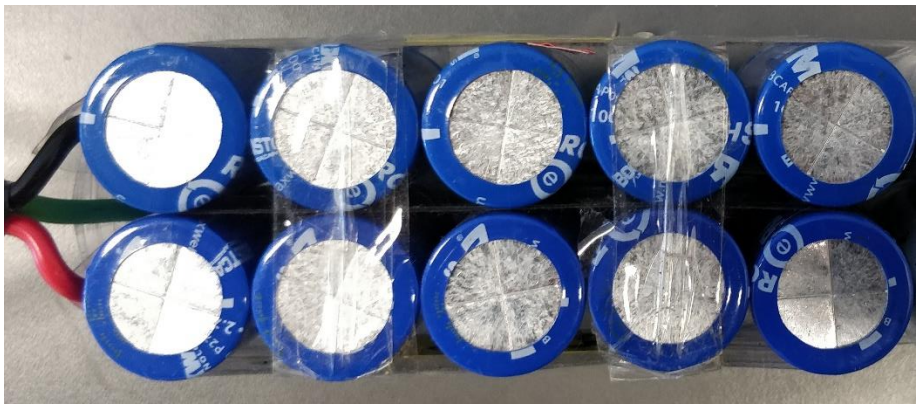

Fig 5.13 10 F 27 V rated SC module

5.5.2 Practical testing of new SC module

The big 166F SC modules in original SCALED were replaced by these newly designed small SC units shown in Figure 5.13 and before applying any surges to this new system, changes in the normal operation of the SCALED were observed. Figure 5.14 depicts the switching waveform of this SC unit.

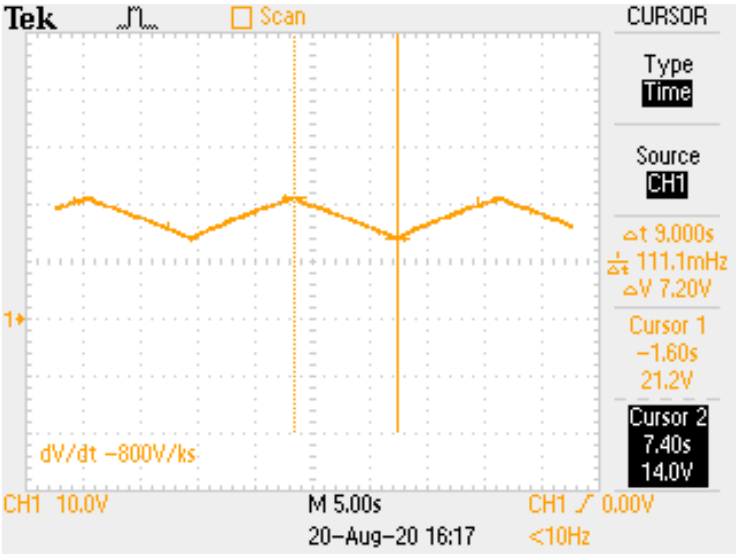

Fig 5.14 Switching waveform of new SC module

From Figure 5.14, it is observed that SC module switches every 9 seconds reflecting that the practical switching time does not match with the expected switching time. This is due to the energy losses in the path as well as due to component losses such as ESR loss within supercapacitors. This means SC module is unable to fulfil the energy requirement of LEDs to keep them in a respective loop of charging or discharging for 60 seconds. 166 F SC module has the total ESR of 7.8 mΩ which is very small compared to the ESR of this SC unit which is 150 mΩ. Due to time constraints it was not possible to carry out more theoretical analysis and the practical experimentation to explain this behaviour of SC unit.

Chapter 6

Conclusion and Future Development

6.1 Conclusion

SC-Assisted topologies (SCA) developed at University of Waikato modifies traditional RC loop by inserting useful load in series and replacing capacitor by supercapacitor resulting in the increased net efficiency of the overall circuit. SCALED is a unique application designed from this SCA concept. It makes use of solar energy to power up 12V 5W LED loads with supercapacitor modules placed in series providing short term DC-UPS capability. Buffer SC bank connected at the input of the system acts as a voltage source in the absence of adequate solar irradiance.

Solar PV panel was subjected to high energy transients in order to observe its effect on SCALED in surge environment. From practical experimentation and mathematical calculations it is concluded that PV panel plays important role in surge protection of SCALED by absorbing part of surge current and energy. Supercapacitors are good surge absorbers due to their large time constants. Surge withstand capability of the SCALED is tested with and without any external surge absorbing components. System is able to withstand surges up to 500V in the absence of surge suppressors. Buffer SC bank connected in parallel protects the control board from these high energy transients. However due to the absence of any surge protective components across the power board, components on the power board were damaged. With MOV as first level of protection and buffer BC bank and LC filter as second level of protection for control board and power board respectively, three component based surge absorbing unit (comprised of V180ZA20P MOV in series with 26µH inductor and 100 µF capacitor) was designed to protect SCALED against these high energy surges with voltage magnitudes greater than 500V.

With this surge absorbing unit connected, SCALED was subjected to surge testing. Even though no component damage was observed, operational delay in PIC of startup and protection block of the control board was encountered. This is because the supply voltage of PIC exceeds above its normal and maximum ratings. No damage was observed to PIC as voltage across it shoots only for the period of few nano-seconds but its reliability is compromised. This delay is small enough compared to switching time (which is in the order of several minutes) of the SC modules and hence has no effect on the normal operation of system. However in order to observe the influence of this delay, size of SC modules were

reduced considerably and new SC units were designed such that the new switching time is now in the order of few seconds. Due to time constraints it was not possible to carry out mathematical analysis to rectify the measurement issues faced and troubleshooting of the circuit.

6.2 Future Development

Voltage spikes are observed at the output of "8V SCALDO and 5V isolated power supply" sub-circuits due to partial surge appearance across them. Need of an in-circuit design modification is necessary to absorb or to minimize this partial surge voltage. To eliminate the operational delay generated by PIC in startup and protection block, it is very important that there should not be any overvoltage condition across its supply terminals. More mathematical analysis and practical experimentation is required to estimate and design new SC unit of suitable capacitance with appropriate voltage rating and minimum ESR to observe the effect of operational delay on the load side of SCALED system.

Surge testing of the solar PV panel was carried out as a part of this project in order to understand its response towards high voltage transients. From practical experimentation and energy calculations, transient model of the PV panel was approximated but more work needs to be done in order to propose the finalised transient model for PV panel.

Appendices

Appendix A

MATLAB code for CSUN250-60P solar panel

Generating I-V and P-V curves

```
clc
close all

Vd=0:38; %range of cell voltage
Isc=8.81; %short circuit current of cell
Ns=60; %number of cells in panel
Voc=0.621*Ns; %open circuit voltage of panel

Tc=0.058; %current temperature coefficient of the cell
Tref=273+25; %standard temperature in kelvin
T=273+25; %temperature in kelvin

Sref=1000; %standard irradiance
S=1000; %irradiance at which panel is operating
S1=800;
S2=600;
S3=400;
S4=200;

Np=1; %number of panels
q=1.6*10^-19; %charge of electron
K=1.38*10^-23; %Boltzman constant
A=1.5; %ideality factor

Rs=0.48; %cell series resistance
Rp=310; %cell shunt resistance

Vt=K*T/q; %thermal voltage of cell
a=Ns*A*Vt;

Ioref=Isc*exp(-Voc/a); %expression for saturation current of cell
Io=Ioref*(T/Tref)^3*exp((q*1.12/(A*K))*((1/Tref)-(1/T))); %saturation
current at given temperature

Iph=(Isc+Tc*(T-Tref))*(S/Sref); %photo current
Iph1=(Isc+Tc*(T-Tref))*(S1/Sref);
Iph2=(Isc+Tc*(T-Tref))*(S2/Sref);
Iph3=(Isc+Tc*(T-Tref))*(S3/Sref);
Iph4=(Isc+Tc*(T-Tref))*(S4/Sref);
Id=Io*(exp(Vd/a)-1); %diode current

I=Iph-Id-(Vd/Rp); %output current of panel
I1=Iph1-Id-(Vd/Rp);
I2=Iph2-Id-(Vd/Rp);
I3=Iph3-Id-(Vd/Rp);
I4=Iph4-Id-(Vd/Rp);

V=Vd-I.*Rs; %output voltage of panel
V1=Vd-I1.*Rs;
```

```
V2=Vd-I2.*Rs;
V3=Vd-I3.*Rs;
V4=Vd-I4.*Rs;

figure('name','current-voltage characteristics','numbertitle','off')
plot(V,I)
hold on
plot(V1,I1)
hold on
plot(V2,I2)
hold on
plot(V3,I3)
hold on
plot(V4,I4)
grid on
legend('1000w/m2','800w/m2','600w/m2','400w/m2','200w/m2')
xlabel('Voltage')
ylabel('Current')
xlim([0 40])
ylim([0 10])

P=V.*I; %output power of panel
P1=V1.*I1;
P2=V2.*I2;
P3=V3.*I3;
P4=V4.*I4;

figure('name','power-voltage characteristics','numbertitle','off')
plot(V,P)
hold on
plot(V1,P1)
hold on
plot(V2,P2)
hold on
plot(V3,P3)
hold on
plot(V4,P4)
grid on
legend('1000w/m2','800w/m2','600w/m2','400w/m2','200w/m2')
xlabel('Voltage')
ylabel('Power')
xlim([0 40])
ylim([0 300])
```

Appendix B

MATLAB code for LSS waveforms at surge voltage of 6.6 kV

Generating open circuit voltage waveform, short circuit current waveform along with power and energy graphs

```
%% Surge waveforms %%

close all
clc

t = 0:1e-6:140e-6; %% Time axis

%% Constants for Voltage wave

Av = 1.037;
T1 = 0.4074e-6;
T2 = 68.22e-6;

%% Constants for Current wave

T3 = 3.911e-6;
Ai = 0.01243e18;

%% Peak Voltage and Current of the Surge

Vp = 6600
Ip = (Vp/2) %% internal resistance of Surge Simulator is 2 Ohm

%% Voltage and Current equations and their waveforms

V = Av*Vp.*(1-exp(-t./T1)).*exp(-t./T2);
I = Ai*Ip.*(t.^3).*exp(-t./T3);

figure('Name','Open Circuit Voltage Waveform','NumberTitle','Off');
plot (t,V);
title('Open Circuit Voltage')
xlabel('time')
ylabel('Voltage')
figure('Name','Short Circuit Current Waveform','NumberTitle','Off');
plot (t,I);
title('Short Circuit Current')
xlabel('time')
ylabel('Current')


%% Power and Energy Waveforms

P = V.*I;
average_power = mean(P)  %% Average value of Power
[max_power,index] = max(P) %% Max value of Power and its index

figure('Name','Power Waveform','NumberTitle','Off')
plot(t,P)
title('Power Wave')
xlabel('time')
ylabel('Watts')
```

```
E = P.*t;
average_energy = mean(E)  %% Average value of Energy
[max_energy,index]= max(E)%% Max value of Energy and its index

figure('Name','Energy Waveform','NumberTitle','off')
plot(t,E)
title('Energy Wave')
xlabel('time')
ylabel('Jouls')
```

Appendix C-1

MATLAB code for LSS waveforms at surge voltage of 6.6 kV

Generating open circuit voltage waveform, short circuit current waveform along with power and energy graphs

```
close all;
clc;

V_surge=[46 216 448 700 880 1140 1400 1600 1800 2080 2320 2560 2720 3040];
%% Surge Voltage observed from Scope
I_surge=[34 192 400 620 820 1080 1360 1600 1680 1920 2160 2400 2560 2800];
%% Surge Current observed from Scope

V_pv = [ 50 132 224 336 416 504 580 700 800 900 960 1200 1160 1280 ];
%% Surge Voltage + Open Circuit Voltage of Solar Panel
R_path = 0.5;      %% Path Resistance
Voc_pv = 35;       %% Open Circuit Voltage of the Solar Panel

V_pv_surge = V_pv - Voc_pv; %% Actual Surge Voltage appeared across the
Solar Panel due to surge

V_drop_observed = V_surge - V_pv_surge; %% Voltage drop during the path
V_drop_calculated_resistive = (R_path*I_surge); %% Voltage drop observed
due to the resistive effect of the path
V_drop_calculated_inductive= V_drop_observed - V_drop_calculated_resistive;
%% Voltage drop observed due to the inductive effect of the path

time = [ 50e-6 26e-6 24e-6 21e-6 21e-6 20e-6 19e-6 19e-6 19e-6 19e-6 19e-6
19e-6 19e-6 19e-6 ];%% Time interval between start and near end of the
surge spike at Solar Panel
energy_surge = V_surge.*I_surge.*time;
energy_solar_panel = V_pv.*I_surge.*time;

figure('Name','Energy sourced by LSS and absorbed by Solar
Panel','NumberTitle','off')
plot(V_surge,energy_surge, '-*')
hold on
plot(V_surge,energy_solar_panel, '-*')
hold off
xlabel('Surge Volatge (V)','FontSize',18)
set(gca,'FontSize',20)
ylabel('energy (J)','FontSize',18)
set(gca,'FontSize',20)
legend({'Energy sourced by LSS','Energy absorbed by Solar
Panel'},'Location','NorthWest','FontSize',22)
grid on

figure('Name','Drop due to path resistance and path
inductance','NumberTitle','Off');
plot(V_surge,V_drop_calculated_resistive, '-*')
hold on
plot (V_surge,V_drop_calculated_inductive, '-*')
hold off
xlabel('Surge Volatge (V)','FontSize',18)
set(gca,'FontSize',20)
ylabel('Voltage drop due to path (V)','FontSize',18)
```

```
set(gca,'FontSize',20)
legend({'resistive drop','inductive
drop'},'Location','NorthWest','FontSize',22)
grid on
```

Appendix C-2

Oscilloscope images when surges were applied on PV panel

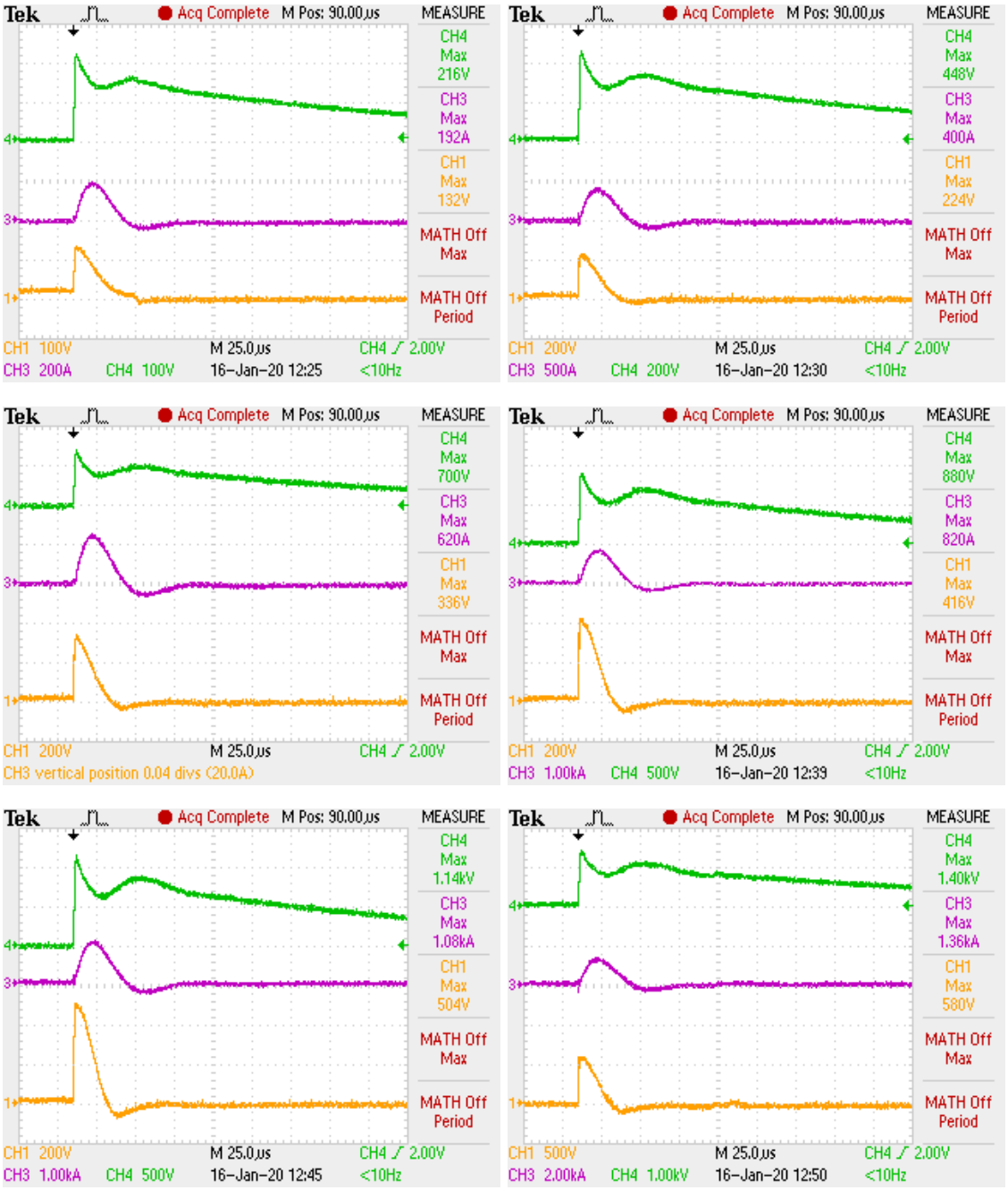

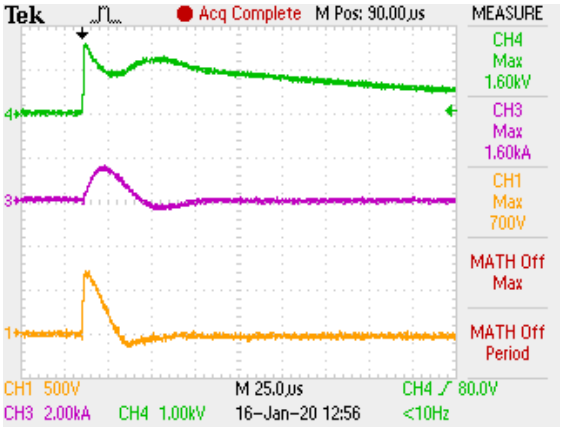
Tek
Acq Complete M Pos: 90.00µs
MEASURE
CH4 Max 1.60kV
CH3 Max 1.60kA
CH1 Max 700V
MATH Off Max
MATH Off Period
CH1 500V M 25.0µs CH4 ∕ 80.0V
CH3 2.00kA CH4 1.00kV 16-Jan-20 12:56 <10Hz

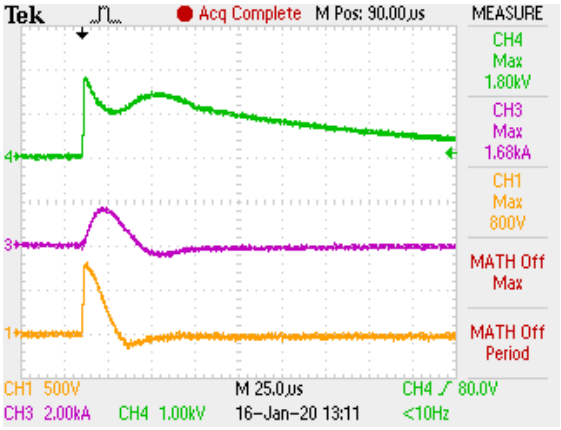
Tek
Acq Complete M Pos: 90.00µs
MEASURE
CH4 Max 1.80kV
CH3 Max 1.68kA
CH1 Max 800V
MATH Off Max
MATH Off Period
CH1 500V M 25.0µs CH4 ∕ 80.0V
CH3 2.00kA CH4 1.00kV 16-Jan-20 13:11 <10Hz

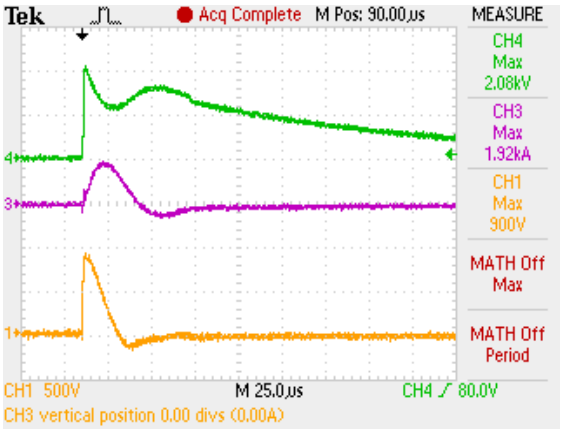
Tek
Acq Complete M Pos: 90.00µs
MEASURE
CH4 Max 2.08kV
CH3 Max 1.92kA
CH1 Max 900V
MATH Off Max
MATH Off Period
CH1 500V M 25.0µs CH4 ∕ 80.0V
CH3 vertical position 0.00 divs (0.00A)

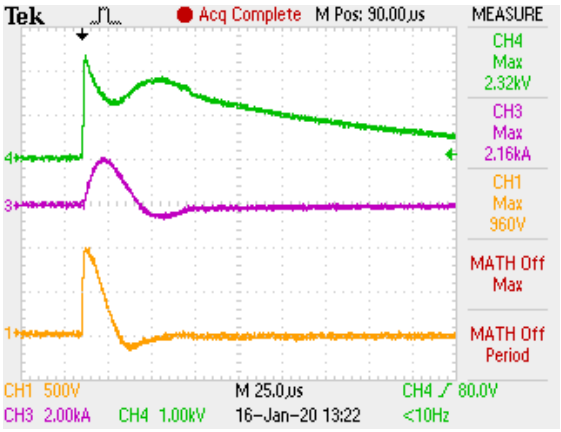
Tek
Acq Complete M Pos: 90.00µs
MEASURE
CH4 Max 2.32kV
CH3 Max 2.16kA
CH1 Max 960V
MATH Off Max
MATH Off Period
CH1 500V M 25.0µs CH4 ∕ 80.0V
CH3 2.00kA CH4 1.00kV 16-Jan-20 13:22 <10Hz

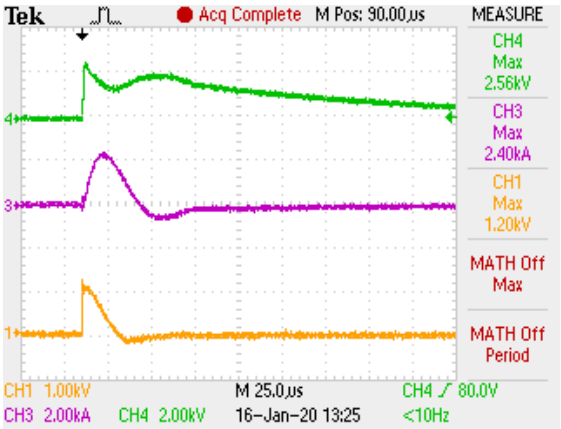
Tek
Acq Complete M Pos: 90.00µs
MEASURE
CH4 Max 2.56kV
CH3 Max 2.40kA
CH1 Max 1.20kV
MATH Off Max
MATH Off Period
CH1 1.00kV M 25.0µs CH4 ∕ 80.0V
CH3 2.00kA CH4 2.00kV 16-Jan-20 13:25 <10Hz

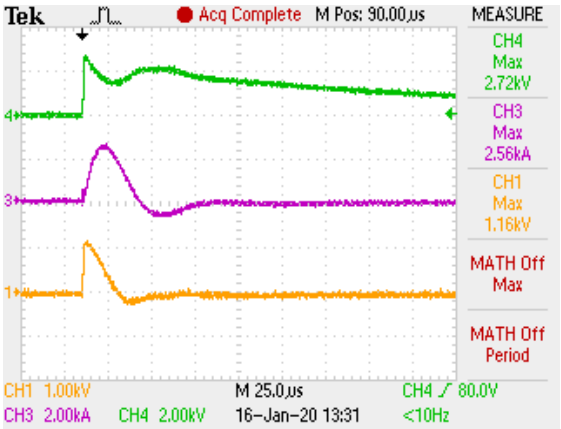
Tek
Acq Complete M Pos: 90.00µs
MEASURE
CH4 Max 2.72kV
CH3 Max 2.56kA
CH1 Max 1.16kV
MATH Off Max
MATH Off Period
CH1 1.00kV M 25.0µs CH4 ∕ 80.0V
CH3 2.00kA CH4 2.00kV 16-Jan-20 13:31 <10Hz

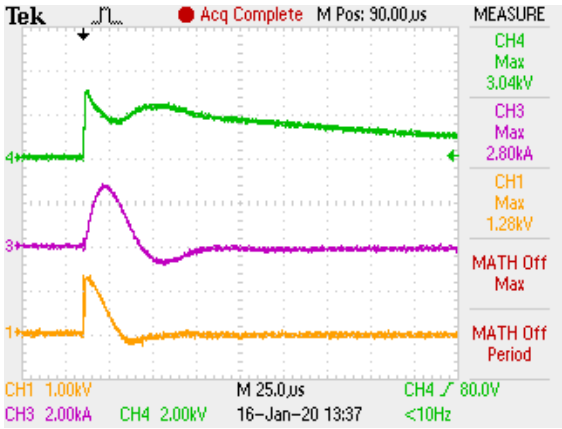
Tek
Acq Complete M Pos: 90.00µs
MEASURE
CH4 Max 3.04kV
CH3 Max 2.80kA
CH1 Max 1.28kV
MATH Off Max
MATH Off Period
CH1 1.00kV M 25.0µs CH4 ∕ 80.0V
CH3 2.00kA CH4 2.00kV 16-Jan-20 13:37 <10Hz

Appendix C-3

LTspice simulation for LSS and PV connected in parallel

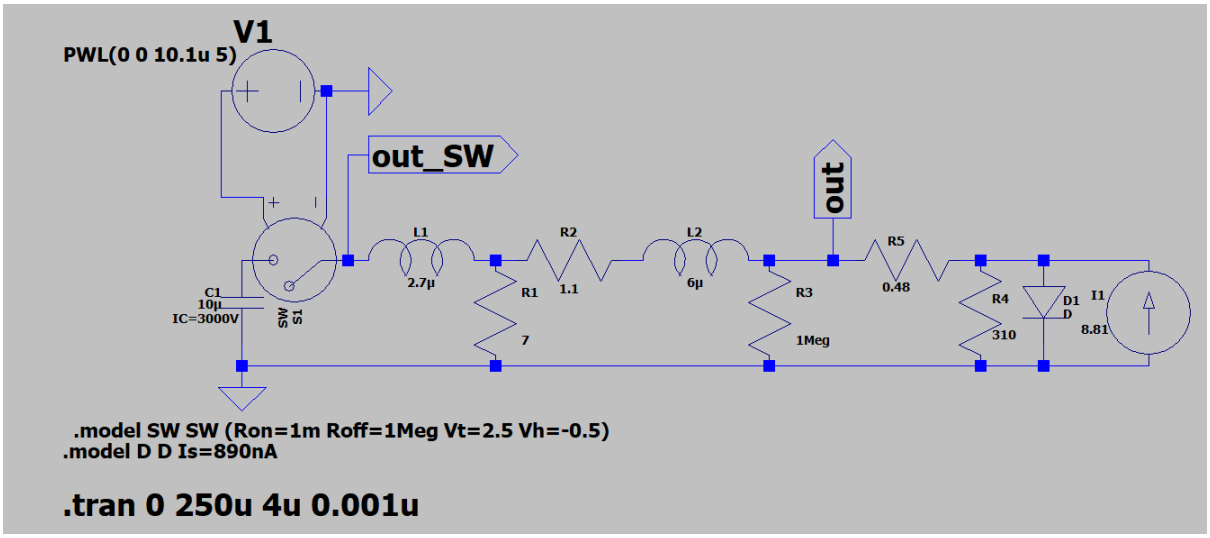

Appendix C-4

MATLAB code for parallel connection of LSS, PV and MOV

Calculating voltage dropped along the path as well as energy supplied by LSS and energy absorbed by PV panel

```
close all;
clc;

V_surge=[50 208 420 620 840 1040 1240 1440 1600 1840 2000 2240 2400 2640];
%% Surge Voltage observed from Scope
I_surge=[20.8 192 440 608 920 1280 1440 1760 1920 2080 2400 2640 2800
3040];     %% Surge Current observed from Scope

V_pv = [ 80 104 128 136 152 176 176 192 216 208 288 232 240 256 ];
%% Surge Voltage + Open Circuit Volatge of Solar Panel
R_path = 0.5;      %% Path Resistance
Voc_pv = 35;       %% Open Circuit Voltage of the Solar Panel

V_pv_surge = V_pv - Voc_pv; %% Actual Surge Volatage appeared across the
Solar Panel due to surge

V_drop_observed = V_surge - V_pv_surge; %% Voltage drop during the path
V_drop_calculated_resistive = (R_path*I_surge); %% Voltage drop observed
due to the resistive effect of the path
V_drop_calculated_inductive= V_drop_observed - V_drop_calculated_resistive;
%% Voltage drop observed due to the inductive effect of the path

time = [ 50e-6 26e-6 24e-6 21e-6 21e-6 20e-6 19e-6 19e-6 19e-6 19e-6 19e-6
19e-6 19e-6 19e-6 ]; %% Time interval between start and near end of the
surge spike at Solar Panel
energy_surge = V_surge.*I_surge.*time;
energy_solar_panel = V_pv.*I_surge.*time;

figure('Name','Energy sourced by LSS and absorbed by Solar
Panel','NumberTitle','off')
plot(V_surge,energy_surge, '-*')
hold on
plot(V_surge,energy_solar_panel, '-*')
hold off
xlabel('Surge Volatge (V)','FontSize',18)
set(gca,'FontSize',20)
ylabel('energy (J)','FontSize',18)
set(gca,'FontSize',20)
legend({'Energy sourced by LSS','Energy absorbed by Solar
Panel'},'Location','NorthWest','FontSize',22)
grid on

figure('Name','Drop due to path resistance and path
inductance','NumberTitle','Off');
plot(V_surge,V_drop_calculated_resistive, '-*')
hold on
plot (V_surge,V_drop_calculated_inductive, '-*')
hold off
xlabel('Surge Volatge (V)','FontSize',18)
set(gca,'FontSize',20)
ylabel('Voltage drop due to path (V)','FontSize',18)
```

```
ylim([0 1600])
set(gca,'FontSize',20)
legend({'resistive drop','inductive
drop'},'Location','NorthWest','FontSize',22)
grid on
```

Appendix C-5

Oscilloscope images for the surges on PV panel with MOV connected

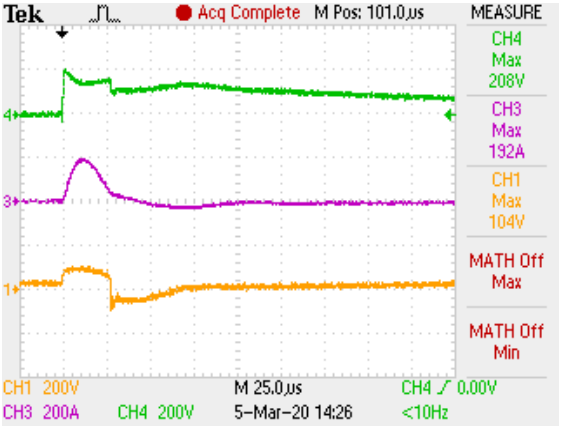

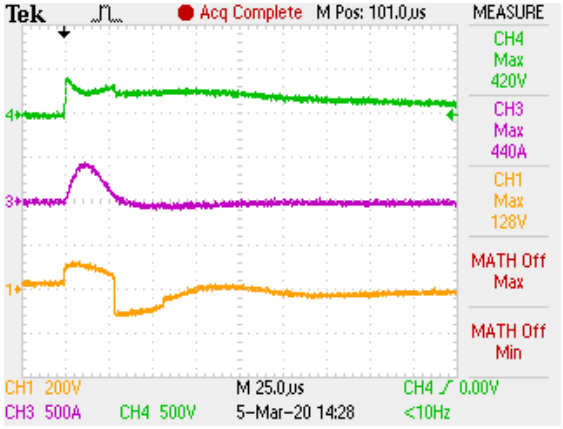

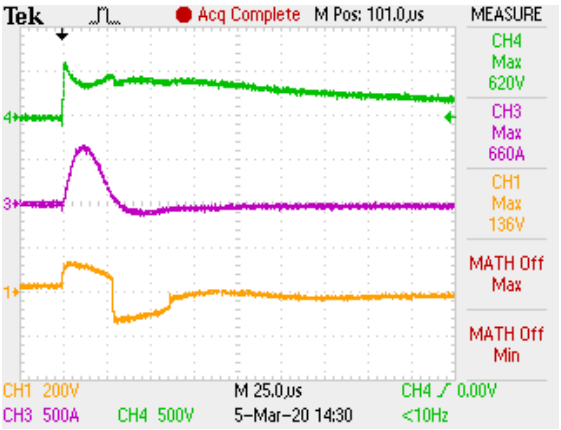

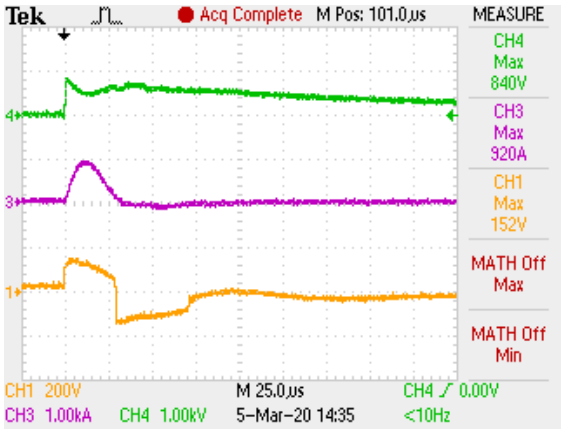

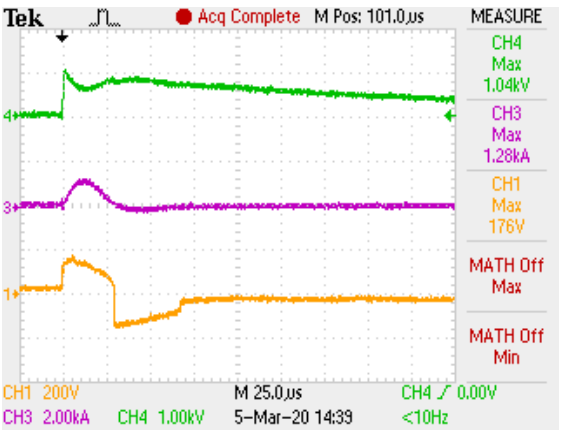

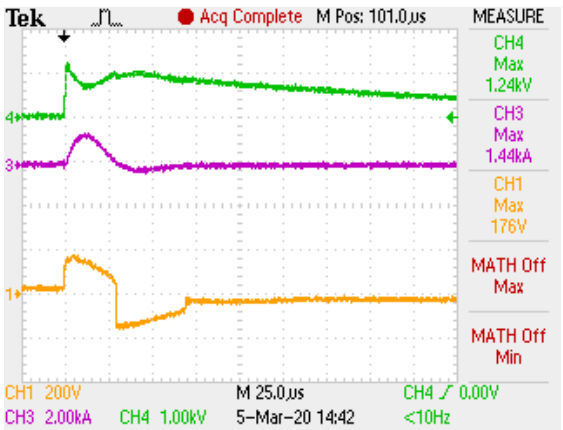

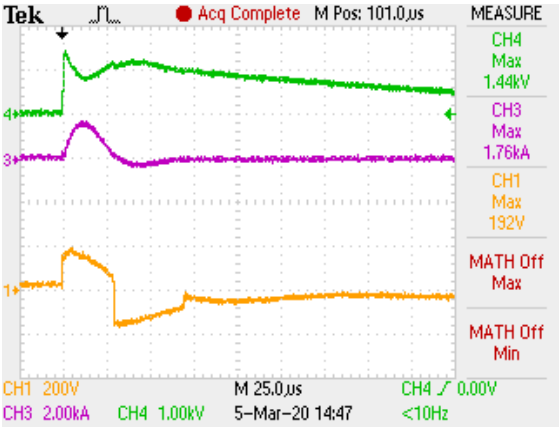
Tek
Acq Complete
M Pos: 101.0µs
MEASURE
CH4
Max
1.44kV
CH3
Max
1.76kA
CH1
Max
192V
MATH Off
Max
MATH Off
Min
CH1 200V
M 25.0µs
CH4 ∕ 0.00V
CH3 2.00kA
CH4 1.00kV
5-Mar-20 14:47
<10Hz

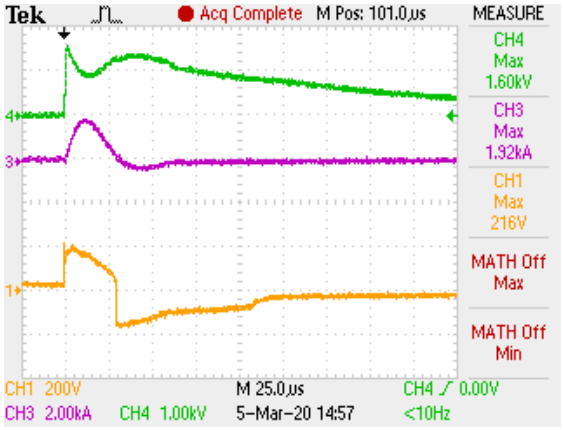
Tek
Acq Complete
M Pos: 101.0µs
MEASURE
CH4
Max
1.60kV
CH3
Max
1.92kA
CH1
Max
216V
MATH Off
Max
MATH Off
Min
CH1 200V
M 25.0µs
CH4 ∕ 0.00V
CH3 2.00kA
CH4 1.00kV
5-Mar-20 14:57
<10Hz

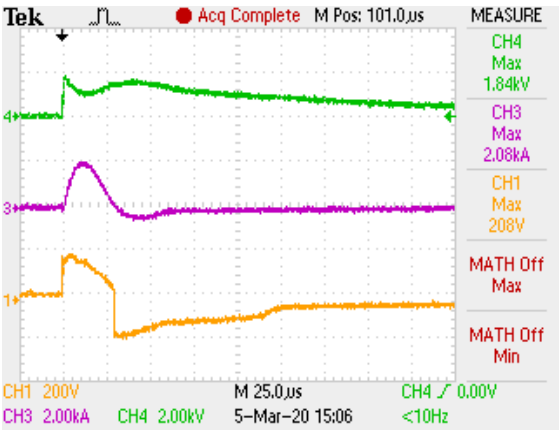
Tek
Acq Complete
M Pos: 101.0µs
MEASURE
CH4
Max
1.84kV
CH3
Max
2.08kA
CH1
Max
208V
MATH Off
Max
MATH Off
Min
CH1 200V
M 25.0µs
CH4 ∕ 0.00V
CH3 2.00kA
CH4 2.00kV
5-Mar-20 15:06
<10Hz

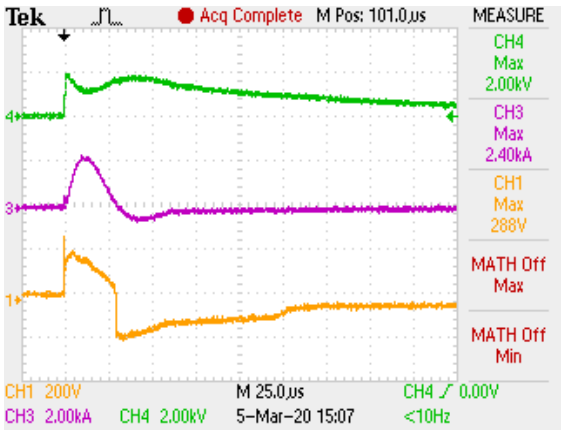
Tek
Acq Complete
M Pos: 101.0µs
MEASURE
CH4
Max
2.00kV
CH3
Max
2.40kA
CH1
Max
288V
MATH Off
Max
MATH Off
Min
CH1 200V
M 25.0µs
CH4 ∕ 0.00V
CH3 2.00kA
CH4 2.00kV
5-Mar-20 15:07
<10Hz

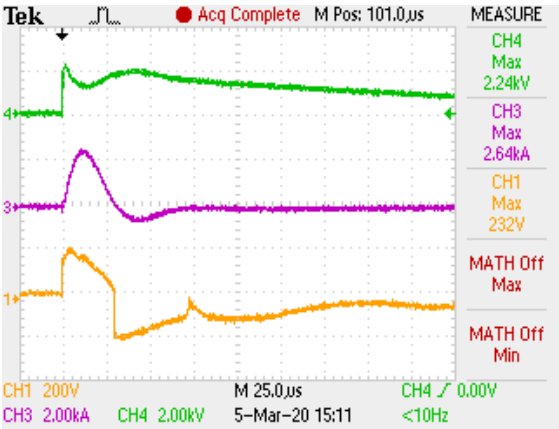
Tek
Acq Complete
M Pos: 101.0µs
MEASURE
CH4
Max
2.24kV
CH3
Max
2.64kA
CH1
Max
232V
MATH Off
Max
MATH Off
Min
CH1 200V
M 25.0µs
CH4 ∕ 0.00V
CH3 2.00kA
CH4 2.00kV
5-Mar-20 15:11
<10Hz

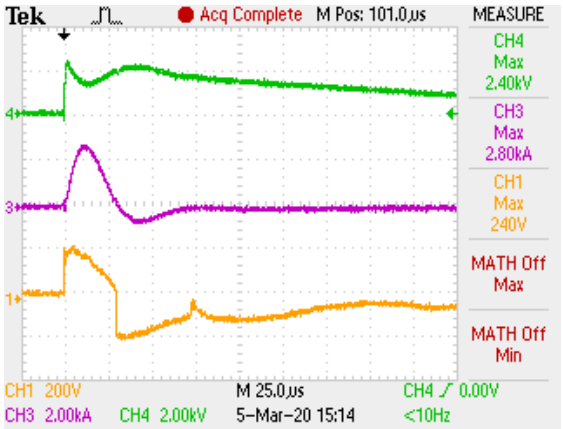
Tek
Acq Complete
M Pos: 101.0µs
MEASURE
CH4
Max
2.40kV
CH3
Max
2.80kA
CH1
Max
240V
MATH Off
Max
MATH Off
Min
CH1 200V
M 25.0µs
CH4 ∕ 0.00V
CH3 2.00kA
CH4 2.00kV
5-Mar-20 15:14
<10Hz

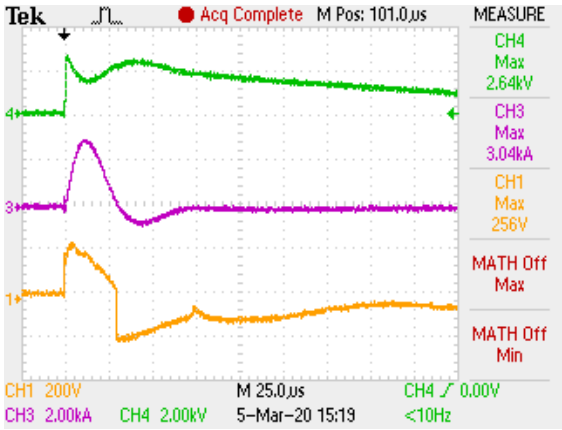
Tek
Acq Complete
M Pos: 101.0µs
MEASURE
CH4
Max
2.64kV
CH3
Max
3.04kA
CH1
Max
256V
MATH Off
Max
MATH Off
Min
CH1 200V
M 25.0µs
CH4 ∕ 0.00V
CH3 2.00kA
CH4 2.00kV
5-Mar-20 15:19
<10Hz

Appendix D

LTspice simulation of surge protective circuit designed for SCALED

MOV is represented by the symbol U1

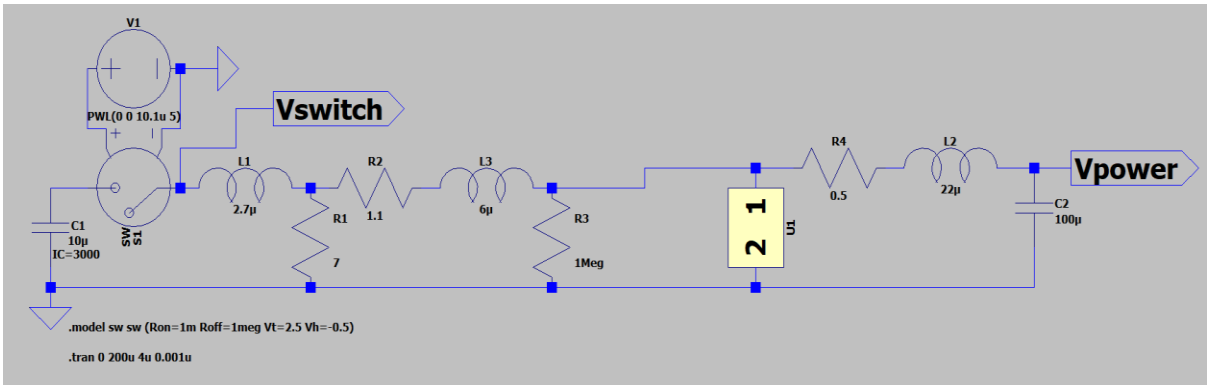

Library file to create symbol for V180ZA20P MOV

Downloaded from

https://www.littelfuse.com/technical-resources_old/spice-models/varistor-spice-models.aspx

```
Edited by: Pranav Udas

.SUBCKT MOV  1 2 PARAMS: T=1 C=1pF L=1nH a1=1 a2=0 a3=0 a4=0
a5=0 a6=100u a7=100u

E_non_lin 3 1  VALUE {T*(a1+a2*(log10(limit(v(4),a7,1g))-
3)+a3/limit(v(4)*.001,a7/1e3,1g)+a4*exp(-
log10(limit(v(4),a7,1g))+3)+a5*exp(log10(limit(v(4),a7,1g))-
3)-(a1+a2*(log10(-limit(v(4),-1g,-a7))-3)-a3/limit(v(4)*.001,-
1g,-a7/1e3)+a4*exp(-log10(-limit(v(4),-1g,-
a7))+3)+a5*exp(log10(-limit(v(4),-1g,-a7))-
3))+limit(v(4)/a7*v(8),-v(8),v(8)))}

L_series  5 6  {L}
H_H1      4 0  VH_H1 1k
VH_H1     5 7 0V
R_R2      0 4  1G=20
R_series  6 2  {a6}
V_V1      3 7  0V
E_x_zero  8 0  VALUE {a1+a2*(log10(a7/1e3)) +a3/(a7/1e3)
+a4*exp(-log10(a7/1e3))+a5*exp(log10(a7/1e3))}
R_x_zero  8 0  1G
```

```
C_parallel     1 5 {C}
.ENDS

.SUBCKT V180ZA20 1 2 PARAMS: TOL=30
X1   1 2  MOV PARAMS: T={1+TOL/100} L=12nH C=1.1nF a1=214.5
a2=11.74 a3=-1.343e-5 a4=2.101e-2 a5=5.953 a6=3.032e-2
.ENDS
```

Appendix E-1

Oscilloscope images for the voltage spikes observed across 8V SCALDO in the event of surge

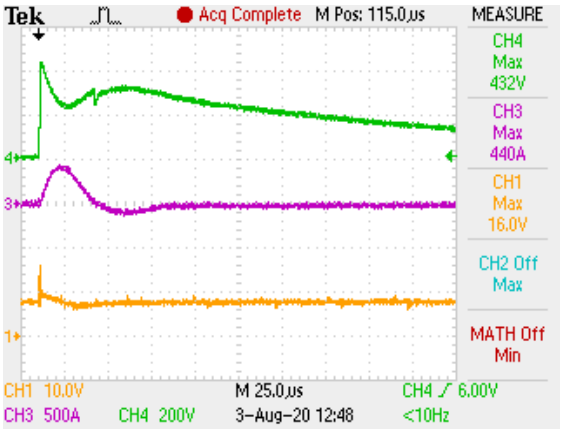

1 kV

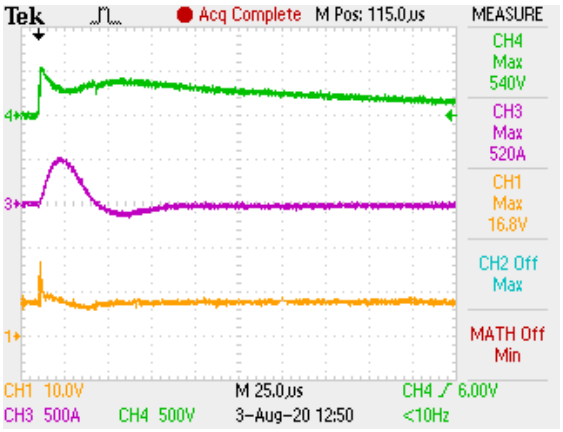

1.2 kV

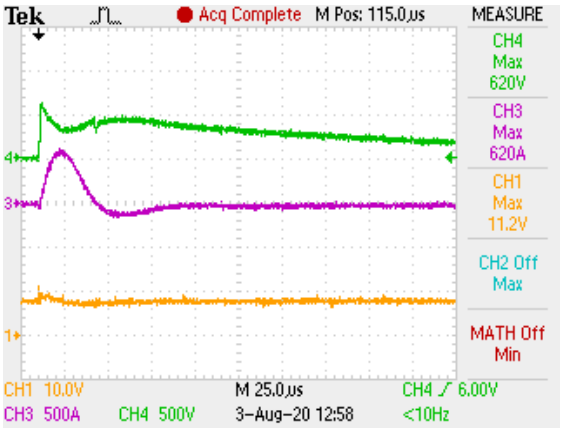

1.4 kV

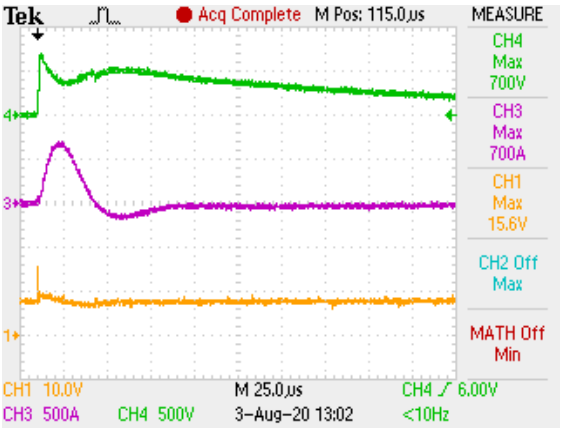

1.6 kV

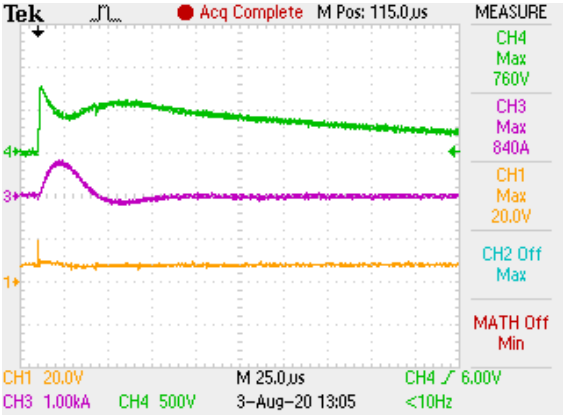

1.8 kV

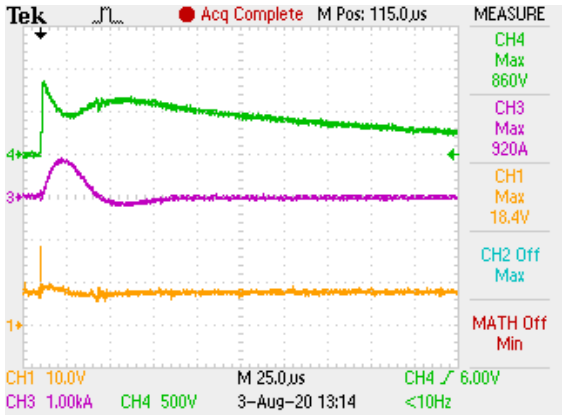

2 kV

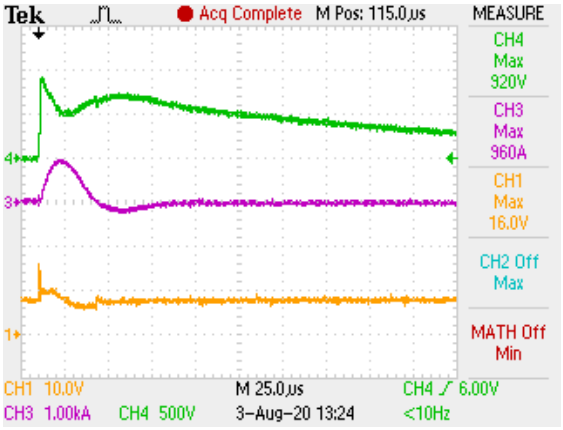

2.2 kV

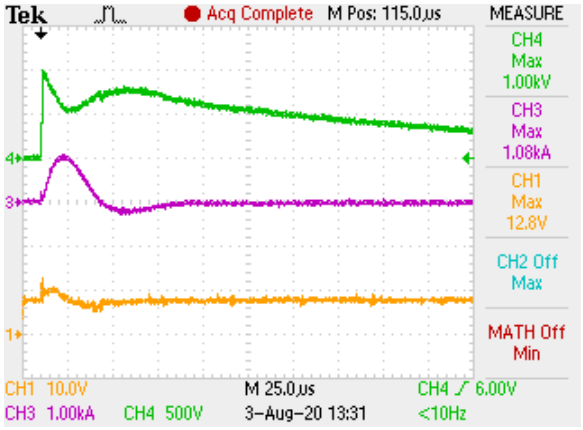

2.4 kV

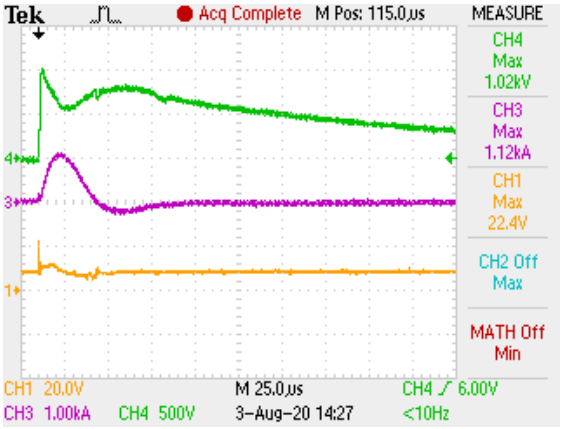

2.6 kV

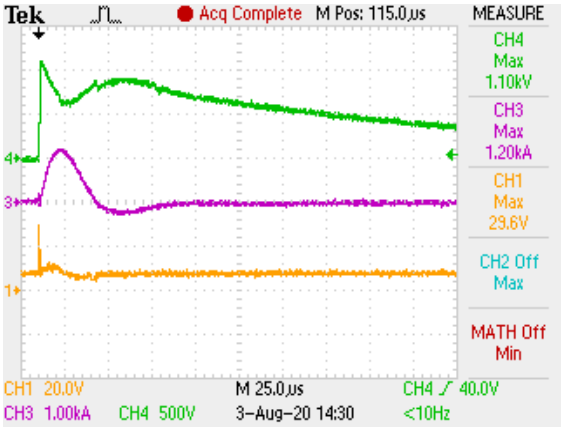

2.8 kV

Appendix E-2

Oscilloscope images for the voltage spikes observed across 5V isolated power supply in the event of surge

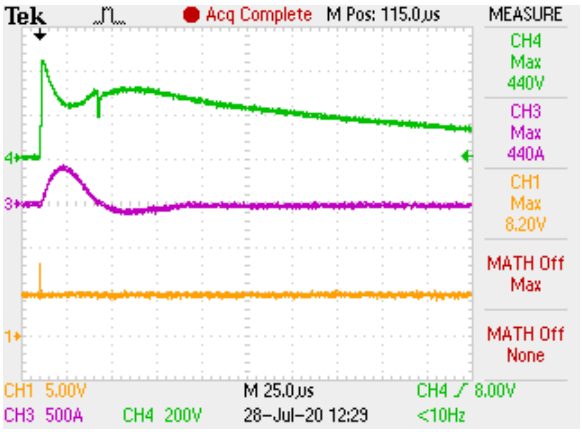

1 kV

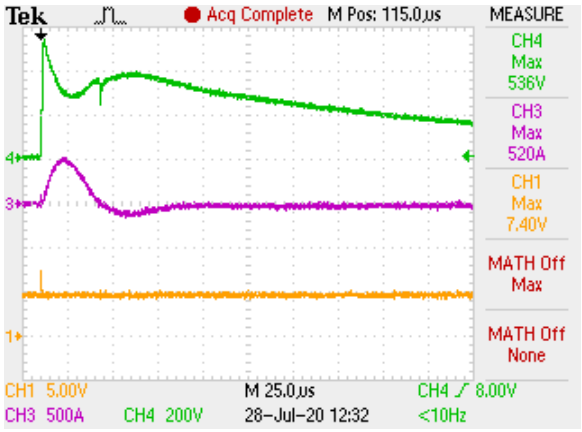

1.2 kV

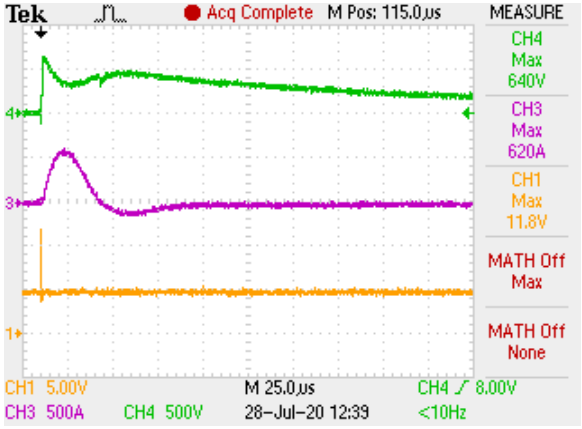

1.4 kV

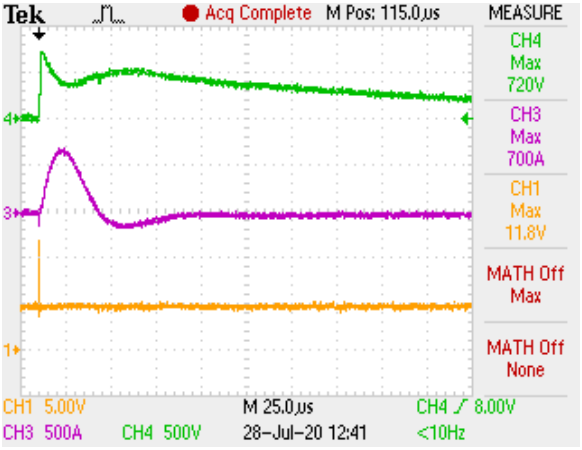

1.6 kV

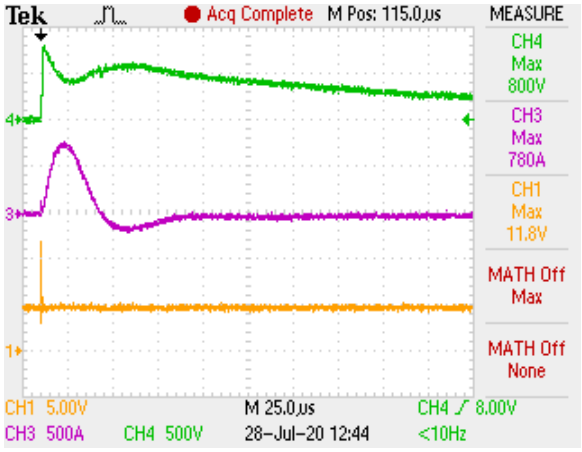

1.8 kV

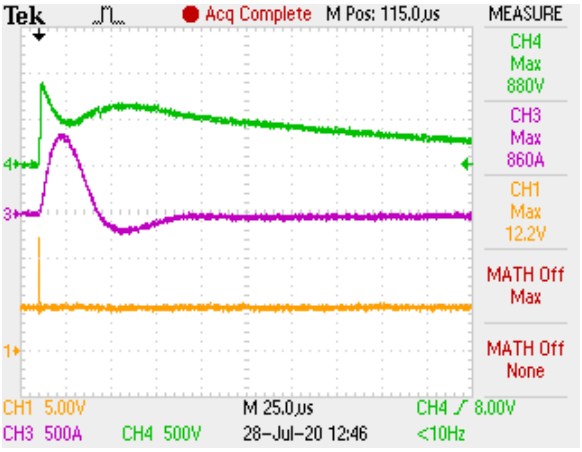

2 kV

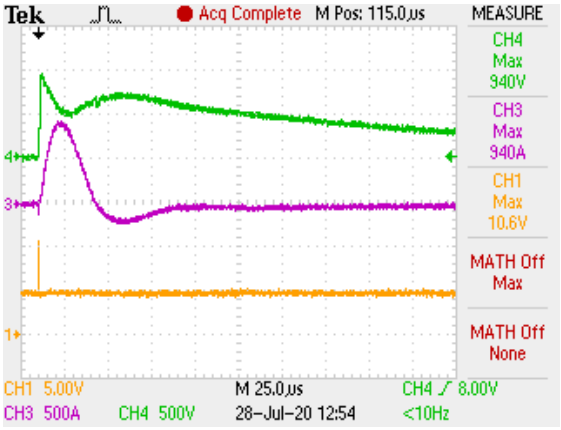

2.2 kV

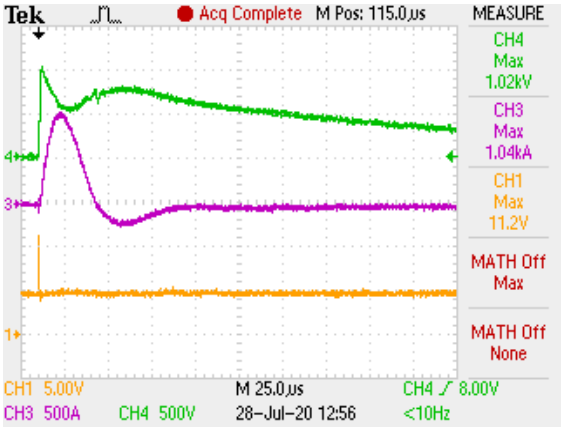

2.4 kV

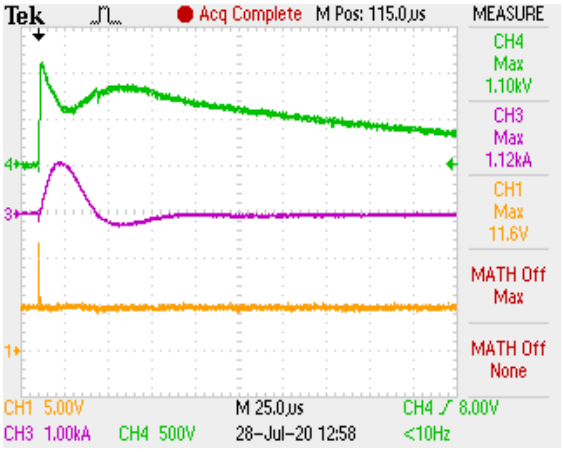

2.6 kV

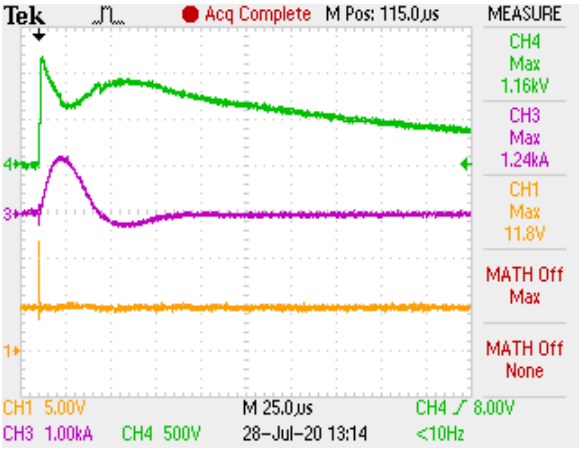

2.8 kV

References

[1] T. Ariyarathna, D. Jayananda, N. Kularatna and D. A. Steyn-Ross, "Potential of supercapacitors in novel power converters as semi-ideal lossless voltage droppers," IECON 2017 - 43rd Annual Conference of the IEEE Industrial Electronics Society, Beijing, 2017, pp. 1429-1434, doi: 10.1109/IECON.2017.8216243.

[2] K. Subasinghage, K. Gunawardane, T. Lie and N. Kularatna, "Design concepts and preliminary implementations of dual output supercapacitor-assisted low-dropout regulators (DO-SCALDO)," 2016 Australasian Universities Power Engineering Conference (AUPEC), Brisbane, QLD, 2016, pp. 1-6, doi: 10.1109/AUPEC.2016.7749346.

[3] J. Fernando, N. Kularatna, H. Round and S. Tálele, "Implementation of the supercapacitor-assisted surge absorber (SCASA) technique in a practical surge protector," IECON 2014 - 40th Annual Conference of the IEEE Industrial Electronics Society, Dallas, TX, 2014, pp. 5191-5195, doi: 10.1109/IECON.2014.7049290.

[4] N. Gurusinghe, N. Kularatna, S. A. Charleston and J. Fernando, "System implementation aspects of supercapacitor based fast in-line water heating system," 2015 IEEE 24th International Symposium on Industrial Electronics (ISIE), Buzios, 2015, pp. 1313-1317, doi: 10.1109/ISIE.2015.7281662.

[5] N. Kularatna, K. Milani and W. H. Round, "Supercapacitor energy storage in solar application: A design approach to minimize a fundamental loss issue by partitioning the load and the storage device," 2015 IEEE 24th International Symposium on Industrial Electronics (ISIE), Buzios, 2015, pp. 1308-1312, doi: 10.1109/ISIE.2015.7281661.

[6] D. Jayananda, N. Kularatna and D. A. Steyn-Ross, "Design approach for Supercapacitor Assisted LED lighting (SCALED) technique for DC-microgrids," 2018 IEEE International Conference on Industrial Electronics for Sustainable Energy Systems (IESES), Hamilton, 2018, pp. 27-31, doi: 10.1109/IESES.2018.8349845.

[7] Amy, B. (2015, October 19). *altE store*. Retrieved June 29, 2020, from The altE blog: https://www.altestore.com/blog/2015/10/how-do-solar-panels-work

[8] Issac, O. (2018, April 2). *solar learning center*. Retrieved June 29, 2020, from solar.com: https://www.solar.com/learn/solar-panel-size-and-weight-comparison-in-2018/

[9] M. G. Villalva, J. R. Gazoli and E. R. Filho, "Comprehensive Approach to Modeling and Simulation of Photovoltaic Arrays," in IEEE Transactions on Power Electronics, vol. 24, no. 5, pp. 1198-1208, May 2009, doi: 10.1109/TPEL.2009.2013862.

[10] Alternative Energy in Power Electronics, edited by Muhammad H. Rashid, Elsevier Science & Technology, 2014. ProQuest Ebook Central, https://ebookcen_tralproquest.com.ezproxy.waikato.ac.nz/lib/waikato/detail.action?docID=1834154.

[11] Blog, S. (2016, December 6). *Infinite Energy*. Retrieved June 28, 2020, from https://www.infiniteenergy.com.au/:https://www.infiniteenergy.com.au/difference-between-max-power-stc-noct/

[12] T. Dragičević, X. Lu, J. C. Vasquez and J. M. Guerrero, "DC Microgrids—Part II: A Review of Power Architectures, Applications, and Standardization Issues," in IEEE Transactions on Power Electronics, vol. 31, no. 5, pp. 3528-3549, May 2016, doi: 10.1109/TPEL.2015.2464277.

[13] Tomislav Dragičević, G. B. (2017, June 27-29). Power architectures, applications and control of DC distribution Systems and Microgrids. *Power architectures, applications and control of DC distribution Systems and Microgrids*. Nürnberg, Nürnberg, Germany.

[14] M. T. Ahmed, T. Gonçalves, A. Albino, M. R. Rashel, A. Veiga and M. Tlemcani, "Different parameters variation analysis of a PV cell," 2016 International Conference for Students on Applied Engineering (ICSAE), Newcastle upon Tyne, 2016, pp. 176-180, doi: 10.1109/ICSAE.2016.7810183.

[15] M. K. Dave, "Modeling of PV arrays based on datasheet," 2016 IEEE 1st International Conference on Power Electronics, Intelligent Control and Energy Systems (ICPEICES), Delhi, 2016, pp. 1-4, doi: 10.1109/ICPEICES.2016.7853617.

[16] CSUN..CSUN250-60P Standard Solar Product datasheet.

[17] D. Jayananda, N. Kularatna and D. A. Steyn-Ross, "Powering 12-V LED luminiaries with supercapacitor-based energy storage in DC-microgrid systems," IECON 2018 - 44th Annual Conference of the IEEE Industrial Electronics Society, Washington, DC, 2018, pp. 1922-1927, doi: 10.1109/IECON.2018.8591511.

[18] D. Jayananda, N. Kularatna and D. A. Steyn-Ross, "Supercapacitor-assisted LED (SCALED) technique for renewable energy systems: a very low frequency design approach with short-term DC-UPS capability eliminating battery banks," in IET Renewable Power Generation, vol. 14, no. 9, pp. 1559-1570, 6 7 2020, doi: 10.1049/iet-rpg.2019.1307.

[19] Nihal Kularatna, A. S. (2019). *Design of Transient Protection System Including Supercapacitor Based Design Approaches for Surge Protectors.* Hamilton, Waikato, New Zealand: Elsevier.

[20] James, S. (2014). Investigation of surge propagation in transient voltage surge suppressors and experimental verification (Thesis, Doctor of Philosophy (PhD)). University of Waikato, Hamilton, New Zealand. Retrieved from https://hdl.handle.net/10289/8830

[21] Fernando, J. (2016). Supercapacitor Assisted Surge Absorber (SCASA) and Supercapacitor Modelling.

[22] Kozhiparambil, P. K. (2011). Development of a Supercapacitor based Surge Resistant Uninterruptible Power Supply (Thesis, Master of Engineering (ME)). University of Waikato, Hamilton, New Zealand. Retrieved from https://hdl.handle.net/10289/5360

[23] S. James, N. Kularatna, A. Steyn-Ross and R. Künnemeyer, "Numerical simulation of surge protection circuits and experimental verification using a lightning surge simulator," IECON 2012 - 38th Annual Conference on IEEE

Industrial Electronics Society, Montreal, QC, 2012, pp. 615-620, doi: 10.1109/IECON.2012.6388757.

[24] S. James, N. Kularatna, A. Steyn-Ross, A. Pandey, R. Künnemeyer and D. Tantrigoda, "Investigation of failure patterns of desktop computer power supplies using a lightning surge simulator and the generation of a database for a comprehensive surge propagation study," IECON 2010 - 36th Annual Conference on IEEE Industrial Electronics Society, Glendale, AZ, 2010, pp. 1275-1280, doi: 10.1109/IECON.2010.5675553.

[25] S. James, N. Kularatna, A. Steyn-Ross and R. Künnemeyer, "Estimation of transient surge energy transferred with associated time delays for individual components of surge protector circuits," in IET Power Electronics, vol. 8, no. 5, pp. 685-692, 5 2015, doi: 10.1049/iet-pel.2014.0212.

[26] N. Kularatna, J. Fernando, A. Pandey and S. James, "Surge Capability Testing of Supercapacitor Families Using a Lightning Surge Simulator," in IEEE Transactions on Industrial Electronics, vol. 58, no. 10, pp. 4942-4949, Oct. 2011, doi: 10.1109/TIE.2011.2109338.

[27] Littlefuse. (n.d.). *Littlefuse*. Retrieved from MOV product catalog and design guide.

[28] Littlefuse. (n.d.). *Littlefuse*. Retrieved from TVS diode product catalog and design guide.

[29] N. Kularatna, J. Fernando and A. Pandey, "Surge endurance capability testing of supercapacitor families," IECON 2010 - 36th Annual Conference on IEEE Industrial Electronics Society, Glendale, AZ, 2010, pp. 1858-1863, doi: 10.1109/IECON.2010.5675392.

[30] *autoblog*. (2019, February 6). Retrieved July 28, 2020, from autoblog.com: https://www.autoblog.com/2019/02/06/tesla-maxwell-technologies-ultracapacitors/

[31] LS(2020, June 25) *User Manual LSUM06R8L 0058F EA*. Retrieved from www.ultracapacitor.co.kr: https://www.ultracapacitor.co.kr:8001/sub/product/LSUM/Manual_LSUM016R8L_0058F_EA.pdf

[32] J. Fernando and N. Kularatna, "Supercapacitor assisted surge absorber (SCASA) technique: Selection of supercapacitor and magnetic components," 2014 IEEE Energy Conversion Congress and Exposition (ECCE), Pittsburgh, PA, 2014, pp. 1992-1996, doi: 10.1109/ECCE.2014.6953664.

[33] Littelfuse. (2020, August 24). *Littelfuse*. Retrieved from Littelfuse ZA varistor_series:https://m.littelfuse.com/~/media/electronics/datasheets/varistors/littelfuse_varistor_za_datasheet.pdf.pdf

[34] Module, L. (2020, August 24). LS ultracapacitor. Retrieved from www.ultracapacitor.co.kr:8001: https://www.ultracapacitor.co.kr:8001/products/lsum

[35] Franco, G., & Kularatna, N. (2017). *Supercapacitors*. Presented at APEC 2017 - Applied Power Electronics Conference 2017, 27-29 March 2017, Tampa, FL.

[36] *Electronics Tutorials*. (2020, September 16). Retrieved from electronic-tutorials.ws: https://www.electronics-tutorials.ws/accircuits/series-resonance.html

[37] *Bunnings Warehouse*. (2020, September 16). Retrieved from bunnings.co.nz: https://www.bunnings.co.nz/arlec-vertical-double-surge-adaptor_p0264599

[38] *PBTech*. (2020, September 16). Retrieved from pbtech.co.nz: https://www.pbtech.co.nz/product/SURBEL2740626/Belkin-SurgeCube-BSV102au.OutletSurgeProtector?qr=GShopping&gclid=EAIaIQobChMIkfnzk5Pt6wIVmiQrCh3q7wIBEAQYASABEgKPlPD_BwE

[39] *MITRE10*. (2020, September 16). Retrieved from mitre10.com.au: https://www.mitre10.com.au/hardware-electrical/electrical/powerboards-timers-adaptors